HOST DEFENCE AGAINST COMPLEX CHALLENGES

PULMONARY HOST DEFENCE AGAINST HETEROLOGOUS INFECTIOUS AND NON-INFECTIOUS CHALLENGES

By

CALEB CRAIG JENTER ZAVITZ, B.Sc.

A Thesis
Submitted to the School of Graduate Studies
in Partial Fulfilment of the Requirement
for the Degree
Doctor of Philosophy

McMaster University
Hamilton, Ontario, Canada

DOCTOR OF PHILOSOPHY (2009) McMaster University
(Medical Sciences) Hamilton, Ontario

TITLE: Pulmonary Host Defence Against Heterologous Infectious and Non-Infectious Challenges

AUTHOR: Caleb Craig Jenter Zavitz, B.Sc.

SUPERVISOR: Dr. Martin R. Stampfli

NUMBER OF PAGES: xvii, 148

Abstract

Lung disease is the leading threat to human health worldwide. In particular, two threats are responsible for the majority of the pulmonary disease burden: infection and tobacco smoke exposure. Efforts to combat these diseases have been hampered by gaps in our understanding of the complex interactions between environmental threats and the host's own immune defences. Indeed, much of the pulmonary disease burden should be ascribed not to direct smoke-, virus- or bacteria-induced damage, but to maladaptive host defence responses against these threats. This is an understudied topic. Efforts to redress this deficiency have been hampered by the lack of available animal models. Thus, the present studies developed and examined models of Heterologous pulmonary infection, in which hosts must defend against two different infections, and of tobacco smoke exposure. In the first study, a critical role for MIP-2 driven pulmonary neutrophilia was elucidated in the pathology associated with bacterial superinfection of influenza virus infection. This study further demonstrated that the timing and sequence in which pathogens were encountered played important roles in determining the outcome of disease, and that viral and bacterial infections have different but long-lived impacts on alveolar macrophages. In the second study, it was determined that cigarette smoke exposure impacts host defence without exhausting T- or B-cells. Collectively, these studies have advanced our understanding of complex lung pathologies, and suggest an important role for the innate immune system in mediating such diseases.

Acknowledgements

"If I have seen a little further it is by standing on the shoulders of Giants"
–Sir Isaac Newton, 1676

I am grateful to all the giants, who have supported me through my life and my career in science. At points, I have surely not made myself easy to help.

First to my supervisor, Martin Stämpfli. Why he took a chance on me is a mystery, but Martin has been a mentor and a friend, and through him, I have received what can only be described as an apprenticeship in science. Equally to Mark McDermott, who inspired me to pursue graduate work in immunology, and who has supported me continuously ever since. I suspect this is because he laid his job or life on the line to get me into the program. And to Jonathan Bramson, who I think Martin added to my committee along with Mark just so future students could be threatened with the prospect of a similar horror. Thanks to their supervision, I became a better scientist.

Were it not for Gord Gaschler and Carla Bauer, I would not have been able to complete my degree. Both are brilliant scientists and tremendously hard workers. Over the last 5 years, they have made themselves available 24 hours a day, 7 days a week. I appreciate the constant help, insightful advice, and withering critiques, but the camaraderie most of all.

Ramzi Fattouh, David Smythe, Clinton Robbins, and Maziar Divangahai – some of the best scientists and best people I know. Their positive effect on my brain while in the lab has been approximately balanced by their devastating effect on my liver while outside of it.

Thanks to the Stampfli and Jordana groups, past and present. Particularly, Katie Fraser- a talented undergraduate student involved with these experiments, Joanna Kasinska and Sussan Kianpour – two excellent technicians, and Marie Colbert and Mary Kirakopolous – administrative assistants extraordinaire.

To my mom- an amazing woman who served as both a mother and a father to me. Her ceaseless love and support is a constant source of comfort.

To Tracy for her patience and understanding through the late nights, early mornings, and missed holidays that this graduate degree demanded.

And finally, thanks to the countless faculty, staff, students, friends, and family who have helped me along the way but whose names I have been forced to omit here. I hope I have expressed my appreciation in person.

Table of Contents

List of Figures

List of Tables

List of Abbreviations

7AAD	7-aminoactinomycin D
AM	alveolar macrophage
ANOVA	analysis of variance
AP-1	activating protein 1
APC	allophycocyanin
APCs	antigen presenting cells
ARDS	acute respiratory distress syndrome
B (-cell)	bursa of Fabricius / Bone-marrow
B. bronchiseptica	*Bordetella bronchiseptica*
B. parapertussis	*Bordetella parapertussis*
B. pertussis	*Bordetella pertussis*
BAL	broncho-alveolar lavage
BCR	B cell receptor
Bpp	*Bordetella parapertussis*
CARD	caspase recruiting domain
CCR	cystine-cystine chemokine receptor
CD	cluster of differentiation
CFA	complete Freund's adjuvant
cfu	colony forming unit
COHb	carboxyhemoglobin
COPD	chronic obstructive pulmonary disease
CpG	unmethylated 5' cytosine-guanine 3' nucleotide
cpm	counts per minute
CRP	C-reactive protein
cRPMI	complete Roswell Park Memorial Institute 1640 medium
CXCL	cystine-X-cystine chemokine ligand
CXCR	cystine-X-cystine chemokine receptor
Cy	cyanine
D	day
DC	dendritic cell
dLN	draining lymph node(s)
DMEM	Dulbecco's modified Eagle's medium
DPT	diphtheria, pertussis, tetanus
EDTA	ethylene diamine tetraacetic acid
EGF	epidermal growth factor
ELISA	enzyme-linked immunosorbent assay
ELR	glutamic acid-leucine-arginine motif
FcR	constant fragment receptor
FGF	fibroblast growth factor
FimH	fimbrial protein H
FITC	fluorescein isothioscyanate
FSC	forwardscatter
GCP	granulocyte chemotactic protein

G-CSF	granulocyte colony-stimulating factor
GFP	green fluorescent protein
GM-CSF	Granulocyte-macrophage colony stimulating factor
GST	glutathione s-transferase
H&E	hematoxylin and eosin
HA	Hemaglutinin
HBSS	Hanks' balanced salt solution
HeLa	Henrietta Lacks
HIV	human immunodeficiency virus
i.n.	Intranasal
i.p.	intraperitoneal
ICAM	intracellular adhesion molecule
IFN	Interferon
Ig	immunoglobulin
IL	Interleukin
IP	inducible protein
IP3	inositol triphosphate
IRAK	IL-1 receptor associated kinase
IRF	interferon regulatory factor
KC	keratinocyte-derived chemokine
LDD	lowest detectable dose
LFA	leukocyte functional antigen
LIF	leukemia inhibiting factor
LN	lymph node(s)
LPS	lipopolysaccharide
M	influenza virus matrix protein
MACS	magnetic activated cell sorting
MBL	mannose binding lectin
MCP	monocyte chemoattractant protein
M-CSF	macrophage colony stimulating factor
MDC	macrophage derived chemokine
MDCK	Madin-Darby canine kidney
MEF	mouse embryonic fibroblasts
MEM	minimum essential medium
MHC	major histocompatibility complex
MIP	macrophage inflammatory protein
MMP	matrix metalloproteinase
MNC	mononuclear cells
MPO	myeloperoxidase
MyD	myeloid differentiation factor
NA	neuraminidase
nAChR	nicotinic acetylcholine receptor
ND	not detected
NF	nuclear factor
NK	natural killer

NP	nucleoprotein
OD	optical density
OSM	oncostatin M
PAMP	pathogen associated molecular pattern
PBMC	peripheral blood mononuclear cells
PBS	phosphate-buffered saline
PCR	polymerase chain reaction
PE	phycoerythrin
perCP	peridinin-chlorophyll protein
pfu	plaque-forming unit
PHA	phytohemagglutinin
PMA	phorbol 12-myristate 13-acetate
PMN	polymorphonuclear neutrophil
poly (I:C)	polyinosinic:polycytidylic acid
PRR	pattern recognition receptor
RANTES	regulated upon activation, normal T-cell expressed and secreted
rbt	rabbit
RIG	retinoic acid inducible gene
RNA	ribonucleic acid
ROS	reactive oxygen species
RPMI	Roswell Park Memorial Institute 1640 medium
RSV	respiratory syncytial virus
RV	rhinovirus
S. aureus	*Staphylococcus aureus*
S. pneumonia	*Streptococcus pneumonia*
SAP	serum amyloid protein
SCF	stem cell factor
SEA	staphylococcal enterotoxin A
SEB	staphylococcal enterotoxin B
SEM	standard error of the mean
SGOT	serum glutamic-oxaloacetic transaminase
SHP	Src homology 2-containing protein-tyrosine phosphatase
SIRP-α	signal inhibitory regulatory protein α
SPA	surfactant protein A
SPD	surfactant protein D
SSC	sidescatter
T-cell	thymocyte
TCN	total cell number
TCR	T cell receptor
TGF	transforming growth factor
TIMP	tissue inhibitor of metalloproteinase
TLR	toll-like receptor
TNF	tumor necrosis factor

TPO	thrombopoietin
TUNEL	terminal deoxynucleotidyl transferase deoxy uridine triphosphate nick end labelling
VCAM	vascular cell adhesion molecule
VEGF	vascular endothelial growth factor
VILI	ventilator-induced lung injury
VSV	vesicular stomatitis virus
vWF	von Willebrand factor
WHO	World Health Organization

Preface

The data contained within this thesis are drawn from two distinct projects- one focusing on the impact of multiple infections on pulmonary host defence and one focusing on tobacco smoke's impact on immune responses. Although different in their foci, these projects were thematically related, in that they developed new knowledge on the impact that common environmental challenges have on the pulmonary host defence response. The work related to the impact of cigarette smoke on immunity has been published in the journal *Cellular Immunology* (1), while some of the data related to heterologous viral-bacterial infection have been compiled into a manuscript which is under review at *Cell Host and Microbe*. In order to prepare this thesis, these published and submitted results have been supplemented with a number of unpublished observations. Additionally, elements of the Introduction and Discussion have been drawn from a previously published book chapter which I co-authored (2). Where I have used previously published work in this manuscript, I have done so with the expressed written consent of the relevant copyright holder.

Certainly this work could not have been completed without a number of other contributors, and that is reflected in the multiple authors listed in my published and submitted manuscripts. With specific regard to the contributions made by my co-authors, in the first manuscript,

Caleb CJ Zavitz, Gordon J Gaschler, Fernando M Botelho, P Gerard Cox, and Martin R Stampfli. 2008. Impact of cigarette smoke on T and B cell responsiveness. *Cellular Immunology* 253(1-2):38-44

Gordon J Gaschler assisted with experiments and critically reviewed the draft manuscript. Fernando M Botelho assisted with experiments. P Gerard Cox provided biological specimens and critically reviewed the manuscript. Martin R Stampfli provided the initial research direction, provided funding for the project, and critically reviewed the manuscript.

In the second manuscript,

Caleb CJ Zavitz, Carla MT Bauer, Gordon J Gaschler, Katie M Fraser, Robert M Strieter, Cory M Hogaboam, and Martin R Stampfli. Submitted 2009. Dysregulated MIP-2 expression drives illness in bacterial superinfection of influenza. Submitted.

Carla MT Bauer and Gordon J Gaschler assisted with or performed experiments under my direction and critically reviewed the draft manuscript. Katie M Fraser assisted with experiments. Robert M Strieter and Cory M Hogaboam provided reagents and critically reviewed the draft manuscript. Martin R Stampfli provided the initial broad idea for the project, provided funding for the project, and critically reviewed the manuscript.

As the lead investigator of both the aforementioned studies, I was responsible for formulating both broad and specific hypotheses, planning and conducting experiments to test them, and analyzing, interpreting and presenting results. Furthermore, I have been solely responsible for the preparation of the current thesis document. I have organized this thesis with

the goal of using my observations in pulmonary infectious- and tobacco-related disease to elucidate some key features of the host-environment interaction.

Chapter 1: Introduction

The lungs are elegantly positioned to perform the obligatory tasks of respiratory gas exchange and short-term acid-base balance. Given the acute and chronic maladies that can arise from interruptions in either of these homeostatic processes, it is not surprising that pulmonary disease represents a leading threat to health, with infection reigning supreme. Despite the widespread application of vaccines, antibiotics, and other therapies, lung infections are the single most pressing threat, not only to pulmonary health, but to human health in general. Specifically, the World Health Organization (WHO) estimates that over 4 million lives are lost each year to lower respiratory tract infections- more than are attributable to the widely recognized human immunodeficiency virus (HIV) and malaria pandemics, or to cardiovascular disease, cancer, or trauma (3). When including the lives lost to *Mycobacterium tuberculosis* infections, upper respiratory tract infections and childhood *Bordetella pertussis* infections, the toll exacted by pulmonary infectious disease climbs further to 5.9 million annually (4).

Tobacco smoke exposure represents another critical threat to pulmonary health and, consequently, also results in widespread death and disability. Smoking is the leading cause of preventable morbidity and mortality in the developed world, causing over 4.8 million deaths per year globally (5), and is projected to be the ultimate cause of over 10 million lost lives per year by 2030 (6). Morbidity and mortality are likely even higher than currently acknowledged, due to the largely unknown impact of

"environmental" smoke, i.e., the combination of exhaled mainstream smoke and uninhaled sidestream smoke to which a non-smoker is exposed by being in the same room as a smoker (commonly termed "second-hand" smoke). Even so, smoking is the dominant and nearly exclusive etiologic factor for chronic obstructive pulmonary disease (COPD), and lung, tracheal and bronchial cancers (7-9), along with non-occupationally related bladder cancer (10). Furthermore, smoking is a risk factor for conditions including but not limited to cardiovascular disease, periodontitis and, indeed, also respiratory tract infection (9, 11-13). Still, over 1.1 billion people continue to smoke, representing one-sixth of the world's population (14).

Critical gaps exist in our understanding of both infectious and tobacco-related disease and these deficiencies have hampered the development of effective interventions for both of these health threats. The interplay between environmental agents and the immune system is one such area, especially with respect to the impact that an environmental insult has on the immune system's responses to subsequent challenges. Indeed, a virus, a bacterium, or cigarette smoke's ability to modulate the immune response against secondary infections, allergens, and other immune stimuli might account for a larger proportion of pulmonary disease than does direct pathogen- or smoke-induced damage.

In this thesis, Chapter 1 (Introduction) provides the background on pulmonary defences, pathogens, tobacco smoke, and animal models of

disease that are necessary to appreciate the subsequent experiments in context, and presents the hypotheses which were tested during the course of these investigations.

1.1: Pulmonary host defences:

The principal function of the lungs is gas exchange. During ventilation, atmospheric air passes it through branching, progressively smaller calibre airways to the alveoli, where gas exchange occurs. Following inhalation, oxygen is transferred to the blood in the alveoli, while carbon dioxide is concurrently transferred out, and ultimately exhaled. Adequate tissue oxygenation demands that ventilation occur every few seconds, without appreciable interruption in order to avoid hypoxia, hypercapnia, and (rapidly) death (15).

The ability to regulate acid-base balance is intrinsic to the process of gas exchange; removing carbon dioxide from the blood decreases the concentration of carbonic acid in the bloodstream, raising the blood's pH. Moreover, the respiratory centre of the brain responds to increasing H^+ concentrations in the cerebrospinal fluid and the plasma by increasing respiratory depth and rate in order to eliminate excess CO_2. Through this process, blood pH is maintained within a homeostatic range of 7.35-7.45. Uncorrected interruptions to the process of ventilation also lead to respiratory acidosis, and would become lethal if the hypoxic consequences did not first kill the host (15).

Although the consequences of a failure in ventilation or respiration are dire, the chances of such an occurrence are not insignificant. To meet their basic metabolic needs through this process, a typical person will need to inhale and exhale over 7500L of atmospheric air on a daily basis. The number of contaminating viruses, bacteria, and other agents such a volume of gas contains is truly staggering. As a result, a multi-layered system of pulmonary defences has evolved to protect the delicate gas-exchange tissues from a constant onslaught of external agents (15).

1.1.1: Upper respiratory tract intrinsic barriers

The first of these layers is composed of the intrinsic defences: pre-formed barriers which prevent the entry of potentially hazardous agents. After air enters the nose, it passes through the nasal turbinates- the first line of defence. The turbinates force the airflow to become turbulent, and large suspended particles have sufficient inertia that they collide with the wall of the nasal passages during the high-speed directional changes before they can penetrate further down the respiratory tree. Humidification of the inhaled gases further increases the mass and diameter of hydrophilic particles, and, thus, even small particles might acquire sufficient mass to carry them out of the airstream and onto the airway wall (16). This apparently simple process is so effective that the respiratory tract of a healthy individual is generally regarded as sterile below the level of the larynx. Recent application of culture-independent molecular microbiological techniques and electron microscopy has called this notion into question by showing that some

bacteria do exist in the distal airways of healthy animals, but compared to the outside environment or other mucosal surfaces such as the gut, the airway remains an impressively clean environment (17). The importance of the intrinsic nasal defences is further underscored by the observation that bypassing the nasal defences, either by mouth breathing or by endotracheal intubation dramatically increases the risks of infection (18, 19).

Mucus forms an integral part of the upper defences in both the nasopharynx and the large airways. Mucus is a viscous polysaccharide produced in and secreted by goblet cells that are intercalated between the airway epithelial cells. Sticky mucus ensures that particles which collide with the airway wall become embedded there and cannot be inhaled further down the airway tree. In the conducting airways, which exist to convey air down to the respiratory airways, no gas exchange occurs (16). The airway epithelium is comprised of thick, columnar cells, underlain by a basement membrane and in some areas by muscle and collagen. This thickness makes the conducting airways more resistant to particle penetration than the delicate, more distal respiratory airways, where gas exchange occurs by simple diffusion. The ciliated epithelium ensures a relatively continuous upward motion of the overlying mucus, commonly referred to as the mucociliary escalator. Through this process, mucus-embedded particles are carried up the respiratory tract to a point where they can either be expelled by sneezing coughing, or swallowing (15). As a result, particles >5μm diameter are generally excluded from the distal airways, and only those particles under

3μm reliably penetrate and deposit in the delicate alveolar sacs, where gas exchange occurs (20).

1.1.2: Resident alveolar defences

With only two thin cells (epithelial and vascular endothelial) totalling 0.2 μm separating the external air from the host's bloodstream, the alveoli represent a site through which foreign agents can gain access to the body (21). Since mucus presents a diffusion barrier that would slow or preclude the exchange of respiratory gases, it is absent from these respiratory airways. Furthermore, the respiratory airways lack the chemical and microbiological barriers present in the genitourinary tract, gastrointestinal tract, and other host-environment interfaces commonly referred to as mucosal surfaces. At those sites, fatty acid layers, low water activity and keratinisation of the skin, and commensal bacteria which compete for niches with potential pathogens all cooperate to prevent the entry of harmful microbes (22). Instead, the alveoli are afforded some protection by a protective layer of phosphatidylcholine-rich surfactant, secreted from type II alveolar cells and Clara cells to reduce pulmonary surface tension, which contains the collectin-family surfactant proteins A and D (SPA and SPD) and mannose binding lectin (MBL), in addition to lactoferrin, lyzozyme, defensins, and secreted immunoglobulin A (IgA), all of which have host-protective functions (23). SPA and SPD bind to and opsonise a wide range of pathogens including viruses, bacteria, fungi, as well as allergens via their C-terminal carbohydrate recognition domains (23). Apart from being directly

microbicidal, surfactant proteins can interact with several receptors in order to influence cellular activity. SPA and SPD's N-terminal non-collagenous domains interact with a multipartite cell surface receptor complex that includes the complement fragment c1q receptor CD93, CD91, and calreticulin, inducing inflammatory mediator production, or by binding to signal inhibitory regulatory protein α (SIRP-α), with the opposite effect (24). By binding to numerous other receptors, the surfactant proteins also increase phagocytosis, bactericidal activity, and the production of inflammatory mediators by binding members of the Toll-like receptor (TLR) family (25, 26). Concurrently, MBL binding to conformationally-restricted sugar residues on pathogen surfaces permits both the activation of the complement protein cascade, which exerts both proinflammatory and directly bactericidal activities, and the activation of cells expressing complement receptors (27). Lactoferrin contributes to the alveolar defences by binding ferric (Fe^{3+}) ions with high affinity, thus denying potential pathogens this source of iron, and by exerting a direct bactericidal effect (28). Lysozyme is a potent hydrolytic enzyme which cleaves the β1-4 glycosidic bonds which are required for bacteria and fungi to maintain cell wall integrity (29). Combined with defensins that can permeabilize bacterial cell walls, and the adaptive immune system's secretory IgA (discussed later), these secreted factors provide a permanent barrier against pulmonary infection that exists even under homeostatic conditions, allowing the inactivation of many potential threats

without the need for the induction of potentially deleterious pulmonary inflammation.

Alveolar macrophages (AMs) have evolved in order to clear the debris created by the previously described alveolar defences, and to provide a permanent cellular host defence presence in the airspaces. AMs are mononuclear cells of hematopoietic origin and, if depleted, are re-populated via the migration of blood monocytes into lung tissue, where they differentiate first into lung tissue macrophages and then ultimately into AMs. (30). These cells are long-lived, however, and under homeostatic conditions persist for years with minimal turnover (31). AMs are responsible for ongoing surveillance, phagocytosis of invading particles, the production of cytokines and chemokines, along with a limited degree of antigen presentation to the adaptive immune system. To fulfil these functions, the AMs rely on an array of germ-line encoded pattern recognition receptors (PRRs). PRRs are limited in their diversity, and recognize and bind to pathogen-associated molecular patterns (PAMPs) that are evolutionarily conserved across a range of infectious agents. The toll-like receptors (TLRs) and the cytoplasmic caspase recruiting domain (CARD) helicases are well-characterized classes of innate PRRs (32, 33), along with many others including the Nod-like receptors and scavenger receptors. Together, these PRRs might play a critical role in heterologous infection because, between them, they can detect both viable and inactivated intra- and extracellular pathogens. TLRs are expressed both on the cell surface and in endosomes, and recognize a range of PAMPs

(reviewed in (34)). Upon binding, all of the TLRs can activate the nuclear factor (NF)-κB and activating protein (AP)-1 transcription factors, leading to the production of inflammatory cytokines including tumour necrosis factor (TNF)α, interleukin (IL)-1β and IL-6, and chemokines including macrophage inflammatory protein (MIP)-2/growth related oncogene (GRO)α/cystine-x-cystine chemokine ligand (CXCL)2 and IL-8/GROβ/CXCL8 (reviewed in(33)). At the same time, TLRs 3, 4, 7, 8, and 9 can activate interferon regulatory factor (IRF)3 and/or IRF7 to produce type-I interferons (IFNs). While TLRs detect extracellular and endosomal PAMPs, CARD helicases such as retinoic acid inducible gene (RIG)-I have evolved to recognize cytoplasmic ones. CARD helicases bind viral ribonucleic acid (RNA) in the cytoplasm and activate IRF3 and IRF7 to produce interferons, as well as NF-κB to produce inflammatory cytokines, but do so in a myeloid differentiation factor (MyD)88-independent manner, thus bypassing adaptor molecules such as IL-1 receptor-associated kinase (IRAK)-1 which is used as a regulator of the balance between inflammatory cytokines and interferons (34).

In addition to the production of inflammatory mediators that recruit immune cells to the lung, AMs also have their own intrinsic antimicrobial functions. Following PRR engagement, macrophages can phagocytose both opsonised- and non-opsonized bacteria, and use both free radicals and lysosme-phagosome fusion to kill the engulfed pathogens (35). During antiviral responses, these same cells secrete cytokines and chemokines

which recruit of antiviral effectors including natural killer (NK) cells, T-cells, and B-cells.

Non-classical immune cells in both the conducting airways and the alveoli also play a critical role in the host defence response. Epithelial cells are frequent targets for viral infection and bacterial adherence. Apart from their aforementioned role in mucocialliary clearance, they are equipped with many of the same PRRs as are macrophages and are potent producers of type I IFNs, which contribute to the induction of an antiviral state in the lungs (36). Beyond that role, epithelial cells also have a role in host defence and in disease pathogenesis via the induction of apoptosis once they become infected (37).

1.1.3: Recruited innate defences

As a result of inflammatory cytokine and chemokine production, immune cells are recruited chemotactically into the sites of infection. Neutrophils (large, poymorphonuclear phagocytes) are typically the first such cells to arrive in the tissue. To begin the process of inflammatory cell recruitment, locally-produced factors such as TNF-α, IL-6, and IL-1 are released by host cells in order to activate the vascular endothelium. These molecules are released particularly from AMs and epithelial cells in response to ligation of their PRRs, and act to increase the calibre of the local capillaries and the expression of selectins and Ig superfamily proteins that bind to receptors on passing leukocytes. Like all leukocytes, neutrophils are then

recruited from the blood into the tissue through a well-understood, four-step process. In the first step, rolling adhesion, E-selectin on the surface of vascular endothelial cells interacts loosely with S-Le^x on neutrophils, causing them to "tumble" along the vascular wall. Subsequent "tight binding" is mediated by firm interactions between integrins such as leukocyte functional antigen 1 (LFA-1) on leukocytes and intracellular adhesion molecule 1 (ICAM-1) on vascular endothelial cells. Next, periplasmic spaces are opened between adjacent endothelial cells to allow the third phase, diapedesis, during which cells actually leave the vasculature and enter the tissue. Finally, cells migrate along chemokine gradients established by cells in the tissue to the site of infection, where they can exert their effector functions (22, 38). In the fragile pulmonary capillaries, an additional mechanism of neutrophil recruitment seems to play an important role, in which stiffening of the vasculature and the neutrophils themselves traps the neutrophils, holding them in place until they can migrate into the lumen of the lung (39).

Once in the tissue, neutrophils have potent antibacterial functions. Firstly, neutrophils are highly phagocytic, rapidly fuse the contents of their phagosomes with lysosomes, and produce oxygen radicals and antimicrobial peptides to kill the engulfed invaders. Furthermore, neutrophils contain toxic granules that include myeloperoxidase (MPO), enzymes, and defensins, which directly kill invaders, and can either exocytose these granules or fuse them with phagosomes (40). Neutrophils are short-lived and undergo

apoptosis shortly after they phagocytose a target, at which point they are taken up by AMs through the process of efferocytosis (41).

1.1.4: Adaptive immunity

There are examples of invertebrate species such as bivalves, which live for decades in pathogen-rich environments, yet rely exclusively on innate immune mechanisms to do so (42). Jawed vertebrates have evolved an additional means of host defence however; although distinct from innate immunity in a number of ways, the hallmark feature of adaptive immunity is the ability to gain experience from one pathogen encounter and respond more effectively to a subsequent encounter with the same agent (43). Adaptive immune responses are energy-intensive and when dysregulated can become deleterious to the host however, and are thus not initiated for every encounter with a potentially pathogenic organism. In this respect, the innate immune system plays a key "gatekeeper" role, because it, and more specifically the antigen presenting cells (APCs) bring about the activation of the adaptive arm of immunity. APCs are able to detect the presence of foreign invaders through their PRRs, then migrate to the lymph node (LN) where they come into intimate contact with T-cells. This critical step is necessitated by the fact that T-cells cannot recognize foreign antigens in their native form, and must instead recognize short, linear peptides which result from the hydrolysis of "non-self" proteins such as those produced by invading pathogens. Moreover, these peptides must be presented to T-cells in the context of the major histocompatibility (MHC) protein on the surface of

an APC. All nucleated cells express MHC I which presents intracellular antigens, such as those derived from viral infections, and can present antigens to activated T-cells in the periphery, whereas macrophages, dendritic cells (DCs), and B-cells are the cells classically thought of as "professional" APCs, because they can present antigens via MHC I and II, not only in the periphery but also in the lymph node, where they prime naive T-cells, resulting in the induction of adaptive immunity.

AMs do migrate to lymph nodes in some models of pulmonary infection (44), but their utility as antigen presenting cells for naive T-cells is dubious , since they are poor inducers of T-cell responses (45-47). AMs are phenotypically similar to immature DCs, having low-level expression of MHC and of the B7 family co-stimulatory molecules necessary for T-cell priming, but are identified by the expression of CD11c and F4/80 – a phenotype not shared with classical, systemic macrophages (48, 49). Instead, the AM system seems dedicated to avoiding the induction of immune responses by preventing the activation of classical antigen APCs. The AM system is believed to be capable of phagocytosing and/or killing approximately $1x10^9$ pulmonary bacteria before any surplus becomes available to populations of epithelial and alveolar DCs which bear the principal responsibility for priming the adaptive immune response (50).

DCs are mononuclear phagocytes of similar lineage to macrophages, but are specialized to engulf small particles, process any antigens contained within their intra- and extra-cellular environment and then present portions

of these to T-cells. Their ability to present not only endogenous antigens (those within their cell margins) such as viruses with which they have been infected, but also exogenous antigens such as extracellular bacteria, and debris, and most importantly their ability to prime T-cell responses in the LNmarks them as professional APCs. Upon ligation of their PRRs, DCs rapidly undergo a process of maturation, in which they cease to uptake new antigens, downregulate their expression of tissue-specific adhesion markers, and induce the expression of lymphatic-specific adhesins, MHC genes, and costimulatory molecules (51).

1.1.4.1: Cellular immunity

T-cells bear the principal responsibility for mediating the cellular component of adaptive immunity. T-cell precursors originate in the bone marrow from the common lymphoid progenitor, but at an early stage of development, they migrate to the thymus where they mature into functional T-cells. Following entry into the thymus, T-cell precursors begin expressing a set of deoxyribonucleic acid (DNA) modification enzymes collectively referred to as the variable-diversity-joiner (V(D)J) recombinase. The V(D)J recombinase facilitates the generation of approximately $1x10^{18}$ unique T-cell receptor (TCR) specificities by randomly fusing various combinations of the V, D, and J gene segments which make up the variable (antigen binding) region of the TCR. This process generates a host's remarkably diverse TCR repertoire without the need to encode $1x10^{18}$ different receptors in the germ line. Due to the random nature of this somatic gene rearrangement,

numerous non-productive and self-reactive TCRs are generated, and T-cells pass through a stringent selection process concurrently with their V(D)J recombination. T-cells undergo positive selection, in which those cells which do not recognize peptides in the context of a host's own MHC are allowed to die, and negative selection, in which those cells which recognize a host's own proteins are killed. Respectively, these selection steps prevent useless and autoreactive T-cells from entering the circulation. Early studies of immunology held that T-cells develop into helper T-cells ("T_H" cells), which express the CD4 co-receptor and are specialized for orchestrating immune responses via the production of immunomodulatory cytokines, or cytotoxic ("killer" T-cells), which express the CD8 co-receptor and are specialized for directly killing infected or otherwise abnormal cells (22). More recently however, it has become clear that this is a gross understatement of the number of T-cell subset in circulation.

In humans and murine models, cells which express a heterodimeric $\alpha\beta$ TCR are in the majority, however a subset of cells instead generate $\gamma\delta$ TCRs by using a more restricted set of V(D)J genes, and home preferentially to mucosal sites . Additional heterogeneity in T-cells is generated after positive and negative selection. Firstly, several subsets of "regulatory" cells, once referred to as "suppressor" cells arises. These cells may be identified phenotypically by their expression of the transcription factor Forkhead box P3 (FoxP3) and their ability to elaborate immunoregulatory cytokines including TGFβ and IL-10, or functionally by their ability to modulate and in many

cases attenuate T-cell responses both *in vivo* and *in vitro*. Indeed, the importance of these cells is apparent because mice genetically deficient in FoxP3, succumb to lethal inflammatory immunopathology shortly after birth (52). Secondly, multiple subsets of T_H cells exist, including T_H1 cells, which preferentially promote cellular immunity via the production of cytokines including IFNγ and TNFα, T_H2 cells, which promote humoral immunity via the production of those including IL-4, 5, and -13, and T_H17 cells, which produce the potent neutrophilia-promoting cytokine IL-17 (22).

Once a T-cell has expressed a functional TCR, a CD4 or CD8 co-receptor, and undergone selection, it is released into the periphery, where it lives as a mature, naive T-cell. Naive T-cells migrate continuously through the LNs until they encounter an APC presenting the peptide for which its TCR is specific. T-cells undergo prolonged contact with these APCs, and initiate a programme of cell division and differentiation, at the end of which they are able to migrate to the periphery where they can participate locally in immune responses, or to remain in the lymph node where they may provide the help necessary to initiate humoral responses (53). Following the execution of their effector functions, T-cells enter a well-defined and pre-programmed phase of contraction, in which the majority of T-cells undergo apoptosis, with the surviving cells forming a relatively stable population of long-lived memory cells. In this memory phase, T cells are commonly thought to fall into two broad categories, consisting of effector-memory T-cells which are excluded from lymph nodes, have a limited ability to self-renew, and are principally

responsible for early, rapid defence upon antigen re-encounter, and central memory cells which are able to migrate through LNs, and have the capacity for self-renewal (54).

1.1.4.2: Humoral immunity

The humoral arm of the adaptive immune system relies on B-cells for the production of highly-specific antibodies which can bind to pathogens or be used to guide cellular immune responses. Like T-cells, B-cell precursors originate in the bone marrow; in contrast however, B-cells undergo maturation in the bone marrow in mammals, or in the bursa of Fabricius in aves, i.e., sites from which B-cells derive their name. In a manner similar to T-cells, B-cells undergo V(D)J recombination in order to generate highly specific lymphocyte antigen receptors referred to as B-cell receptors (BCRs) when bound to the cell surface, or as Ig (antibodies) when secreted. In similar fashion to TCRs, BCRs have a distal variable region which mediates antigen binding, and a long, proximal constant domain which mediates the BCR's binding to receptors and cells. Following development and maturation, B-cells undergo a process of selection, by which autoreactive cells are eliminated from the repertoire, and are then released into the circulation as mature, naive IgM^+, IgD^+ B-cells. IgM and IgD are the proteins which result from splice variants of a single primary RNA transcript, and are members of a family of immunoglobulin isotypes that includes IgA, IgD, IgE, IgG, and IgM. Each of these isotypes has a different constant domain and, thus, different functional properties. IgA antibodies are frequently produced

at mucosal sites, usually exist in dimeric form, and are involved in preventing pathogen attachment and in pathogen neutralization. IgE antibodies are found typically bound to mast cells and are involved in allergic sensitization. IgG antibodies are found predominantly in the blood and tissues, but are found at mucosal surfaces due to local synthesis and/or transudation from sera, and mediate a variety of functions including neutralization, complement fixation, and opsonisation. IgM, and its cell-associated relative IgD, are the first antibodies produced following infection and typically low antigen-binding affinity, but are particularly efficient at activating complement (22).

Following activation, T-cells can activate B-cells via a cognate interaction, providing stimulatory signals, along with the cytokines necessary to instruct the appropriate isotype switching of a given B-cell. The B-cell then undergoes a program of intense proliferation, affinity maturation to increase the avidity of its BCR for a given target antigen, and ultimately differentiation into a plasma cell which constitutively secretes high levels of immunoglobulin, or a memory cell which can quickly respond following re-exposure to an antigen (22).

1.1.5: Immune regulation in the lungs

Although direct viral or bacterial damage to respiratory epithelial cells presents a hazard to the lungs' critical gas exchange ability, the threat posed by immunopathology is at least as great. In order to prevent damage to the lungs, several overlapping systems conspire to prevent or attenuate immune

responses in the lungs. Firstly, AMs, the principal alveolar sentinels, are poor inducers of adaptive immune responses, and can avoid the induction of T-cell immunity via inhibitory effects on the DCs that prime T-cell responses, or can directly suppress established T-cell responses in a paracrine manner via the production of IL-10, prostaglandins, and transforming growth factor (TGF)-β (55-57) or through direct contact interactions with inhibitory receptors on T-cells (58). Secondly, the expression of CD200 on the airway epithelium provides a strong inhibitory signal to AMs, promoting their immunoregulatory function, especially in the context of infection (59). As a corollary to this, AMs have high levels of CD200R expression relative to systemic macrophages, which might partially account for their notably hyporesponsive phenotype (59). In addition to AMs, DCs in the airway produce high levels of IL-10 under homeostatic conditions, but IL-10 levels are dramatically increased following infection, which dampens immune responses even further (60).

1.2: Threats to pulmonary host defence

1.2.1: Pulmonary viral infection

The lungs are a frequent target for viral infection, with respiratory epithelial cells representing the most common targets for infection. The most commonly experienced respiratory viral infections in man include those with rhinovirus (RV), respiratory syncytial virus (RSV), and influenza virus (61). Upper respiratory tract infections with RV and RSV commonly lead to symptoms of the common cold, including the hyperproduction of mucus, local

pain, sneezing, and coughing (62). Although these can lead to severe disease in individuals with co-morbidities such as asthma or COPD, these infections are not typically life-threatening in a healthy individual (63). The *Orthomyxovirus* influenza on the other hand is the most important respiratory virus in the world today, causing approximately 1 billion infections, 3-5 million cases of serious illness and 500,000 deaths in an average non-pandemic year. Moreover, during pandemics, it has eclipsed all other causes of death combined. The 1918 influenza virus pandemic killed 40 million people in just one year, the single greatest loss of life in human history, and depressed worldwide population growth for 10 years (64, 65). Influenza virus infects the upper respiratory tract, but can also penetrate to the lower airways, leadings to pulmonary inflammation, mucus production, and concomitant respiratory distress. As a result, influenza virus-induced pneumonia is the leading infectious cause of death in Canada, and influenza infection causes significant morbidity and mortality even in populations which have vaccination programs in place (66-69). Influenza's ability to survive and cause disease in the face of vaccination programs is due in part to the range of serotypes circulating in a host population, and in part to the existence of diverse animal reservoirs including aves, sus, equus, and numerous sea mammals (70).

The influenza virus genome is elegantly organized to support the existence of multiple serotypes, and to support the periodic generation of pandemic strains through the use of its animal reservoirs. The genome of

influenza viruses A and B comprises eight single (-) stranded RNA segments, while that of 'C' class viruses comprises only 7. Alternative reading frames and RNA splicing permit the generation of up to 11 different proteins from these RNA segments (71). Antigenic variations in matrix protein (M), and nucleoprotein (NP) composition divide influenza viruses into three genera: influenza virus A, B, and C. Influenza A viruses are further divided into serotypes on the basis of their hemagglutinin (HA) and neuraminidase (NA) glycoproteins. Fifteen HA and nine NA serotypes have been identified (67). The influenza virus is constantly undergoing "antigenic drift" in which accumulated mutations to the HA and NA genes result in the generation of subtypes to which there is little or no pre-existing immunity in the population. Thus, vaccines used in prior years have little effect on immunity to currently circulating influenza virus strains. Such mutations are extremely unlikely to result in radical changes to virulence. The development of a pandemic strain is generally thought to be the result of "antigenic shift." In a case of antigenic shift, re-assortment between unrelated strains occurs after an organism is simultaneously infected with more than one subtype of the virus. This process is facilitated by the segmented nature of the viral genome which allows easy recombination by exchanging RNA segments (72). Current fears surrounding avian influenza H5N1 are due to the possibility that a highly virulent avian virus which is incapable of human-to-human transmission will exchange genes with a less virulent but easily transmissible human virus to yield a pandemic strain. Although vaccination, surveillance,

and treatment strategies appear to have contained the threat so far, a small but alarming number of clustered infections recently detected within Vietnamese families may be the first signs of human-to-human transmissibility of a highly pathogenic avian influenza virus (73). At the same time, the H1N1 "swine" influenza virus pandemic (with A/California/04/2009 and subsequent related serotypes) has underscored the difficulty of containing an outbreak once it has established itself (74).

Although influenza virus is currently believed to be the leading respiratory viral threat to human health and is the subject of intense study around the globe, recently there has been an increasing awareness of a gap in our understanding not only of influenza virus, but infectious diseases in general. To date, the overwhelming majority of studies have examined a single disease-causing organism and its interaction with a host. Although important for understanding disease, studies premised on such approaches fail to take into consideration the fact that hosts can be, and frequently are, infected with more than one pathogen, either concurrently or consecutively. These "co-" or "heterologous" infections are common in man, and are also important modifiers of morbidity and mortality.

1.2.2 Heterologous pulmonary infection

It has long been acknowledged that a substantial fraction of influenza-virus related death and disability results not exclusively from primary viral disease, but from secondary infection with bacteria unrelated

("heterologous") to the virus. In fact, recent analyses point to secondary bacterial pneumonia, not primary viral disease, as the predominant cause of death in the three 20th century influenza pandemics (75), and suggests that the remarkable lethality of the 1918 influenza strain may have been due to its ability to instigate a secondary bacterial pneumonia (76). Deaths to secondary bacterial infection commonly result from immunopathology, rather than bacterial infection *per se,* and once initiated, immunopathology in the form of sepsis and septic shock can progress independently of the bacterial burden. Specifically, even if hosts suffering from heterologous infections are treated with sterilizing antibiotics, they still frequently succumb to pathologic inflammation (77-79). Several clinical trials using corticosteroids (80), granulocyte colony stimulating factor (G-CSF) (81), hemofiltration (82), or neutralizing antibodies against endotoxin or TNF-α (83) have largely failed to prevent host progression to septic shock, failed to reduce mortality, and raised concerns about the risks of non-specifically suppressing an infected host's immune defences.

A number of mechanisms have been proposed through which viral infection predisposes the host to bacterial infection. Viruses can act first by lysing epithelial cells and disrupting the respiratory epithelium, thus exposing the basement membrane and permitting bacterial attachment during influenza virus epidemics (84-88) and in experimental models (89, 90). In epithelial cells that escape direct lysis, influenza virus and other viruses can then increase bacterial adherence by upregulating the expression of

receptors to which bacteria can bind (89). Viral infection can also impair ciliary function, further reducing mucocilliary clearance of bacteria in the airway (91, 92). Additionally, viral insult can compromise innate antibacterial immunity by inducing granulocyte apoptosis through overproduction of type I interferons (IFNs) (93), impairing macrophage responsiveness to bacterial TLR ligands by reducing NF-κB activity (94), and reducing macrophage antibacterial function (92, 95). Activation of the adaptive antiviral system can furthermore compromise host defence against subsequent bacterial challenge (96, 97). Whether the life-threatening bacterial pneumonia seen in heterologously-infected individuals simply represents an appropriate immune response to a magnified bacterial burden, or the results of a fundamental alteration in immunity brought on by two divergent immune insults, remains to be elucidated.

1.2.3: Cigarette smoke exposure

In a similar fashion to sequential pulmonary infections, cigarette smoke exposure represents not only a key threat to human health, but also a complex challenge to the immune system. Smoking causes over 4.8 million premature deaths per year globally (5) and is the only leading cause of death that is on the rise (6). In the United States alone, cigarette smoking (irrespective other forms of tobacco) causes over 438,000 deaths per year, while smoking-attributable economic losses total more than US $92 billion per year (98).

Smoking is widely understood to be the dominant and nearly exclusive etiologic factor for diseases including lung, tracheal, bronchial, and bladder cancers, and COPD (8). In fact, the global burden of these diseases can almost exclusively be attributed to tobacco smoke exposure, marking them as "smokers' diseases" (8, 9). Furthermore, smoking has been associated with significantly increased risks of cardiovascular disease, periodontitis, respiratory tract infections, Crohn's disease, and rheumatoid arthritis (9, 11, 12, 99). Despite these and other health consequences, over 1.1 billion people continue to smoke, representing one-sixth of the global population, and one-third of the population over the age of 15 (14). Although smoking prevalence in the developed world has fallen significantly in the last 40 years, an estimated 930 million of the world's 1.1 billion smokers live in developing countries, where smoking prevalence continues to rise, and is reaching epidemic proportions (14, 100). Moreover, increasing numbers of women are beginning to smoke, even as male smoking begins to plateau (101). Thus, the morbidity and mortality attributed to smoking is expected to rise, particularly in the developing world, until at least 2030 (102).

The burden of tobacco-related disease is staggering; however, it remains a fact that not all smokers will develop a smoking-related disease. Since non-smokers typically do not develop smoking related diseases, it seems most plausible that smoking is necessary but not sufficient for the development of diseases such as COPD. It is currently thought to be most likely that COPD development requires smoke exposure in a genetically-

susceptible host, coupled with other factors such as pulmonary infections (103). In these cases, the immune system must not only face a pulmonary infection, but it must do so while simultaneously coping with the ill effects of cigarette smoke exposure.

Cigarette smoke is an extremely multifarious mixture, containing over 4000 chemicals, many of which have toxic, carcinogenic, and other negative effects on biological systems (104). Although the direct, damaging effects of these chemicals on host cells and tissues are major factors in the development of COPD, cancer, and other diseases, it has been proposed that many of smoke's deleterious health effects are caused, at least in part, by smoke's effect on the immune system (reviewed in (7, 105)). For example, carcinogens contained within smoke can cause lung cancer, but smoking's deleterious effects on immune recognition and clearance of those cancerous cells might be similarly important. In parallel, it is difficult to determine if smoke's direct, toxic effects on pulmonary cells lead to airway enlargement and emphysema, or if reduced immune function allows infections that would otherwise remain innocuous, to progress into pathological conditions that destroy lung tissue. In practice, both direct and immune-mediated effects are likely to prove critical to smoke's health effects.

1.3: Animal models of pulmonary disease

Constructing models of human disease is not a simple task, and it is critically important that the results obtained in any model be interpreted in light of the known strengths and limitations of that system.

1.3.1: Pulmonary infection

Research into the impacts of bacterial superinfections on influenza virus responses have been hampered by the lack of relevant model systems. Although many clinical isolates of bacteria are available, when inoculated into animals, often these are found to be non-infectious. Conversely, many animal pathogens do not cause appreciable disease in man and are thus ill-suited for modeling human healthcare problems. *Bordetella* bacteria are a convenient exception to the rule, in that they infect both mice and humans, and cause an identifiable pathology in both cases (106-108). Moreover, influenza virus-*Bordetella* bacterial co-infections have been reported (109). Thus, the *Bordetellae* are ideally suited to serve in experimental models of pulmonary infectious disease.

The species of the *Bordetella* genus are small, Gram-negative beta proteobacterial aerobes (110). Of the eight members in this genus, three are of particular interest in terms of mammalian respiratory infection: *B. pertussis, B. parapertussis, and B. bronchiseptica.* While *B. bronchiseptica* infects a wide range of mammals, *B. pertussis* and *B. parapertussis* principally infect the human respiratory tract during childhood, where they cause disease characterized by a "whooping" cough. Whooping cough occurs approximately 1 week after a catarrhal phase of mild, dry cough. During the

ensuing 2-6 week paroxysmal phase, repeated bouts of 5-10 forceful coughs occur, followed by a characteristic "whoop" as the patient attempts to rapidly inhale. This phase gives whooping cough both its name and its health effects such as hypoxia, pneumonia, difficulty eating and pulmonary hypertension, (111), and is followed by a convalescent phase of approximately 2 weeks, during which the symptoms subside (112). Since *B. pertussis* and *B. parapertussis* are indistinguishable by common microbiological culture and serology tests, their relative contributions to the whooping cough burden have not yet been definitively established. It is known that they are both important participants in this disease, as determined by polymerase chain reaction (PCR) analysis. Although thought of as a childhood problem, *Bordetella* outbreaks in adults and particularly the elderly have been reported with increasing frequency in recent years (113-115). Vaccination has been part of the routine childhood vaccination strategy in the developed world for many years as a component of the diphtheria, tetanus, pertussis (DTP) vaccine, but estimates of vaccination efficacy range from 60-90%, and over 50% of infections occur in previously vaccinated individuals. *B. parapertussis* in particular seems to be problematic within the vaccinated population, although the mechanism underlying this phenomenon is presently unknown (116-119).

1.3.2: Cigarette smoke exposure

The majority of the studies assessing immune function in smokers or in animal models of smoking have been observational and have not provided

detailed cellular or molecular mechanisms to explain the immune impairments seen in smokers. Moreover, many of the studies that are of a more mechanistic nature have been conducted from a toxicological standpoint and have not used functional immune data, such as cytokine secretion, immunoglobulin production, phagocytic ability, or protection. Since the B-cells of the adaptive immune system have a pivotal role in respiratory mucosal immunity, and T-cells are important in orchestrating mucosal immune responses, these cells are fascinating targets for smoking-related research.

Exposure to cigarette smoke or its components has previously been shown to suppress responses to both T-independent and T-dependent B-cell antigens in both animal models and in man (120, 121). It has been postulated that this phenomenon might be mediated by nicotine, one of the most studied compounds contained within tobacco smoke (122). Lymphocytes expressing the nicotinic acetylcholine receptor (nAChR) can bind free nicotine, including that derived from cigarette smoke, and in response activate downstream signal transduction cascades. Constant exposure of a host to nicotine is proposed to constitutively activate protein tyrosine kinases in splenocytes, leading to concomitant phospholipase Cγ1 activation, and subsequently to depletion of the IP_3-mediated Ca^{2+} stores that the nAChR must share with other receptors. It is believed that the exhaustion of these intracellular Ca^{2+} stores upon which both the T-cell receptor (TCR) and B-cell receptor (BCR) rely is what renders T- and B-cells

unresponsive to stimulation in some experimental models (123). Evidence to support this as a plausible mechanism for interference with immune cell activation has been provided by a recent finding that murine B-cells express the nAChR, and that B-cells from mice genetically deficient in various nAChR subunits ("knockout" mice) mount exaggerated responses to anti-CD40 immunoglobulin treatment (124). Unfortunately, these mechanistic studies do not correlate with findings in human smokers, and might represent either fundamental differences between murine and human immunology, or represent toxic levels of smoke exposure, as opposed to those commonly seen in humans (125).

1.4: Summary and hypotheses

The single-agent:single-host models commonly used in experimental research are important for elucidating fundamental features of the host defence response. However, these models do not account for the fact that hosts are frequently exposed to multiple insults (simultaneously and sequentially), and that one exposure or one immune response can profoundly effect on the way a host responds to a second challenge. Thus, the focus of this thesis was on the development of an advanced understanding of host defence responses against such complex challenges. To that end, five specific objectives were pursued:

1) To develop and characterize a model heterologous pulmonary infection;

2) To determine the impact of a viral or bacterial challenge on the host defence response to a heterologous bacterial or viral challenge;
3) To determine the impact of a viral or bacterial infection on alveolar macrophage responses to heterologous challenges;
4) To develop and characterize a model of cigarette smoke exposure's impact on T- and B-cells.
5) To determine the impact of moderate smoke exposure on lymphocyte responses.

These objectives were completed and a more thorough understanding of the host defence response against complex infectious and non-infectious environmental challenges was developed. With respect to heterologous infection, MIP-2 was identified as a potent therapeutic target for the treatment of bacterially-complicated influenza infection. Specifically, it was established that MIP-2 driven pulmonary inflammation, rather than pathogen burden is the threat to life in bacterial superinfection of influenza virus. Additionally, a potential regulatory function for the AM was elucidated in such infections, and it was demonstrated that this regulatory phenotype can persist for a prolonged period of time. With regard to cigarette smoke-related disease, it was demonstrated that in both mice and humans, cigarette smoke does not directly impair adaptive immune cells, and likely exerts its deleterious effects on adaptive immunity by impairing the underpinning innate immune mechanisms. Collectively, these experiments demonstrated the importance of the innate immune system in determining the outcome of

subsequent adaptive immune responses, but also the health and survival of the host.

Chapter 2: Methods and Materials

2.1: Polymicrobial infectious disease experiments

2.1.1: Animals: Female C57BL/6 mice (6–8 wk old) were purchased from Charles River Laboratories (Montreal, PQ, Canada) and kept in specific pathogen free conditions on a 12 h light-dark cycle with food and water provided *ad libitum*. Cages, food, and bedding were autoclaved. Animal were handled in class II biosafety cabinets by gloved, gowned, and masked staff. Experiments were approved by the McMaster University Animal Research Ethics Board.

2.1.2: Infectious agents: *B. parapertussis* strain 12822 (ATCC, Manassas, Virginia) has previously been genetically sequenced (126), studied microbiologically (106), and studied in the murine respiratory tract (127). Bacteria were maintained on Bordet-Gengou agar (Difco, Oakville, Ontario, Canada) containing 15% defibrinated ovine blood (Lampire Biological Laboratories, Pipersville, PA). Liquid culture bacteria were grown at 37°C overnight on a shaking incubator in Stainer-Scholte broth (128).

The H1N1 influenza A (A/FM/1/47) virus used in this study was a genetically sequenced, plaque-purified preparation that was biologically characterized with respect to mouse lung infections (129, 130).

At the time of infection, mice were anesthetised with Isoflurane® (Pharmaceutical Partners of Canada Inc., Richmond Hill, ON), and then given 2.5×10^5 pfu of influenza virus in 35 μL of phosphate-buffered saline (PBS), or 5×10^5 cfu of log-phase *B. parapertussis* in 35μl of PBS intranasally (i.n.).

Mice were individually weighed before infection and throughout the course of experimentation, and health status was scored by a blinded investigator as previously reported (131).

2.1.3: Tissue and cell collection and isolation: At sacrifice, blood was collected by retro-orbital bleeding using heparin-coated capillary tubes (Fisher Scientific, Pittsburgh, PA). Total leukocytes were counted after lysing erythrocytes, and cell smears were prepared and stained with Hema 3 (Biochemical Sciences Inc., Swedesboro, New Jersey, USA) for differential cell determination by enumerating a minimum of 300 cells per slide. To isolate sera, animals were bled retro-orbitally with non-heparinized Pasteur pipets, and sera were obtained by incubating whole blood for 30 min at 37°C, followed by centrifugation. Samples were stored at -20°C until assayed.

The lungs were removed, tracheas were cannulated, and broncho-alveolar lavage (BAL) was obtained. The lungs were lavaged with PBS (250 then 200 μL for determination of BAL cellular inflammation and inflammatory mediator expression, or 500 then 5x1000μL for collection of AMs for culture). After each instilment, the fluid was collected and pooled. Total cell counts were then determined using a haemocytometer. In accordance with previous publications, cell numbers are presented in cells/mL in order to minimize the impact of inter-animal differences in volume of lavage fluid covered. BAL supernatants were stored at -20°C for later analyses of inflammatory mediators by enzyme-linked immunosorbent assay (ELISA). Centrifugal cell smears for differential cell counts were prepared by resuspending cell pellets

in PBS, followed by cytocentrifugation onto plain glass slides in a Cytospin centrifuge (Shandon, Thermo scientific, Burlington, ON) at 10x*g* for 2 min. Cells were stained by Hema 3 (Biochemical Sciences, Swedesboro, NJ), and differential cell enumerations were performed by counting at least 300 cells per preparation. Standard hemacytological criteria were used to classify mononuclear cells, neutrophils, and eosinophils. For histology, the lung lobes were inflated with 10% formalin under gravity pressure equivalent to 20 cm H_2O, embedded in paraffin, and 3-µm-thick sections were prepared and stained with hematoxylin and eosin (H&E). Images were collected with OpenLab software (version 3.0.3; Improvision, Guelph, ON, Canada) via a Leica camera and microscope (Leica Microsystems, Richmond Hill, ON, Canada).

2.1.4: Bacterial burdens and viral titres: For determination of lung bacterial burdens and viral titres, lung lobes were collected in 1mL of PBS and then homogenized with a Polytron PT 1200C (Kinematica, Littau-Lucerne, Switzerland). 25 µL of serially-diluted fresh homogenates in PBS were plated onto Bordet Gengou blood agar plates and grown for 3 days at 37°C to enumerate viable bacteria. Homogenates were stored at -80°C prior to determination of viral titres on Madin-Darby canine kidney (MDCK) cell monolayers. MDCK cells grown to confluence in 6-well tissue culture plates were rinsed twice with warm PBS to remove sera, and 200 µl of serially-diluted samples were added. Plates were rocked and incubated at 37°C for 30 minutes, after which 2 mL of 0.65% agarose (BioShop Canada,

Burlington, ON, Canada) in minimum essential medium (MEM) supplemented with 1% L-glutamine, 1% penicillin and streptomycin, and 1µg/mL trypsin were added to each well. Once the agarose solidified, the plates were incubated at 37ºC for 2 days. Cells were fixed using Carnoy's fixative and plaques were enumerated after Giemsa staining.

2.1.5: Vesicular stomatitis virus (VSV) plaque reduction assay: Type I IFN bioactivity was measured in BAL samples by plaque reduction assay as previously described (130). This assay has the advantage of detecting biologically active interferon, as opposed to total interferon protein levels, as would be assessed by ELISA. Briefly, BAL samples were assessed for their ability to protect primary IFN regulatory factor-3 (IRF)-deficient mouse embryonic fibroblasts (MEFs) (kindly provided by Dr. Karen Mossman, McMaster University) from infection with a VSV expressing green fluorescent protein (GFP) under an endogenous viral promoter (VSV-GFP, kindly provided by Dr. Brian Lichty, McMaster University). The replication efficiency of VSV is decreased, as type I IFN present in BAL is able to produce an antiviral state in MEFs. IRF-3-deficient MEFs are incapable of producing IFN; however, they are capable of responding to exogenous interferon to produce an antiviral state (132).

Cells were removed from BAL samples by centrifugation and monolayers of MEFs were incubated with serial dilutions of supernatants for 24 hours in 24 well plates. Subsequently, supernatants were removed and MEFs were infected with 4×10^3 pfu of VSV-GFP in serum free α-MEM. Viral

inocula were replaced with Dulbecco's modified Eagle's Medium (DMEM) containing 1% methylcellulose following 40 minutes of incubation at 37°C. GFP fluorescence intensity was measured 24 hours later on a Typhoon Trio (GE Healthcare, Piscataway, NJ) imager and quantified using ImageQuant™TL (GE Healthcare) software.

2.1.6: Flow Cytometry: Lungs were cut into ~2 mm pieces, shaken for 1 h at 37°C in 150 U/mL collagenase III (Gibco/Invitrogen, Burlington, ON) in Hanks' balanced salt solution (HBSS), pressed through nylon mesh, erythrocytes were lysed in hypotonic ACK lysis buffer (0.5M NH_4Cl, 10 mM $KHCO_3$, 0.1nM disodium ethylenediaminetetraacetic acid (Na_2edta), pH 7.2–7.4), washed twice in HBSS and enumerated using a haemocytometer.

$2x10^6$ cells were plated in 96-well, round-bottom plates, and non-specific FcR-mediated antibody binding was inhibited by incubating the cells for 15 minutes on ice with 50 μl of anti-CD16/CD32 antibodies (purified, clone 93, eBiosciences, SanDiego, CA). Cells were then stained for 1h at room temperature with a Phycoerythrin (PE)-conjugated $H2^{Db}$ tetramer loaded with influenza virus A/FM/1/47 $NP_{366-374}$ (Baylor College of Medicine protein core lab, Houston, TX). Cells were washed and then resuspended in the staining cocktail for 30 min on ice. Antibodies used in this study include anti-CD11c (Fluorescein isothiocyanate (FITC), HL3, BD Biosciences), anti-CD11b (PE, M1/70, eBiosciences), anti-CD4 (PE-610, RM4-5, Invitrogen), anti-CD69 (PerCP-Cy5.5, H1.2F3, BD), anti-NK1.1 (PE-Cy7, PK136, eBiosciences), anti-MHC II (APC, M5/114.15.2, eBiosciences), anti-Gr-1

(Alexa Fluor 700, RB6-8C5, eBiosciences), anti-CD45R (APC-Alexa Fluor 750, RA3-6B2, eBiosciences), anti-CD3 (Pacific Blue, eBio500A2, eBiosciences), and anti-CD8 (Pacific Orange, 5H10, Invitrogen). For flow cytometric determination of apoptosis, cells were further stained with biotinylated Annexin-V (BD) and streptavidin-Qdot800 (Invitrogen) and 7-aminoactinomycin D (7AAD) (BD), or with the *in situ* cell death detection kit according to the manufacturer's protocol (Roche, Laval, QC). Cells were washed, and $3x10^4$–$3x10^5$ forwardscatter/sidescatter (FSC/SSC)-gated events were collected per sample on an LSRII flow cytometer for flow cytometric analyses, or a FACSVantage digital cell sorter for cytochemistry. Data were analysed using FlowJo software (Tree Star, Ashland, OR).

2.1.7: Myeloperoxidase assay: Myeloperoxidase (MPO) was measured as described by Drannik *et al.* (131) using a modification of the technique described by Diaz-Granados *et al.* (133). Briefly, 0.5mL of lung homogenate was mixed with 0.5mL of 5mg/mL hexadecyltrimethylammonium bromide (Sigma-Aldrich, Oakville, ON) in potassium phosphate buffer (pH 6.0) and centrifuged at 10,000xg for 2 minutes. 20 μl of supernatant was then added to 200μL of the reaction mixture (16.7 mg of *o*-dianisidine (Sigma-Aldrich), 90 mL of distilled H_2O, 10 mL of potassium-phosphate buffer, and 50 μl of 1% H_2O_2) in a 96 well plate. Optical densities (ODs) were obtained by spectrophotometer at 1 minute intervals at 450 nm. MPO activity was expressed as units/g lung tissue,

where one unit of MPO was defined as the amount of enzyme capable of degrading 1 μmol of H_2O_2 per minute at room temperature.

2.1.8: Lung and BAL cytokine measurements: Bead array-based analysis of cytokines in lung homogenates was performed by Rules Based Medicine with the Rodent multi-Analyte Profile (Austin, Texas, USA). The least detectable dose (LDD) was determined as the mean + 3 standard deviations of 20 blank readings. Results below the LDD were assigned a value of 0. Means of 4 independent mice in each treatment group and time were visualized in a "heat map" using Excel (Microsoft, Seattle, WA, USA). Individual scales were applied to account for the large numerical differences between the mediators. Levels of key cytokines were confirmed in the BAL and additional lung homogenate samples by DuoSet ELISAs (R&D Systems, Minneapolis, MN, USA) according to the manufacturer's specifications.

2.1.9: MIP-2 neutralization and CXCR2 blockade: Anti-MIP-2 and anti-CXCR-2 antibodies (kind gifts from Drs. Cory Hogaboam (University of Michigan Medical School) and Robert Strieter (University of Virginia) respectively) were generated by the respective collaborators as previously described (134), and have previously been characterized in models of infectious disease (135). Briefly, a rabbit was immunized with multiple intradermal injections of 20 pg of recombinant MIP-2 emulsified with complete Freund's adjuvant (CFA), then boosted 10 days later with the same antigen in incomplete Freund's adjuvant. Blood was collected from the rabbit 10 days later. Antiserum was isolated and heated for 30 minutes at 55°C to

inactivate complement proteins, then transferred from the collaborator's lab to McMaster University. Here, antiserum was passed over Protein A-Agarose columns (Pierce Biotechnology, Fischer Canada, Nepean, ON) and purified immunoglobulins were quantified by Bradford assay (Bio-Rad), both according to the manufacturer's instructions. To neutralize MIP-2 *in vivo*, mice were given an intraperitoneal (i.p.) administration of 25 μg of purified anti-MIP-2 immunoglobulin once daily, commencing 3 days post-*B. parapertussis* infection, and continuing throughout the period of observation.

Goat anti-murine CXCR2 serum was generated by Dr. Strieter's staff as described in Mehrad *et al.* (135). Briefly, goats were immunized at multiple intradermal sites with a carrier-free peptide encompassing the ligand-binding domain of the murine CXCR2 (Met-Gly-Glu-Phe-Lys-Val-Asp-Lys-Phe-Asn-Ile-Glu-Asp-Phe-Phe-Ser-Gly) in CFA, as described in (136). To block CXCR2 ligand binding, 0.5mL of anti-CXCR2 immune serum was administered i.p., on the same schedule as that for anti-MIP-2. Control mice were given a 0.5mL daily i.p. administration of normal goat serum.

2.1.10: Detection of pathogen-specific antibodies by ELISA: Influenza virus- and *B. parapertussis*-specific antibodies were detected in the BAL or sera using a minor modification of the procedure previously described (130). Briefly, MaxiSorp plates (Nalge NUNC International, USA) were coated overnight at 4°C with a lysate from influenza virus-infected Henrietta Lacks (HeLa) cells, or with a lysate from log-phase growth *B. parapertussis* bacteria. Coated wells were blocked with 1% casein in PBS for 2 h at room

temperature. After washing, sera and BAL samples, serially diluted in PBS, were incubated overnight at 4°C, washed, and developed with biotin-labelled, anti-mouse IgG or IgA (Southern Biotechnology Associates, Birmingham, AL), respectively. Plates were washed and incubated with alkaline phosphatise-streptavidin for 1 h at room temperature. The colour reaction was developed with p-nitrophenyl phosphate tablets (Sigma) in diethanolamine buffer (pH 9.8).

2.1.11: Alveolar macrophage culture: AMs in the BAL were counted by hemacytometry, recovered by centrifugation, and resuspended in RPMI supplemented with 10% FBS (Sigma-Aldrich, Oakville, ON, Canada), 1% L-glutamine, 1% penicillin/streptomycin (Invitrogen, Grand Island, NY, USA), and 0.1% 2-mercaptoethanol (Invitrogen) (cRPMI) at $5x10^5$ macrophages/mL. $5x10^4$ AMs/well were plated in 96 well-flat bottom plated, and allowed to adhere for 2 hours at 37°C in a humidified incubator with 5% CO_2. Each well was then washed 3 times with 37°C PBS to remove nonadherent cells, and adherent AMs were cultured in 100µL/well of cRPMI, 1µg/ml lipopolysaccharide (LPS) (Invivogen, San Diego, CA, USA) in cRPMI or 10µg/ml of Poly I:C in cRPMI for 6 or 24hrs. Supernatants were aspirated and frozen at -20°C for later analyses, and adherent cells were fixed by adding 100 µL/well of Carnoy's fixative. After fixation, cells were stained with Hema III solution for verification of plated cell density.

2.2: *Ex vivo* studies of tobacco smoke-induced immune dysfunction

2.2.1: Smoke exposure protocol: Mice were exposed 5d/wk to the mainstream smoke of 2 or 4 cigarettes (1R3, Tobacco and Health Research Institute, University of Kentucky) for 2-6 months using a smoke exposure system developed for guinea pigs (137) and adapted for mice (138). To control for handling, groups of control mice were placed into restrainers only (sham-exposure).

2.2.2: Serum carboxyhemoglobin (COHb) and cotinine levels: Mice were anesthetised using Isoflurane®. COHb and cotinine were monitored as indicators of exposure to nicotine-containing tobacco smoke. For COHb, blood samples were obtained by retroorbital bleeding into heparinised clinitubes (Radiometer Copenhagen, Denmark). COHb saturation was assessed at the Hamilton Regional Laboratory Medicine Program (McMaster University Medical Centre, Hamilton, Ontario, Canada) by spectrophotometry. Cotinine levels were measured by ELISA (Bio-Quant, San Diego CA) in sera obtained by incubating whole blood for 30 min at 37°C, followed by centrifugation.

2.2.3: Murine cell isolation: Mice were anaesthetized using Isoflurane® and euthanized by exsanguination. Spleens, cervical and mediastinal lymph nodes, and lungs were dissected and placed into ice cold HBSS.

Spleens were pressed through 40 μm pore nylon mesh filters (BD Falcon). Lymph nodes were triturated between the frosted ends of sterile glass microscope slides. Cell suspensions were filtered through nylon mesh,

centrifuged at 250 x *g* for 10 min at 4°C, and erythrocytes were lysed in ACK buffer. Leukocytes were washed in HBSS and resuspended in RPMI 1640.

Splenic B-cells were isolated on an AutoMACS magnetic sorter (Miltenyi Biotec, Toronto, ON, Canada) by negative selection from splenocytes using a B-cell isolation kit (Miltenyi Biotec). Recovered cell populations were routinely >93% pure $CD19^+$ B-cells as judged by flow cytometry.

Lungs were perfused with 15 mL of HBSS via the right ventricle, cut into ~2 mm pieces, shaken for 1 h in 37°C 150 U/mL collagenase III (Gibco) in HBSS, pressed through steel mesh, and filtered through nylon mesh. Cells were washed twice in HBSS and layered on 30% Percoll® (Amersham Biosciences, Uppsala, Sweden) underlaid with 60% Percoll®. After centrifugation at 914xg for 30 min at 20°C, mononuclear cells were isolated by aspiration from the 30%-60% interface, recovered by centrifugation at 250xg for 10 minutes, washed in 10 mL of HBSS, and analysed by flow cytometry or processed for tissue culture as described later.

2.2.4: Human peripheral blood mononuclear cell isolation: Blood from current cigarette-smoking subjects and never-smoking control subjects (Table 1) was obtained by venipuncture into heparinised Vacutainers® (BD biosciences) with informed consent. Peripheral blood mononuclear cells (PBMCs) were obtained by centrifugation on Ficoll-Paque+® (Amersham) according to the manufacturer's instructions, and were stored in $N_{2(l)}$ for later

analyses. Experiments were approved by the St. Joseph's Healthcare Hamilton Research Ethics Board, Hamilton ON.

2.2.5: Flow cytometry: Fluo-4, phorbol 12-myristate-13-acetate (PMA) and Ionomycin were purchased from Sigma (St. Louis, MO, USA). Anti-mouse B220-[APC] (RA3-6B2), CD3e-[PE] (145-2C11), CD4-[PE-Cy5.5] (RM4-5), CD8-[APC-AlexaFluor750] (53-6.7), CD19-[FITC] and -[PE-Cy5.5] (1D3) and anti-human CD3-[FITC] (UCHT1), CD8-[PE-Cy5] (L307.4), and CD19-[APC-Cy7] (SJ25C1) (BD Pharmingen, and eBiosciences, San Diego, CA) and CD4-[APC] (M-T466) (Miltenyi) antibodies were used. For cell phenotyping experiments, $1x10^6$ cells were pre-treated with 0.5 μg anti-CD16/CD32 antibodies for 15 min to inhibit nonspecific binding of fluorescent antibodies, stained for 30 min, washed, fixed in 1% paraformaldehyde and counted on a FACSCanto or LSR II flow cytometer (BD, Sunnyvale, CA). $1x10^5$ events were acquired based on FSC and SSC plots, and analysed in FlowJo (Tree Star, Ashland, OR).

For calcium flux assays, cells were loaded with the calcium-binding dye Fluo-4 and incubated with or without 0.005μg/ml of anti-CD3 (2C11) antibodies. Samples were stained also for CD4 and CD8 to detect T cells or for CD19 to detect B cells. Cells were stimulated to flux calcium by either cross-linking of 2C11 bound antibodies with anti-Armenian hamster IgG antibodies (1.8μg, Jackson Immunoresearch, West Grove, PA) to detect T cell calcium signalling, or by adding 2.6ug of anti-IgM antibodies (Jackson Immunoresearch) to detect B cell calcium signalling.

2.2.6: Cell culture and supernatant analyses: $4x10^5$ splenic, or $2x10^5$ LN, lung mononuclear (MNC) or PBM cells/well were cultured in 96-well plates in 0.2 ml of cRPMI (RPMI 1640 with 1% L-glutamine (Sigma), 10% fetal bovine serum, 1% penicillin/streptomycin, and 0.1% 2-mercaptoethanol (Gibco)). Cells were incubated at 37° C in 5% CO_2, 95% sterile humidified air. Anti-mouse and anti-human IgM $f(ab')_2$ antibodies (Jackson Immunoresearch), anti-mouse CD40 antibodies (FGK4.5, a gift from Dr. J Bramson, McMaster University), anti-mouse and anti-human CD3 (Pharmingen), and phytohemagglutinin (PHA (Sigma)), staphylococcal enterotoxins A and B (SEA and SEB (Sigma)), and recombinant human CD154 and IL4 (Sigma) were used as indicated. Immunoglobulin and cytokine levels in culture supernatants were determined by ELISA (Bethyl Laboratories, Montgomery, TX, and R&D Systems, Minneapolis, MN, respectively) according to the manufacturer's protocols.

2.2.7: Thymidine incorporation proliferation assays: On the third day of culture under the conditions described above, triplicate cell cultures were pulsed overnight with [^{3}H]-Thymidine (1 μCi/well, PerkinElmer, Boston, MA) in cRPMI. Cells were harvested onto UniFilter-96 GF/C filter plates (PerkinElmer) by suction, and the filter plates were allowed to air dry. After drying, 200 μl of MicroScint-O liquid scintillation fluid (PerkinElmer) per well, and incorporation of radioactive thymidine was determined using a Topcount NXT scintillation counter (Packard Instrument Company, Meriden, CT).

2.3: Data analyses

Data were expressed as the means ± SEMs. Graphs in this thesis were prepared using SigmaPlot version 11 (Systat Software, Chicago, IL) or GraphPad Prism version 5 (GraphPad Software, LaJolla, CA). Unpaired Student's t-tests were used for 1-factor, 2-group comparisons (Mann-Whitney rank sum test if the data were not normally distributed), 1-way ANOVA for 1-factor, >2-group comparisons, and 2-way ANOVA for 2-factor comparisons. Additional details and interpretation are indicated in figure legends. Differences were considered statistically significant at $p < 0.05$.

Chapter 3: Results

3.1: Polymicrobial infectious disease

3.1.1: Establishment of a murine model of pulmonary infection with *B. parapertussis*. Bacteria from frozen stocks were cultured on Bordet-Gengou blood agar plates for 3 days before being inoculated into Stainer-Scholte broth. As shown in Figure 1a, *B. parapertussis* had a lag phase of approximately 18 hours in liquid culture, followed by an exponential growth phase which lasted for a further 12 hours. Serially-diluted samples of log-phase cultures were plated onto Bordet-Gengou Blood agar plates, and the OD of the sample at 600 nm (OD_{600}) was found to correlate with the number of viable bacterial colonies, via the algebraic notation $y = mx + b$, to yield the function

$$[\text{bacteria}] = (OD_{600}) \times (4.9 \times 10^9 \text{ cfu/ml}) \qquad \text{(Equation 1)}$$

over the linear range of OD_{600} values from 0.8 to 1.5. Based on these calculations, groups of C56BL/6 mice were infected i.n. with *B. parapertussis* doses ranging from $5x10^5$ to $5x10^8$ cfu, and weight loss was monitored as shown in Figure 1b.

The $5x10^5$ cfu/mouse dose was chosen for subsequent study because it has previously been used by others (127), and because it reliably infected mice without leading to significant weight loss (figure 1b). *B. parapertussis* established infection in all lung lobes by day 7 (Figure 1c), and persisted in the lungs for at least 14 days (Figure 1d). Infection resulted in a very modest inflammatory response, with neutrophilia apparent 7 days post-infection, and

mononuclear inflammation evident on day 14 (Figure 1e). Taken together, these results demonstrated the successful establishment of a reproducible model of pulmonary bacterial infection in a well-studied strain of experimental animals.

3.1.2: Influenza infection impairs host defence against *B. parapertussis*. Having established this model of bacterial infection, the impact that *B. parapertussis* would have when introduced into an animal already suffering from an influenza viral was examined (i.e., a heterologous infection condition).

To model heterologous infection, mice were first infected i.n. with influenza virus, using a model of influenza virus infection that has previously been established (130), and then given an i.n. inoculation of *B. parapertussis* 5 days later (D5). Mice infected with *B. parapertussis* alone did not become overtly ill, and did not lose body weight when compared to control mice, while mice infected with influenza virus lost 22.1 ± 2.3 % (n=8, Figure 2a) of their original body weight at the peak of illness, and began recovering 8 days post-influenza infection (day 5+3). Mice infected with both influenza virus and *B. parapertussis* lost significantly more body weight (30.4 ± 1.6 %, n=8) than did mice given either pathogen alone, operationally defined as "bacteria-only" or "virus-only" infected mice (Figure 2a). Moreover, 25% of heterologously-infected mice succumbed to infection, while control and single-infection mice suffered no mortality (Figure 2b). In all subsequent experiments, heterologously-infected mice were provided with

additional feeding and hydration measures to prevent mortality. Although heterologous infection did not impact the animals' ability to completely clear influenza virus from the lungs by day 5+7 (12 days post-influenza infection, data not shown), it did significantly impair *B. parapertussis* clearance when measured on day 5+7 ($3.7 \pm 2.6 \times 10^4$ *B. parapertussis* cfu/mL in bacteria-only mice vs. $2.6 \pm 0.42 \times 10^6$ cfu/mL in heterologously-infected mice) and 5+14 ($2.2 \pm 1.2 \times 10^2$ cfu/mL vs. $5.9 \pm 1.2 \times 10^3$ cfu/mL) (Figure 2c). These findings confirmed that influenza virus infection has a long-lasting, deleterious impact on antibacterial host defence, as has previously been reported with respect to other bacteria (139). Notably, greater doses of *B. parapertussis* than these alone did not cause mortality, prolonged illness, or weight loss when administered to naive mice (Figure 1b), thus suggesting that increased bacterial burden was not the independent cause of the observed morbidity and mortality. In subsequent experiments, the notation "Dx+y" was used to denote animals infected with the first pathogen on day 0 of experimentation, challenged x days later with a second pathogen, and sacrificed y days after challenge.

3.1.3: Effect of viral dose on the outcome of heterologous infection. To determine if reducing the severity of the initial viral insult might reduce the impact of a subsequent bacterial challenge, mice were infected with 7.2×10^4 or 2.5×10^3 pfu of influenza virus, and then challenged with *B. parapertussis* 5 days later. At an i.n. dose of 7.2×10^4pfu (approximately 1/6 of the inoculums used in the aforementioned

experiments), influenza virus infection alone still led to body weight loss, and in similar fashion, exacerbated body weight loss in heterologously-infected mice (Figure 3a). At a still lower dose of $2.5x10^3$ pfu (1/200 the inoculums used in the experiments described earlier), body weight loss was not seen in either group (Figure 3b), but influenza virus infection still had a deleterious effect on clearance of *B. parapertussis* from the respiratory tract (Figure 3c).

3.1.4: Heterologous infection impacts adaptive immune responses without impairing immune protection. The deleterious effects of heterologous infection might extend beyond the acute phase of infection, and impact the formation of immune memory. When mice were allowed to convalesce for 7 weeks following infection, numbers of cells specific for influenza virus nucleoprotein residues 366-374 ($NP_{366-374}$, the immunodominant CD8 T-cell epitope as measured in the MHC I tetramer assay) in the lungs were decreased in heterologously-infected mice, as were influenza-virus specific IgG titres in the sera and IgA titres in the BAL. In contrast, *B. parapertussis*-specific antibody titres were unchanged between bacteria-only and heterologously-infected mice in sera and were undetectable in the BAL (Figure 4a, b). Any alterations observed in antigen specific immune responses did not appear to have functional consequences. Specifically, convalescent mice were re-challenged with influenza virus or *B. parapertussis*; those which had previously been given a heterologous infection were as well-protected against bacterial or viral re-challenge compared to their single-infected controls, both in terms of pathogen

clearance (Figure 4c) and pulmonary inflammation (Figure 4d). Upon re-challenge, while bacterial burdens were somewhat increased in influenza virus- or heterologously-infected mice compared to PBS- or *B. parapertussis*-treated mice, the difference was not statistically significant after allowing for the effects of prior *B. parapertussis* infection ($p=0.101$). In a similar fashion, the effect of prior *B. parapertussis* infection (either alone or as part of a heterologous infection) on the bacterial burden following re-challenge was not significant after accounting for influenza virus' effects ($p=0.058$). Collectively, these data suggested that while heterologous infection attenuated aspects of the adaptive immune response, it did not impact overall immune protection.

3.1.5: Heterologous infection significantly worsens inflammatory responses in the murine lung. To further examine the early host defence response in heterologous infection, mice were given an intranasal administration of PBS or influenza virus, and then challenged 5 days later with PBS or *B. parapertussis*. Visual examination of heterologously-infected lungs at the time of sacrifice 7 days post-challenge (D5+7) revealed discolouration and overt haemorrhage. Further examination by flow cytometry revealed small but significant differences in lymphocyte subsets (Table 2), but also a dramatic increase in the frequency of Gr-1^{bright} (Ly-$6G^{bright}$) cells in the lungs of heterologously-infected mice (52.0 ± 6.3%), which was not observed in control mice, or mice infected with *B. parapertussis* or influenza virus alone (9.8±0.5%, 9.6±1.2%, and

11.8±0.6%, respectively) (Figure 5a,b). Gr-1^{bright} cells have been classified as neutrophils but also might represent populations of monocytes and/or DCs. Therefore, these cells were isolated by fluorescence-activated cell sorting, and were found to be >95% pure neutrophils by standard cytologic criteria (Figure 5c).

Upon histological examination of the lungs, mild and moderate perivascular and peribronchiolar inflammation was noted in mice infected with either *B. parapertussis* or influenza virus respectively, whereas heterologously-infected mice had a greater extent of both types of inflammation, along with extensive inflammatory cell infiltration into both the respiratory and the conducting airways. These inflammatory exudates were replete with neutrophils on D5+7 and mononuclear cells on D5+14 (Figure 5d and e). Consistent with this, BAL inflammation was significantly greater in heterologously-infected mice than in mice that received either infection alone. On day 5+7, heterologously-infected mice had significantly elevated numbers of total inflammatory cells as compared to *B. parapertussis*-infected, influenza virus-infected, or vehicle-only control mice, with neutrophils accounting for the vast majority of this increase (Figure 5f, upper panel). A further seven (7) days later, BAL inflammation remained elevated in heterologously-infected mice as compared to *B. parapertussis*-infected, influenza virus-infected, or vehicle-treated control mice, and this increase was comprised principally of mononuclear cells (Figure 5f, lower panel).

3.1.6: Increased inflammation precedes increased bacterial burden in heterologous infection. To investigate whether the increased inflammation observed in heterologously-infected hosts on day 5+7 was a response to an increased bacterial burden early in infection, mice were sacrificed 1 and 3 days post-bacterial challenge. BAL inflammation was equivalent between heterologous and influenza virus-only mice on day 5+1, but on D5+3, heterologously-infected mice had a greater pulmonary inflammatory response, with significantly increased numbers of neutrophils, but not mononuclear cells (Figure 6a). Importantly, bacterial burdens were unchanged at both of these timepoints, thus indicating that exacerbated inflammation was not the result of an increased bacterial burden (Figure 6b). Equivalent bacterial burdens early after infection also suggested that the increased bacterial burdens in heterologously-infected animals on day 5+7 and 5+14 were not the result of increased adherence or decreased mucocilliary clearance early in infection. Increased inflammation did not appear to be a response to increased viral burdens either, since viral burdens were equivalent between influenza virus-only and heterologously-infected mice at both timepoints (Figure 6d), despite significant reductions in type I IFN production in the BAL at both timepoints (Figure 6e).

3.1.7: Increased recruitment, not decreased apoptosis, drives pulmonary inflammation in heterologously-infected lungs. Since type I IFNs play important roles in regulating inflammation through the induction of granulocyte apoptosis, reduced type I IFNs might result in decreased

neutrophil apoptosis and a consequent accumulation of neutrophils in the lungs of heterologously-infected mice. No reductions were noted in the number of cells staining positive in the terminal deoxynucleotidyl transferase-deoxy uridine triphosphate nick end labelling (TUNEL) reaction- a marker of late apoptosis at any timepoint examined (Figure 7a). In order to exclude the possibility that necrotic neutrophils were accumulating in the lungs, neutrophil viability was assessed by 7-aminoactinomycin D (7AAD) exclusion; although a statistically significant increase in neutrophil death on D5+7 was detected, the increase was small (<1.5% compared to influenza virus-only infected mice, and <1% compared to *B. parapertussis*-only infected mice (Figure 7b)). Concordantly, MPO levels in lung homogenates on day 5+7 (Figure 7c) reflected the numbers of neutrophils observed in those lungs (Figure 5b), thus suggesting that the neutrophils in the lungs of heterologously-infected mice were viable, and capable of producing effector molecules.

Since reduced apoptosis did not appear to be responsible for the accumulation of neutrophils in the lungs of heterologously-infected mice, increased recruitment might instead explain such accumulation. A bead-array based analysis of cytokine and chemokine expression in lung homogenates taken from all groups of animals on days 5+1, 5+3, 5+7, and 5+14 was next conducted (Figure 8a and Tables 3-6). Over this timecourse, a number of mediators were induced by influenza virus or *B. parapertussis* alone, and many were further elevated following heterologous infection. Most striking

was the intense increase in the expression of the CXCR2 ligands MIP-2 (elevated 33-fold with respect to influenza virus-only infected mice and 23-fold compared to *B. parapertussis*-only mice on D5+7) and keratinocyte-derived chemokine (KC) (10- and 3-fold increased, compared to influenza- or *B. parapertussis*-alone), both of which are potent neutrophil chemoattractants. The expression of these mediators was confirmed by ELISA (Figure 8b) and, in agreement with the bead-array data, MIP-2 but not KC was increased at the day 5+3 timepoint, when inflammation in heterologously-infected mice was first beginning to arise. This analysis was extended, and it was found that both MIP-2 and KC were significantly elevated in the BAL of heterologously-infected mice on D5+7 (Figure 8c). Systemic production of MIP-2 was not detected in the sera, and while *B. parapertussis* infection resulted in increased serum KC levels compared to naïve animals, expression was not significantly different between heterologously-infected mice and their *B. parapertussis*-only controls (Figure 8d). This pointed to locally-produced MIP-2 as a potential cause for the profound neutrophilia in heterologously-infected mice and it was therefore considered as a therapeutic target.

3.1.8: Critical role of MIP-2 in heterologous pulmonary inflammatory pathology. To examine neutralization of MIP-2 as a therapeutic avenue in the treatment of the immunopathology which ensues following heterologous infection, mice were infected with influenza virus and challenged with *B. parapertussis* 5 days later. Commencing on day 5+3, a

timepoint when heterologous mice can be differentiated from influenza virus-only infected mice on the basis of weight loss and/or pulmonary inflammation, a daily i.p. injection of neutralizing anti-MIP-2 antibodies or control IgG was administered. Anti-MIP-2 antibody treatment resulted in a significant improvement in animals' clinical scores on day 5+7, as well as decreased weight loss over the course of treatment (Figure 9a, b). Neutralization of MIP-2 had no impact on bacterial burden in these mice, but did significantly reduce pulmonary neutrophilia (Figure 9 c, d), thereby pointing to inflammation as a cause of heterologous infection-related illness, rather than simply a response to increased pathogen burdens. Since granulocyte chemotactic protein (GCP)-2 and KC (both of which are ELR^+ neutrophil chemokines that share the CXCR2 receptor with MIP-2), were also elevated in heterologously-infected mice, it was hypothesized that blockading CXCR2, rather than just one ligand, might provide a more pronounced therapeutic effect. On the contrary, blocking antibodies against CXCR2 resulted in increased bacterial burdens and reduced weight recovery when administered on the same treatment regime as the anti-MIP-2 antibody treatment (Figure 10a, b). In parallel experiments, the administration of anti-CXCR2 antibodies to mice infected only with *B. parapertussis* resulted in similar, significant impairments to bacterial clearance from the lungs.

3.1.9: Effect of influenza virus infection on alveolar macrophage responses. The potential cellular sources of the overproduced MIP-2 observed in the lungs of heterologously-infected mice were next

investigated. AMs were seen as a potential source, because they play a critical role in pulmonary host defence, are targets for influenza virus infection, have been shown to elaborate cytokines and chemokines, and modulate their production of inflammatory mediators following exposure to environmental cues (94-96, 140), Thus, isolation and study of AMs isolated from the lungs of mice 5 days after influenza infection was undertaken. At this timepoint in the aforementioned study of *in vivo* heterologus infection, influenza virus-exposed AMs would have been challenged with *B. parapertussis*. When isolated from the lung and cultured in the presence of bacterial LPS, rather than producing elevated levels of the inflammatory mediators AMs from influenza-infected mice produced significantly less TNF-α, KC, MIP-1α, and MIP-2 than did cells from uninfected mice (Figure 11). This attenuation appeared to selectively affect responses to LPS, since inflammatory mediator production in response to the viral mimic poly (I:C) was not impaired. AM desensitization to LPS stimulation persisted for an extended period of time after influenza virus infection; a modest but significant reduction in inflammatory mediator elaboration was noted from AMs isolated from influenza virus-infected mice 14 days post-infection, i.e., at a timepoint when virus has been cleared from the lungs but inflammation still persists, and 84 days post-infection, when both infection and inflammation have resolved.

3.1.10: Effect of timing on the outcome of heterologous infection. Given the prolonged effect that influenza virus infection had on

AMs, prior influenza virus infection might impact also on *in vivo* host defence processes. When mice were superinfected 14 days post-influenza virus infection, heterologously-infected mice showed only modestly increased inflammation compared to single-infection controls, without the dramatic neutrophilia that was apparent in mice infected 5 days post-influenza infection (Figure 12). The impact of influenza virus infection on antibacterial immune responses waned with time, but still persisted for at least 90 days post-infection. At a timepoint when mice have resolved both the influenza infection and the ensuing inflammation, challenge with *B. parapertussis* still resulted in altered inflammatory responses and bacterial clearance in mice previously infected with influenza virus, but differences were even less pronounced than in mice challenged 14 days post-influenza (Figure 13).

3.1.11: Effect of pathogen sequence in heterologous infection.

The order in which two pathogens were encountered might play a role in determining the outcome of a heterologous infection. To explain this, mice were infected first with *B. parapertussis,* then challenged with influenza virus 7 days later, a timepoint when bacterial burden is high and inflammation is well-established. Mice infected with *B. parapertussis* lost significantly less weight when challenged with influenza virus than did those given only sterile PBS prior to viral challenge (Figure 14a). Along similar lines, these heterologously-infected mice had similar levels of BAL inflammation compared to single-infection controls when sacrificed 5 days post-influenza virus infection, rather than the exacerbated neutrophilia seen in animals

given influenza then *B. parapertussis* (Figure 14b). Finally, AMs isolated from *B. parapertussis*-infected mice did not mount attenuated responses to bacterial LPS or poly (I:C), unlike those from influenza virus infected hosts (Figure 15).

3.2: Cigarette smoke's effect on *ex vivo* lymphocyte function. In addition to investigations into polymicrobial heterologous infections, another complex immune challenge that is common in humans was considered, in which the host must defend itself against challenges encountered over the background of cigarette smoke exposure. To begin these studies, whether exposure to moderate levels of cigarette smoke would result in lymphocyte exhaustion, as has previously been reported with high levels of smoke exposure was studied.

3.2.1: Splenocytes from smoke-exposed animals respond normally to B-cell stimuli *ex vivo*. To investigate the impact of cigarette smoke on splenocyte responses to mitogens, mice were exposed to the mainstream smoke of 2 cigarettes per day for 2-4 months. In earlier work, it was demonstrated that 2 months of smoke exposure is sufficient to decrease pulmonary DCs, alter allergic sensitization, impair alveolar macrophage function, and impair antiviral, antibacterial, and antitumor immunity (131, 141-144). In the present study, this level of smoke exposure resulted in significantly elevated carboxyhemoglobin (COHb) and cotinine levels, indicators of carbon monoxide and nicotine exposure, respectively. Smoke-exposed animals displayed 13.6 ± 0.7% COHb saturation levels immediately

post-exposure, compared to 3.8 ± 0.3% in sham-exposed animals (n=12 and 13 respectively, $p<0.001$). COHb saturation fell in smoke-exposed animals to sham-exposed levels within 24 hours of smoke exposure. Sera cotinine levels averaged 160 ± 56 ng/ml in smoke-exposed mice, significantly elevated over those seen in sham-exposed animals (0.8 ± 0.2 ng/ml, $p=0.005$ by Mann-Whitney rank sum test, used due to abnormally distributed data). These levels were similar to those which have been described in human smokers (145, 146), and are several-fold lower than those described in alternative models (123), thus suggesting this as a model of moderate smoke exposure.

Stimulation of splenocytes with anti-IgM $f(ab')_2$, a Ca^{2+} dependent B cell mitogen, induced robust proliferation, which peaked after 72 hours of culture (Figure 16a). Results were not significantly different between smoke and sham, and background counts were equivalent between smoke and sham cells (3947±602 vs. 2468±1138 cpm).

Whether smoking exerted an effect on responsiveness to costimulation through the CD40 molecule, a stimulus not known to be dependent on Ca^{2+} fluxing, but which is critical in T-dependent B-cell activation was next determined. Proliferative responses in splenocyte populations treated with an agonistic anti-CD40 antibody were studied, and no effect of smoke on these cells was revealed (Figure 16b).

To determine if greater frequency of cigarette smoke exposure resulted in immune cell unresponsiveness, exposure was increased to 4

cigarettes per day. Splenocytes from smoke- and sham-exposed animals proliferated equivalently in response to *ex vivo* stimulation with anti-IgM $f(ab')_2$ or anti-CD40 (Figure 16c, d).

To determine if exposure to cigarette smoke has functional consequences on processes other than proliferation, the ability of these mitogens to stimulate immunoglobulin secretion from splenocytes was evaluated. In accordance with prior studies, anti-IgM $f(ab')_2$ treatment did not induce IgG secretion, but anti-CD40 treatment led to significant IgG secretion, which was similar between smoke- and sham-derived cells (Figure 16e and f). Since COHb and cotinine levels were similar between 2- and 4-cigarette per day animals, all subsequent experiments were performed using animals exposed to the smoke of 4 cigarettes per day in order to maximize the amount of smoke the animals received within the confines of a moderate exposure model. The similarity between 2- and 4-cigarette per day cotinine levels may be explained by the 4h time lag between exposure to morning and afternoon cigarettes in this model. The half life of cotinine in C57BL/6 mice is just 37.5 minutes (147), and a 4h time lag between exposures might prevent cotinine accumulation, whereas continuous smoke exposure, as is used in models reporting higher cotinine levels, may permit it.

3.2.2: Peripheral B-cells are unaffected by *in vivo* exposure to cigarette smoke. Whether differences in BCR responsiveness in smoke-exposed animals might be masked by differences in B-cell numbers between smoke- and sham-exposed animals, or by a countervailing effect of smoke on

other cells was evaluated next. Viable splenocytes were counted by Trypan Blue exclusion using a haemocytometer, and B-cells were enumerated as $B220^+CD19^+$ leukocytes by flow cytometry. Similar splenocyte numbers were observed in smoke- and sham-exposed animals ($4.6 \pm 0.6 \times 10^7$ and $4.3 \pm 0.6 \times 10^7$ per animal; n=10 and 8 respectively, p=0.65) as were similar $B-220^+CD19^+$ B-cell percentages (27 ± 3% and 29 ± 9% of the lymphocyte gate respectively, n=5) and absolute numbers ($16.8 \pm 4.1 \times 10^6$ and $10.8 \pm 5.9 \times 10^6$ B-cells/spleen respectively, n=3-5) (Figure 17a and b). Splenic B-cells were magnetically sorted by negative selection from smoke- and sham-exposed animals, and cultured in the presence of anti-IgM $f(ab')_2$ or anti-CD40 antibodies. As was the case with unsorted splenocytes, anti-IgM $f(ab')_2$ treatment did not induce the production of IgG, while treatment with anti-CD40 antibodies produced robust secretion of IgG into culture supernatants (Figure 17c and d). No differences were found in either the proliferation or IgG secretion of B-cells isolated from smoke- and sham-exposed animals, and background counts were equivalent between smoke and sham cells (1813±609 vs. 1794±378 cpm).

3.2.3: *Ex vivo* T-cell responses are unaffected by *in vivo* smoke exposure. Since a direct effect of smoke on B-cells could not be discerned, the ability of T-cells to respond to T-cell mitogens, and consequently their ability to support humoral responses was evaluated. The proliferation of both splenocytes and magnetic activated cell sorting (MACS)-enriched splenic T-cells was evaluated, and no differences were found in responsiveness to

common Ca^{2+} dependent T-cell mitogens, including soluble anti-CD3 (Figure 18a), as well as PHA, SEA, and SEB (data not shown). Background counts were equivalent between smoke and sham cells (3947±602 vs. 2468±1138 cpm for splenocytes, 1811±607 vs. 1969±345 cpm for enriched T-cells. The secretion of IFNγ from cells stimulated *ex vivo* was also examined as an indicator of T-cell function, and no differences were found between cells from smoke- and sham-exposed animals (Figure 18b).

3.2.4: Lymphocytes from smoke- and sham-exposed animals are equivalently activated *in vivo* and *ex vivo*. Although proliferative responses were equivalent between cells from smoke- and sham-exposed animals under all conditions tested, it remained possible that the analyses of cellular events such as proliferation might mask a more subtle effect of smoke on molecular events of activation. The expression of CD69 and CD25 were evaluated as indicators of early and late lymphocyte activation, respectively, and no differences were found in the proportions of $CD69^+$ or $CD25^+$ B- or T-cells by flow cytometry of freshly isolated splenocytes (Table 7). To elucidate any impact of cigarette smoke exposure on the early molecular events of lymphocyte activation, the abilities of B- and T-cells to generate a calcium flux in response to cross-linking of their antigen receptor was studied, and, at variance with prior reports (122, 123), none was found. As shown in Figure 19A, $CD4^+$ (top) and $CD8^+$ (bottom) T cells isolated from sham and smoke-exposed mice induced an equivalent magnitude of calcium signalling after cross-linking of CD3, and anti-IgM-induced stimulation of

calcium fluxing was also similar between $CD19^+$ B cells of sham and cigarette smoke-exposed mice (Figure 19B).

3.2.5: Locally-derived lymphocytes are unaffected by *in vivo* exposure to cigarette smoke. Given that draining lymph nodes (dLNs) are crucial to the induction of adaptive immune responses, lymphocytes isolated from the cervical lymph nodes were examined. No differences in proliferation were found between cervical lymph node cells isolated from smoke- and sham-exposed animals when cultured in the presence of soluble, agonistic anti-IgM $f(ab')_2$, anti-CD40, or anti-CD3 antibodies (Figure 20a). Further, proliferative responses of cells from within the lungs themselves were assayed. Although lung mononuclear cells did not proliferate in response to anti-IgM $f(ab')_2$ treatment, cells derived from smoke- and sham-exposed proliferated equivalently in response to anti-CD40 or anti-CD3 antibody stimulation, (Figure 20b and data not shown). Background counts were equivalent between smoke- and sham-derived cells (2096±291 vs. 4483±872 cpm for lymph node cells, 5188±1690 vs. 4674±1764 cpm for lung mononuclear cells).

3.2.6: PBMCs from human smokers proliferate normally when stimulated. Given the disparities observed between the present data and previous reports in a rat model of intense cigarette smoke exposure (123, 148), human smokers' lymphocytes were examined for evidence of reduced responsiveness to receptor-mediated signalling. PBMCs were isolated from fresh venous blood samples drawn from asymptomatic current smokers and

age-matched never-smoking controls. In agreement with the present murine model, lymphocytes from current human smokers proliferated equivalently to their non-smoking counterparts when stimulated with soluble anti-IgM $f(ab')_2$, CD154 (CD40L) + IL4, or anti-CD3 antibodies (Figure 21). No changes in B- or T-cell frequencies were noted between smokers' and non-smokers' cells by flow cytometry, and background counts were equivalent between smokers' and never-smokers' cells (797±147 vs. 495±82 cpm). These findings indicated that lymphocyte unresponsiveness is not responsible for the immune dysfunction observed in human smokers.

Chapter 4: Discussion

The immune system is constantly challenged by exogenous threats, ranging from infectious agents like viruses and bacteria, to toxic components of pollution and cigarette smoke, to innocuous particles such as allergens. From the work of several generations of immunologists, a detailed understanding of the immune system's interaction with these agents has been developed. The studies by which this understanding was garnered have typically been conducted in animal models wherein a specific pathogen-free host is exposed to a single agent, and then monitored over time. Although important for understanding disease, studies premised on such reductionist approaches fail to take into consideration the fact that hosts can be, and frequently are assaulted by with more than one challenge, either concurrently or consecutively.

Indeed, both the present work and that of others has shown that the level of immune activation in a given tissue critically affects the response to a coincident challenge. Moreover, prior antigen exposures and immune activation can have a long-lived impact on future challenges, both through the formation of classical immune memory, and, as has been shown more recently, by leaving an indelible mark on the innate immune system (94, 149). To gain a thorough understanding of these phenomena, a model of heterologous pulmonary infection was developed.

4.1: Heterologous infection

The initial focus of these experiments was on the bacterial pneumonia which frequently complicates natural influenza virus infections, using a novel model of heterologous pulmonary infection in which mice were infected with influenza virus, then challenged 5 days later with the Gram-negative bacterium *B. parapertussis*. *B. parapertussis* was chosen not only for its clinical relevance, but also because it productively infects the murine respiratory tract for a period of at least 2 weeks (Figure 1d). The bacteria most commonly associated with natural cases of bacterial superinfection such as *Streptococcus pneumonia* (*S. pneumonia*), *Staphlococcus aureus* (*S. aureus*), and *Haemophilus influenzae* (75) are cleared quite quickly from the murine respiratory tract. Notably, at the dosage given intranasally in the present work, *B. parapertussis* infection on its own was an apparent sub-clinical event, causing no apparent illness or weight loss in naive animals, and only minimal pulmonary inflammation (Figure 1). Given that weight loss and symptom scores are relatively insensitive measures of illness in mice, future studies should consider the use of additional objective measurements such as body temperature change in order to evaluate whether this model is in fact a sub-clinical one. Common, otherwise commensal respiratory microflora cause severe human disease when superimposed over the background of conditions such as influenza infection (75) or COPD (150) in humans. The present study is the first to recapitulate this phenomenon in a mouse model with influenza virus infection.

Lungs from heterologously-infected mice were hemorrhagic upon gross examination, while microscopic and flow cytometric examination revealed a BAL and tissue inflammation which was substantially greater than what would be anticipated based on the sum of the *Bordetella*- and influenza-virus induced responses on their own (Figure 5). This inflammation was comprised principally of neutrophils 7 days post-*Bordetella* infection, and mononuclear cells a week later (Figure 5). Viral burdens were unaffected by heterologous infection, and although bacterial burdens were increased late in the course of infection, they were within the range of inoculums delivered to naive animals without inducing any significant pathology (Figure 6). Furthermore, it was observed that a primary infection with live *B. parapertussis* protected against subsequent influenza virus challenge (Figure 14), and others have similarly found that exposure to bacterial ligands such as FimH (151) or CpG DNA (152, 153), or viral ligands such as poly(I:C) (154) protected against subsequent virus challenge. Mechanistically, the present study demonstrated that AMs from bacterially infected mice responded competently to both viral and bacterial TLR ligands *ex vivo*, which was at odds with the reduced sensitivity to bacterial TLR ligands exemplified by AMs from influenza virus infected mice. More generally, whereas extracellular bacteria, bacterial ligands, and viral ligands are all potent activators of innate immune responses and may provide local protection against a later viral challenge, infection with live intracellular pathogens has been proposed to establish a disadvantageous environment for antibacterial host defence. Evidence

suggests that viral infection results in the lysis of epithelial cells, exposing the relatively "sticky" basement membrane to which bacteria can adhere, and in upregulation of bacterial adhesion factors on surviving cells (89). Thus, whether early changes in bacterial burdens might drive this pulmonary neutrophilia was explored. In contrast, no evidence of an increased bacterial burden was found in the first 3 days post-infection and, instead, it was noted that inflammation arose *prior to* differences in bacterial burdens (Figure 6). In the future, studies using heat-killed bacteria may help to further clarify the role of pathogen burden in determining the outcome of heterologous infection. In similar fashion, a further dose-response curve could be completed, to include lower doses than the $5x10^5$ cfu minimum tested in figure 1, and those lower doses then tested in heterologous infection.

In the present studies, severe pulmonary inflammation correlated with increased production of a wide range of mediators, and was specifically attributable to an overproduction of the inflammatory chemokine MIP-2/CXCL2/GRO-β (Figure 8, 9). Here, it was demonstrated that therapeutic immunoneutralization of MIP-2, beginning 3 days post-challenge, was an effective therapy in heterologously-infected mice, which improved the clinical condition, weight recovery, and pulmonary neutrophilia, without altering bacterial burdens. By showing that inflammatory immunopathology was the real threat to life in heterologously-infected hosts, the present investigations supported the notion that overly vigorous pulmonary immune responses cause the majority of illness, as has been proposed in prior influenza

pandemics, and the present H1N1 swine influenza outbreak (74). Importantly, anti-MIP-2 was given also to influenza virus- or *B. parapertussis*-only infected mice, without any apparent deleterious effect. In contrast, blockade of the entire CXCR signalling axis with antagonistic anti-CXCR2 antibodies resulted in dramatically impaired antibacterial immunity in bacteria-only and heterologous mice, as well as reduced weight recovery in those given heterologous infections when compared to mice treated with normal goat sera (Figure 10). Others have made analogous findings; in a model of pulmonary *Pseudomonas aeruginosa* infection, CXCR2 blockade attenuated pulmonary neutrophilia, but impaired bacterial clearance and reduced survival, while neutralization of MIP-2 significantly reduced neutrophilia, without compromising host defence (155).

In other models of severe lung pathology, more complete interference with the CXCR2 signalling axis has shown a positive effect; genetic deletion or immunoneutralization of CXCR2 or its ligands attenuated the pathology of ventilator-induced lung injury (VILI) in mice (156). VILI is an aseptic cause of acute respiratory distress syndrome (ARDS), a disease which kills 26 to 44 percent of those it afflicts (157, 158). VILI-minimizing strategies reduce mortality in ARDS by minimizing CXCR2 signalling, reducing neutrophil recruitment and neutrophilic injury (156, 159). Simultaneously, in cases of ARDS resulting from infectious causes such as heterologous pneumonia, the merits of preventing immunopathology must be weighed against the potentially deleterious effects of dampening the antiviral and antibacterial

host defence responses. While overexpression of MIP-2 might drive inflammatory immunopathology, clearly some signalling through CXCR2 is required for adequate antibacterial immunity.

Taken together, the disparity between the present findings with MIP-2 neutralization and CXCR2 blockade suggest important pathological and protective roles for CXCR2 ligands in pulmonary host defence. Clinically, BAL levels of the CXCR ligands IL-8 and KC correlate with the severity of pulmonary neutrophilia in ARDS and pneumonia (159). In this regard, KC is highly expressed in heterologously-infected mice, as is (GCP)-2, another CXCR2 ligand. When MIP-2 is neutralized, these and other CXCR2 ligands, as well as cystine-cystine chemokine receptor (CCR) ligands (which have evolved in mice to compensate for a species-wide deficiency in CXCR1), might partially overcome the loss of MIP-2, and allow coordination of a response which is effective for host defence, without causing immunopathology. In the present model of heterologous infection, the bacterial pathogen used does not cause major disease on its own. Whether neutralization of MIP-2 will provide benefit in models of heterologous infection that utilize more virulent pathogens such as *S. pneumonia* remains to be determined; there is a risk that attenuating pulmonary neutrophilia might unacceptably impair host defence. While this possibility cannot be dismissed, in a mouse model of heterologous infection, antibody-mediated neutrophil depletion did not damage the anti-pneumococcal response any further than that already achieved by influenza virus infection (160).

Specifically, influenza virus infection impaired pulmonary neutrophils' ability to phagocytose labelled *S. pneumonia*, and to produce ROS to an extent that neutrophils became functionally irrelevant to the *in vivo* anti-pneumococcal response.

Heterologously-infected mice had dramatically increased pulmonary expression of MIP-2, however the cellular source of this chemokine remains an unresolved question. AMs are important producers of inflammatory mediators during pulmonary infection, but do not appear to be responsible for the overproduced MIP-2, KC, MIP-1α, and TNFα in heterologously-infected mice. On the contrary, AMs from influenza virus-infected mice produced less of these mediators than did cells from control mice, and might therefore play a key role in the host`s attempts to regulate immune responses and avoid immunopathology. Prior work by Didierlaurent *et al.* (2008) showed that AMs isolated from mice months after influenza virus infection have attenuated production of inflammatory mediators in response to bacterial TLR challenge, at a timepoint when *in vivo* bacterial challenge similarly results in reduced pulmonary inflammation, via a mechanism that involves reduced NF-κb nuclear translocation. The present findings go further and provide evidence that AMs are desensitized to bacterial stimuli even 5 days post-influenza virus infection, when the lung as a whole is hypersensititive to the same stimuli. The present study also failed to recapitulate on Didierlaurent *et al.*'s findings of reduced *in vivo* inflammation in previously influenza virus-infected mice. In the present experiments, the magnitude of the heterologous

infection-induced inflammation was inversely correlated with the time lag between viral and bacterial infection, but at no timepoint did influenza virus infected-mice mount *reduced* responses to bacteria when compared to previously naive controls. Interestingly, when mice were re-challenged with *B. parapertussis* 90 days post-influenza virus infection, heterologously-infected mice only developed more severe inflammation (and exacerbated bacterial burdens) than their single-agent infected controls after 3 or 7 days of infection- a timepoint which has not been examined in previously published models, since pathogens were used which are cleared within less than a week. This delayed-onset exacerbation of inflammation might be a feature specific to the present model's use of *B. parapertussis* as a bacterial pathogen; *B. parapertussis* is a poor stimulator of TLR4-mediated immunity, an adaptation that allows it to escape the host defences of both naive and immunized hosts. As a result, *B. parapertussis* induced minimal inflammatory responses in naive mice, and prior influenza virus infection might cause such a small impact on B. parapertussis-induced inflammation that the effect cannot be detected. With more acutely pathogenic agents such as *S. pneumonia* or *S. aureus*, these effects might be revealed, as has been reported in Didierlaurent *et al.* (94). Alternatively, the influenza viruses used in the present study and other work may have different effects on susceptibility to bacterially-induced inflammation.

The question of what then drives MIP-2 overexpression only in heterologously-infected mice remains important, because it is the source of

the observed morbidity. The pulmonary defences must concern themselves not only with the prevention of infection, but also with the avoidance of inflammatory disease which would compromise gas exchange. Consequently, a number of mechanisms have evolved that maintain a high degree of ignorance and tolerance to foreign invaders. In order to shift the "immune rheostat" (reviewed in (161)) towards a pathological state of inflammation like that observed in the present study, these mechanisms must be overcome. Recent work by Shahangian and colleagues (162) might provide a clue to explain this phenomenon. They showed that mice with a genetic deficiency in the IFNα receptor produced more KC and MIP-2, and mounted more robust inflammatory responses during viral-bacterial superinfection than did wild type controls (162). In this regard, one of the most important findings in the present study is that heterologously-infected mice have reduced pulmonary interferon titres compared to influenza virus-only infected mice (Figure 6). Since early reductions in type-I IFNs were noted in heterologously-infected animals, this might have permitted the later increases in MIP-2 expression. A notable difference between Shahangian's study and the present results is that in their model, acute influenza infection attenuated inflammatory responses to bacterial challenge, rather than exacerbating it, so the *administration* of MIP-2 and KC, rather than their *removal* was used as a therapy (162). While work by Didierlaurent and colleagues (94) have elaborated a similar phenomenon which began weeks and continued for months after the resolution of influenza virus infection,

reduced lung inflammation is not a feature of *acute* bacterial superinfections of influenza virus in humans. In such cases, a surfeit of inflammation, rather than a deficit, is commonly noted, and is implicated in disease pathogenesis.

That the intense and prolonged inflammatory response seen in heterologously-infected hosts is incapable of clearing the pulmonary bacterial load is an intriguing observation- more neutrophils would be expected to have a greater antibacterial capacity than would a smaller number. While neutrophils are required for *B. parapertussis* clearance (127), it is important to note that influenza virus infection impairs neutrophil function to the extent that even partial depletion of neutrophils from influenza virus-infected mice does not further damage antibacterial host defence (160). In addition, AMs are second only to respiratory epithelial cells as a target for influenza virus, and direct viral infection may further compromise their antibacterial function, as has been reported in other models (95, 96). Moreover, the presence of neutrophils, whether functional or not, in the influenza virus-infected airway at the time of bacterial challenge is a key difference between bacterial-only and heterologously-infected mice. These cells must be cleared by AMs, which also play a crucial role in the early pulmonary antibacterial response. Efferocytosis has been shown to compromise their antibacterial function by inducing the release and autocrine activity of prostaglandin E2 (41), thus having to clear the influenza virus-associated neutrophilia might place these macrophages at an immediate disadvantage when next tasked with clearing a bacterial infection. A self-reinforcing vicious circle may then arise, in which

ever-increasing neutrophil recruitment actually impairs resident antibacterial host defence cells, until ultimately the adaptive immune system arrives to clear the pathogen. In the future, studies to examine the function of neutrophils and alveolar macrophages isolated from heterologously infected mice may shed additional light on this hypothesis. The fact that the formation of immune memory was not substantially impacted by heterologous infection (Figure 4) is consistent with the finding that survivors of the 1918 influenza pandemic, many of whom presumably suffered from bacterial superinfections of their influenza virus infection, demonstrate robust B-cell responses against influenza antigens even some 80 years later (163). The key issue seems to be that the host must survive the initial pneumonia for long enough to arm and utilize the adaptive arm of immunity.

It has been commonly stated that the "Spanish" influenza virus which swept the globe in 1918-1919 was remarkably lethal. Elegant work by McAuley and colleagues (2007) has recently called that notion into question. Their experiments suggest not the 1918 virus's intrinsic lethality, but its ability to predispose hosts to a fatal secondary bacterial infection as its most remarkable feature (76). Indeed, secondary bacterial pneumonia, not primary viral disease causes the majority of deaths during influenza pandemics (75), and viral-bacterial co-infections lead to worse symptoms than single-agent ones even during seasonal influenza (164). Thus, it might be that a given influenza pandemic is only as lethal as its ability to promote bacterial superinfection, and that a given superinfection is only as lethal as

its ability to cause a lethal inflammatory immunopathology. Through prophylactic or early therapeutic interventions against the causative pathogens, the extent of the inflammation and improve outcomes might be limited. Beyond a certain threshold (in time or in magnitude of infection); however, strategies which directly alleviate inflammation warrant consideration.

Collectively the present results demonstrate that a normally sub-clinical respiratory bacterial infection can become life-threatening when superimposed over the background of an influenza virus infection. This effect is mediated not by microbial pathogenesis *per se*, but rather by an inappropriately potent pulmonary neutrophilia, which arises independently of the increased bacterial burden. Most importantly, selective neutralization of the ELR^+ CXCR2 ligand MIP-2 attenuates pulmonary inflammation and improves animals' health and weight recovery without impacting on bacterial burden. It is non-trivial that neutralization of MIP-2 provides a dramatic benefit even when administered days after the establishment of heterologous infection; this treatment regimen is clinically practical, and might show additional efficacy if administered sooner after infection.

4.2: Cigarette smoke exposure

Cigarette smoke impairs both innate and adaptive immunity, but the underlying mechanisms are poorly understood. Previous reports using rats suggested that exposure to the smoke from high-tar (22.8 mg/cigarette),

high-nicotine (1.46 mg/cigarette) cigarettes equivalent to 2-3 packs/day for a 70 kg human, or to nicotine itself renders lymphocytes anergic through depletion of the intracellular Ca^{2+} stores necessary for signal transduction (123). Since most smokers consume one pack per day or less (165), the present study questioned whether the same mechanisms were responsible for the immune impairment observed in human smokers or in more moderate models of smoke exposure. Thus, the purpose of the current study was to evaluate the relative importance of lymphocyte unresponsiveness in determining the immune dysfunction observed in human smokers, who are not typically exposed to the high levels of smoke used in previous studies.

The present studies utilized a widely studied murine smoke exposure system that causes emphysema (138), altered immunity including reduced numbers of pulmonary DCs (143), reduced antigen presentation (166), altered humoral responses (143, 144), delayed clearance of pulmonary bacteria (131, 167), impaired antiviral host defence (142), and impaired NK-cell mediated tumor surveillance (141). COHb and cotinine are commonly used as short- and long-lived biomarkers of cigarette smoke exposure, and are semi-quantitative indicators of a host's level of exposure. In the present study, smoke exposure led to sera COHb which many laboratories consider normal for a human smoker (168) and sera cotinine levels comparable to those reported in moderate human smokers (145, 146). Whether the functional deficits observed in these animals could be attributed to T or B cell unresponsiveness was addressed in the present investigations.

To examine smoke's local and systemic effects on B-cells, lung-, draining lymph node-, and spleen-derived lymphocytes from smoke- and sham-exposed animals were stimulated with anti-IgM $f(ab')_2$ and anti-CD40 antibodies. Based on previous reports of attenuated antibody responses in this and similar model systems (143, 144, 148), and in human smokers (169), Ca^{2+} signalling was expected to be impaired in B-cells from smoke-exposed animals. Contrary to that hypothesis however, no impairment in proliferation was observed in cultured cells from any compartment. It was interesting to note that lung-derived cells did not proliferate in response to treatment with anti-IgM antibodies. The present results suggest that while B-cells in the lymphoid organs are mostly mature, naive B-cells with IgM BCRs, those which have migrated into peripheral tissues such as the lungs represent a population almost exclusively comprised of IgM^- B-cells, and would instead express isotype-switched IgG or IgA on the cell surface. In further investigation, flow cytometry indicated that smoke- and sham-exposed animals have equal percentages of B- and T-cells in all the compartments studied here. Thus, magnetic sorting was employed to isolate B- and T-cells from smoke- and sham-exposed animals, to possibly unmask any subtle differences in lymphocyte responsiveness that might be hidden by a countervailing effect of smoke on other cells. This is the first analysis of the behaviour of smoke- exposed B-cells in isolation, and it effectively demonstrated that splenic B- and T-cells from smoke-exposed animals

proliferated and secreted effector molecules normally when stimulated *ex vivo*.

Although proliferation is a clinically important marker of lymphocyte responsiveness, the primary effector function of B-cells is Ig production, and T-cells orchestrate immune reactions through the secretion of immunomodulatory and effector cytokines. Thus, the impact of cigarette smoke on IgG and IFNγ as markers of B-cell and T-cell function, respectively, was evaluated. It was noted previously that IgG, and particularly IgG2a production is reduced in response to *in vivo* adenovirus challenge (144), Reduced production of Th1 cytokines by T-cells might provide a mechanism for this phenomenon, however cells from smoke- and sham-exposed mice secreted equivalent amounts of IgG and IFNγ. The *ex vivo* stimulation of B- and T-cells with agonistic ligands cannot fully recapitulate the features of *in vivo* humoral responses, including antigen processing, presentation, DC licensing, T-cell stimulation and costimulation, B-cell activation, and a complex cytokine environment.

In this model of tobacco-related disease, exposure to cigarette smoke principally impacts cells of the innate immune system, including NK cells, DCs, and macrophages (141, 143). It has previously been observed that smoke exposure can impact humoral responses (143, 144), but as evidenced in the present study, no direct effect of smoke on T- and B lymphocytes of the adaptive immune system could be discerned. Impacts on humoral and cellular adaptive immunity may be the result of smoke's well-documented

effects on innate immune cells. By decreasing pulmonary DCs (143), or impairing other processes necessary to prime adaptive immune responses, smoke might alter the establishment of adaptive immunity as has been reported by others (166). Similarly, it is possible that a dose-dependency exists in cigarette smoke's immunomodulatory effects. Sera cotinine levels in the smoke-exposed animals studied here were at least 6-fold lower than the levels reported in studies by Kalra *et al.* (2000), who showed decreased Ca^{2+}-dependant signalling (123), as were levels in human smokers, suggesting that the level of exposure used in studies that have shown Ca^{2+} depletion are not reflective of a typical human smoker. At moderate doses of cigarette smoke, antigen receptor signalling might be unaffected, and effects on epithelial, DC, and NK cells might predominate while at much higher doses, direct effects on BCR and TCR responsiveness might appear.

Addressing where on this spectrum a human smoker falls is an important issue. In order to determine if the present mouse model accurately reflected human smokers, PBMCs from human volunteers who had never smoked were compared with those from current smokers. In agreement with results from the present animal studies, no impairment was found in the proliferative responses of smokers' PBMCs to polyclonal B- and T-cell mitogens. No studies have documented a decrease in lymphocyte proliferation among smokers, and, in fact, one study reported increased CD3/CD28-induced proliferation of PBMCs from heavy smokers (125). Species differences might explain the variance between the present results

and others, and it is possible that rats' lymphocytes are particularly susceptible to smoke-induced Ca^{2+} depletion. It is crucial to note that the human smokers, whom the rat is purported to model, are not similarly susceptible. Alternatively, the duration of smoke exposure might play a role in smoke's effect on lymphocyte unresponsiveness, as prior work observed unresponsiveness after 8 but not 3 months of smoke exposure (123). Although the present experiments extended out to 6 months of smoke exposure in mice, it is crucial again to note that in humans who have smoked for a mean of over 25 pack years each, no lymphocyte unresponsiveness was observed. Thus, although lymphocyte unresponsiveness can be induced in some animal models, the present data suggest that other mechanisms mediate the immune impairments observed in human smokers (170) and animal models of moderate smoke exposure (131, 141-144), including impairments to the innate immune system which underpins adaptive immunity. A mounting body of evidence points to AM dysfunction as a key factor in the pathogenesis of smoking-related disease, and this might provide a link between smoke exposure and adaptive immune dysfunction.

The present study indicates, both in cells from human smokers and from a murine model previously shown to induce marked immune dysfunction, that the ability to mount a host defence response might be altered without discernable effects on the responsiveness of T and B cells. In a widely-studied murine model of moderate cigarette smoke exposure, it was found that T- and B- lymphocytes responded competently to a wide range of

Ca^{2+}-dependant and also Ca^{2+}-independent activators (section 3.2). Similar findings were obtained in PBMCs from human smokers, and showed that smoke exposure led to marked immune dysfunction without a detectable impairment of lymphocyte signalling. Thus, the present work supports the notion that, in accord with other studies, smokers' adaptive immune responses might be impaired, not by a direct effect of smoke on adaptive immune cells, but rather by an effect on the APCs and other innate cells which activate them.

4.3: Future directions:

At the conclusion of this project, there remain some fascinating avenues for further investigation. Firstly, the cellular source of the overproduced MIP-2 observed in heterologously-infected animals should be examined. A histochemistry project could probe heterologously-infected lung sections to quickly determine the tissue localization of MIP-2 protein, and point to the cell cells responsible. Given that the present work rules out the AM, vascular endothelial cells are the most likely candidates for overproducing MIP-2. Endothelial cells are capable of producing MIP-2, and express a number of PRRs which might be activated during heterologous infection, including TLR-4 and nucleic acid detection helicases including RIG-I and TLR3 (22, 171-174).

Secondly, the mechanism underlying influenza virus-induced AM desensitization should be further investigated. Although Didierlaurent *et al.*

(2008) have attributed this phenomenon to reduced NF-κb nuclear translocation, no explanation has been forthcoming to, in turn, explain the reduced translocation (94). One of the most attractive candidate mechanisms is the induction of the Src homology 2 domain-containing protein tyrosine phosphatases (SHPs). SHPs might play a key role in determining whether infected cells such as epithelial cells, endothelial cells, and AMs induce an antiviral state, characterized by the production of type-I IFNs, or an inflammatory or an antibacterial state, characterized by the production of proinflammatory cytokines. In fact, these enzymes are the only known molecules capable of oppositely regulating expression of these two distinct classes of antimicrobial and antiviral effectors (175). SHP-1 expression promotes type I IFN production by inhibiting IRAK1 activity, which in turn results in a suppression of NF-κB-induced inflammatory cytokine production (176). This effectively biases the immune response following TLR activation away from the production of proinflammatory cytokines, but still permits, and in fact enhances the TLR- and CARD helicase-induced production of type-I IFNs. Genetic deletion of SHP-1 results in a pattern of high proinflammatory cytokine/low type-I IFN production that is similar to that seen in the lung homogenates from the present model of heterologous infection (175). At the same time, viral infection induces SHP-1 expression in glial cells (177), which would be hypothesized to result a pattern of low inflammatory cytokines and high interferon production- at least the former of which is observed in AMs (Figure 11 and (94)), which are a known target for influenza virus infection.

Thus, viral alterations of SHP function could explain the paradoxical effect that heterologous infection has on inflammatory cytokine and type-I IFN production in the whole lung and in AMs.

Thirdly, the role of MIP-2 in human lung infections must be examined if the present findings are to be translated into clinically useful knowledge and therapies. To date, no data exist on whether upregulation of MIP-2/GROα is a feature of human lung infections, although expression of another GRO-family chemokine, GRO-β, correlates well with the level of pulmonary neutrphilia in patients with bacterial pneumonia and ARDS. Moreover, a key distinguishing feature between infection with highly pathogenic influenza viruses and more benign serotypes is the development of a "cytokine storm" (178)in which systemic overproduction of inflammatory cytokines and chemokines leads to immunopathology. MIP-2 expression could be examined by ELISA in BAL samples obtained from pneumonic patients, or by immunohistochemistry on pathology specimens from the victims of bacterially superinfected influenza virus, either in pandemics or seasonal influenza outbreaks.

In regard to the impact of cigarette smoke on host defence responses, elucidating the mechanisms underlying smoke`s deleterious effects has proven to be complicated. The contrast between the present study's findings and previous report of lymphocyte exhaustion highlight a critical need to develop accurate animal models, and validate them against clinical observations. A large body of literature exists which documents the effects of

smoke-conditioned medium, various models of *in vivo* smoke exposure, and numerous ex vivo assays. In many cases, these studies are not replicated in humans, and are either contradictory or cannot be reliably compared to each other because of differences between the models. Thus, there might be a substantial gap between what researchers have reported smoke does in model systems, and what it actually does in humans. One finding which has repeatedly been replicated in animal models and in humans is the fact that smoking impacts on humoral immune responses. The present study rules lymphocyte exhaustion out as a potential cause for this phenomenon, again in both animals and humans. Thus, a deficit must exist in antigen processing, presentation, antigen-specific T-cell activation, or antigen-specific B-cell activation in order to explain a deficit in humoral responses without a global deficit in B-cell responsiveness. Since smokers' humoral responses are specifically attenuated against antigens encountered via the respiratory system rather than other routes of exposure (169), the pulmonary APC system is the most likely source of this defect. Earlier work has suggested that smoke exposure reduces pulmonary DC numbers (143), and their ability to prime $CD4^+$ T-cell responses by reducing their expression of the CD80 and CD86 costimulatory molecules (166). An investigation should therefore be conducted into the mechanisms by which smoke affects DCs, with an eye towards identifying therapeutic targets.

4.4: Synthesis and conclusion

The present findings are applicable in a number of areas; MIP-2 may prove a useful therapeutic target in the treatment of severe pneumonia, while the findings in smoke-exposed animals suggest that vaccination strategies in smokers need not be concerned with lymphocyte exhaustion as a potential obstacle. However, one of the most interesting applications for the tools developed in these experiments is in the development of models for the study of acute exacerbations of COPD. Over 90% of all cases of COPD can be explained by active (primary) smoking, and most of the remaining 10% are attributable to passive (second-hand) exposure to smoke. At the same time, microbial colonization of the airway, is a common feature, along with recurrent exacerbations, in which an environmental stimulus (typically of infectious aetiology) precipitates a sustained worsening of symptoms. Mixed viral-bacterial infections make up a substantial fraction of these exacerbations, especially the most serious ones. All of these elements have been examined in the process of conducting the present studies.

More than is the case for perhaps any other disease, models of chronic obstructive disease have proven elusive. Specifically, it has been argued that no complete models of stable COPD or acute exacerbation currently exist. (2). In part, this may reflect a fundamental lack of understanding of the disease processes that underlie the pathogenesis of this syndrome. The best approach to solving this deficit is to model the key etiologic factors of COPD, including cigarette smoke exposure, persistent inflammation, bacterial colonization, and repeated exacerbating insults. The present studies provide

a platform from which COPD studies can be launched, with mice being exposed to cigarette smoke, repeatedly colonized with an immune system-evading bacterial pathogen, and challenged with a relevant viral pathogen.

The focus of the present studies was on developing an understanding of complex immune challenges, in the interests of better understanding the complex host-environment interactions that occur in the real world every day. With that in mind, the goal of future experiments should not only be to develop a further understanding of heterologous pulmonary infection, or tobacco smoke exposure. These are important goals on their own, but this work provides new tools that, when appropriately combined, can shine new light on even more complex diseases such as COPD.

Chapter 5: Figures, tables, and legends

Figure 1: Establishment of a pulmonary infectious disease model with *Bordetella parapertussis*. **(a)** *B. parapertussis* was grown exponentially in Stainer-Scholte broth as monitored by increasing light absorbance at 600 nm. **(b)** Mice were inoculated intranasally with 10-fold increasing doses of log-phase *B. parapertussis* and weight loss relative to pre-infection weight was monitored. n=4 per group. Circles represent groups given sterile media only. Black, green, blue, and red squares represent groups given $5x10^5$, $5x10^6$, $5x10^7$, and $5x10^8$ cfu respectively. Data are expressed as the means ± SEMs, and peak weight loss was analysed by 1-way ANOVA. **, and *** denote a significant difference at $p<0.01$ and <0.001 respectively compared to mice given sterile media only. **(c)** seven (7) days post-infection, bacteria were found in all lung lobes of animals given $5x10^5$ cfu of *B. parapertussis* (n=5 mice per group) and **(d)** bacteria persisted for at least 14 days post-infection. n=3-17 per mice per group, pooled from 3 independent experiments). **(e)** Pulmonary inflammation was monitored in the broncho-alveolar lavage in terms of total cell number (TCN), polymorphonuclear neutrophils (PMNs), and mononuclear cells (MNCs) in *B. parapertussis*-infected (filled bars) and PBS-exposed (open bars) mice. n=4-5 per group. Data are expressed as the means ± SEMs and are analysed by unpaired T-test. * denotes $p<0.05$ compared to PBS-exposed mice at the same timepoint.

Figure 1

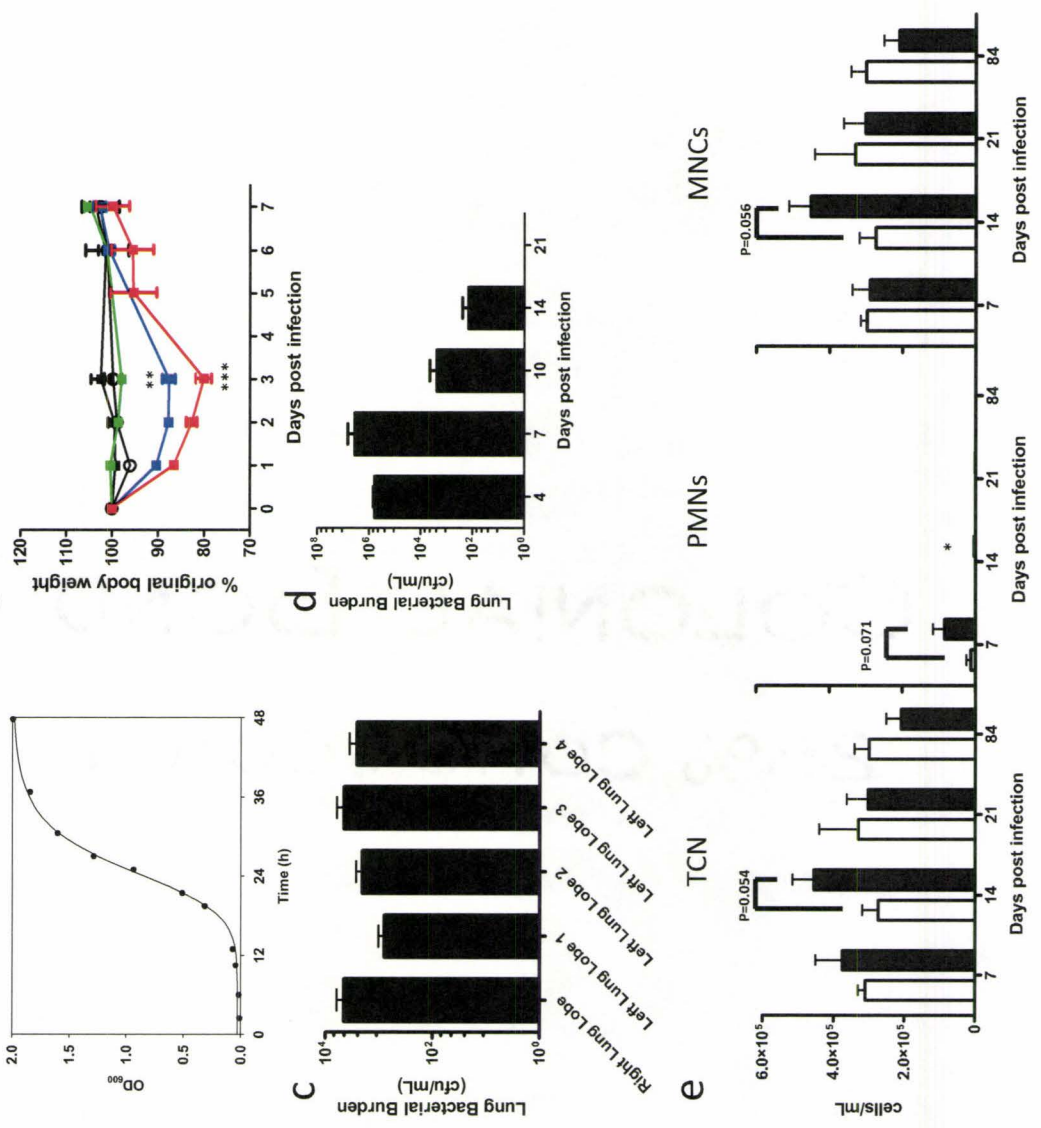
a
OD600
Time (h)
b
% original body weight
Days post infection
**
***
c
Lung Bacterial Burden (cfu/mL)
Right Lung Lobe
Left Lung Lobe 1
Left Lung Lobe 2
Left Lung Lobe 3
Left Lung Lobe 4
d
Lung Bacterial Burden (cfu/mL)
Days post infection
e
TCN
PMNs
MNCs
cells/mL
P=0.054
P=0.071
P=0.056
*
Days post infection

Figure 2: Influenza virus impairs host defence against *Bordetella parapertussis*. (a and b) Initially, mice (n=5-10 per group) were given sterile PBS (grey icons) or $2.5x10^5$ pfu of influenza virus (black icons) intranasally and, 5 days later, sterile PBS (squares) or $5x10^5$ cfu *B. parapertussis* (triangles), with weight loss and mortality monitored. **(c)** Mice were given PBS (open bars) or influenza virus (filled bars), then challenged with *B. parapertussis* 5 days later. Lung bacterial burden was determined 7 (left of the break) and 14 (right of the break) days post-challenge. n= 4-5 per group. Data are expressed as the means ± SEMs and were analysed by 2-way ANOVA for weights and bacterial burdens, and by Mantel-Cox log-rank test for survival curves. *, †, and ‡ denote a significant difference at $p<0.05$ compared to PBS+PBS, PBS+*B. parapertussis*, and influenza+PBS-exposed mice, respectively. 2 icons denote differences at $p<0.01$; 3 icons denote differences at $p<0.001$. Data are representative of at least two independent experiments.

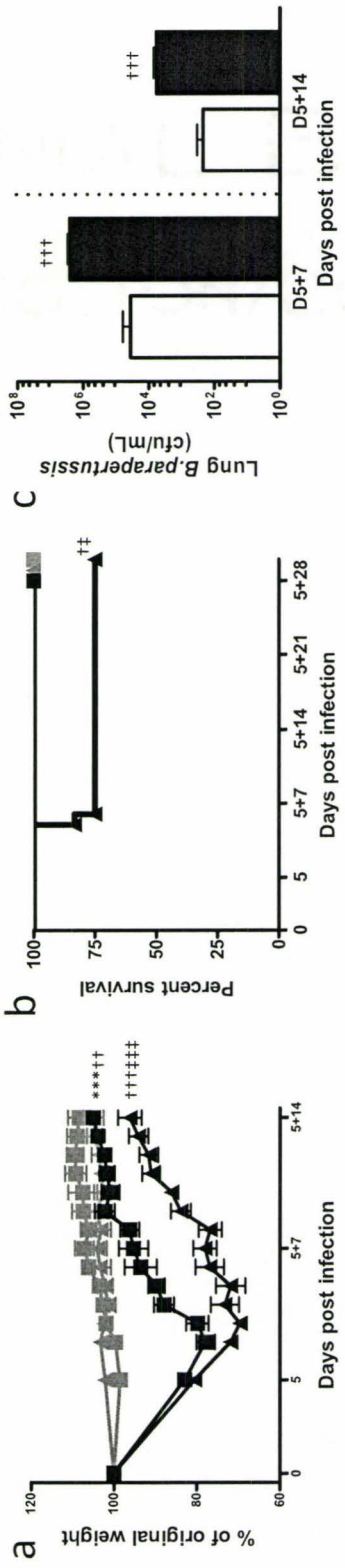
a
% of original weight
120
100
80
60
0
5
5+7
5+14
Days post infection
*****
†††††
‡‡‡‡‡
b
Percent survival
100
75
50
25
0
0
5
5+7
5+14
5+21
5+28
Days post infection
‡‡
c
Lung B.parapertussis (cfu/mL)
10^8
10^6
10^4
10^2
10^0
D5+7
D5+14
Days post infection
†††
†††

Figure 2

Figure 3: Viral dose differentially affects the features of heterologous infection. Mice were given sterile PBS (grey icons) or reduced doses of influenza virus (black icons) intranasally, and then 5 days later sterile PBS (squares) or *B. parapertussis* (triangles). **(a)** Weight loss in mice given $7.2x10^4$ pfu of influenza virus or PBS, followed by PBS- or *B. parapertussis* 5 days later. **(b)** Weight loss in mice given $2.5x10^3$ pfu of influenza virus or PBS, followed by PBS- or *B. parapertussis* 5 days later. **(c)** Lung bacterial burden in mice given $2.5x10^3$ pfu of influenza virus or sterile PBS, then challenged with PBS (open bars) or *B. parapertussis* (filled bars). Data are expressed as the means ± SEMs and are analysed by 2-way ANOVA. ***, †††, and ‡‡‡ denote significant differences at $p<0.001$ compared to PBS+PBS, PBS+*B. parapertussis*, and influenza+PBS-exposed mice, respectively.

Figure 3

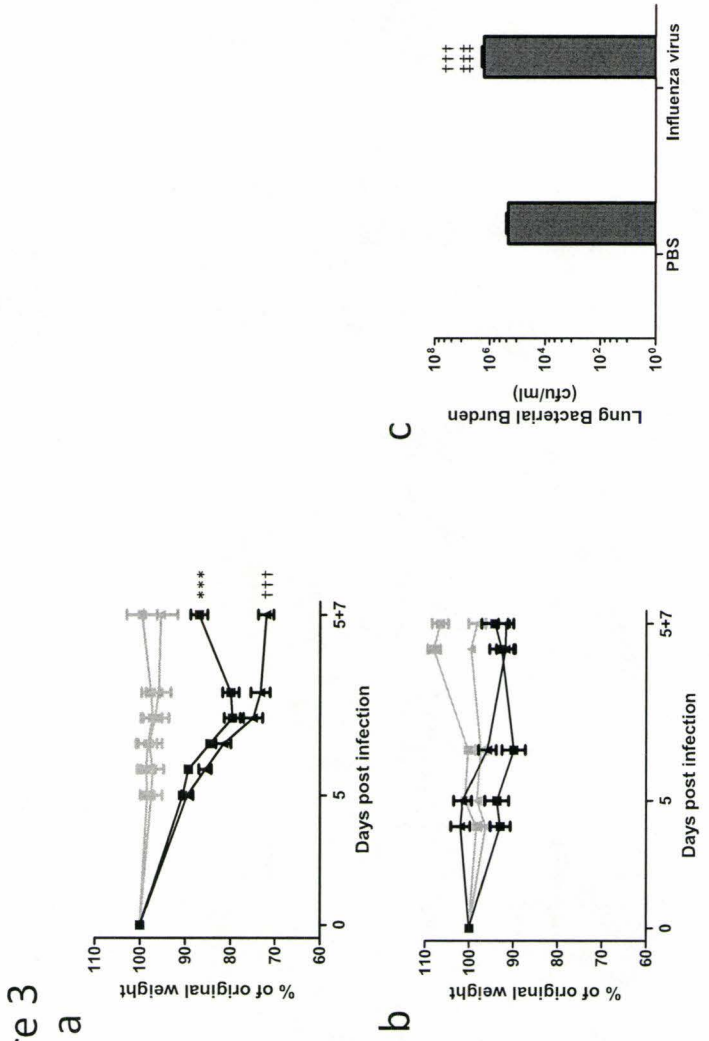
a
% of original weight
110
100
90
80
70
60
0
5
5+7
Days post infection
***
†††
b
% of original weight
Days post infection
c
Lung Bacterial Burden (cfu/ml)
10^8
10^6
10^4
10^2
10^0
PBS
Influenza virus
†††
‡‡‡

Figure 4: Heterologous infection alters adaptive immune responses without impairing protective immune memory. (a) Mice were given sterile PBS or influenza virus intranasally, and then 5 days later sterile PBS (open bars) or *B. parapertussis* (filled bars). Influenza virus $NP_{366-374}$-specific CD8+ T-cells were enumerated following a 7 week convalescence by tetramer-based flow cytometry in enzymatically digested lungs. **(b)** 7 weeks post-challenge, influenza virus- (upper panel) and *B. parapertussis*-specific (lower panel) antibodies were determined by ELISA in the sera for IgG (left panel) and broncho-alveolar lavage (BAL) for IgA (right panel) of mice given sterile PBS (grey icons) or influenza virus (black) intranasally, and then 5 days later sterile PBS (square icons) or *B. parapertussis* (triangles). Convalescent mice were re-challenged with influenza virus (top panel) or *B. parapertussis* and **(c)** pathogen burden and **(d)** BAL neutrophilia was determined 5 days later for influenza virus infection, and 7 days later for *B. parapertussis* infection. n=4-7 per group. ND denotes not detected. Data are expressed as the means ± SEMs and were analysed by 2-way ANOVA. *, †, ‡ and § denote a significant difference at $p<0.05$ compared to PBS+PBS, PBS+*B. parapertussis*, influenza virus+PBS, and influenza virus+*B. parapertussis*-exposed mice respectively. 2 icons denote differences at $p<0.01$; 3 icons denote differences at $p<0.001$. Data are representative of two independent experiments.

Figure 4

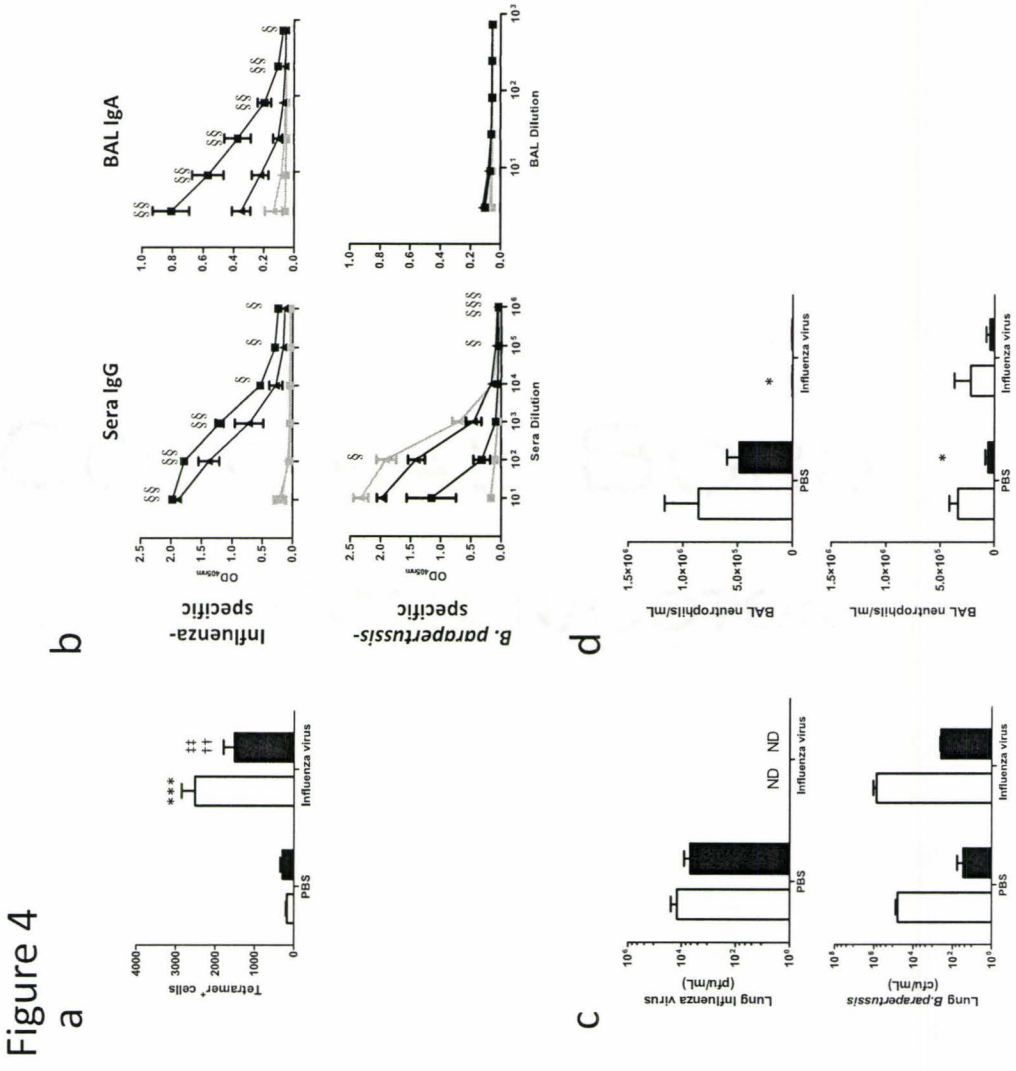
a
Tetramer+ cells
PBS
Influenza virus
b
Sera IgG
BAL IgA
Influenza-specific
B. parapertussis-specific
OD405nm
Sera Dilution
BAL Dilution
c
Lung Influenza virus (pfu/mL)
Lung B.parapertussis (cfu/mL)
ND
d
BAL neutrophils/mL

Figure 5: Heterologous infection leads to severe pulmonary inflammation. Mice were given sterile PBS or influenza virus intranasally as indicated, and 5 days later sterile PBS (open bars) or *B. parapertussis* (filled bars). **(a)** Representative flow cytometry plots of the lung digests of heterologously-infected animals on D5+7. **(b)** Aggregate data from the experiment represented in (a), with n=4 per group. **(c)** Representative cytocentrifuge preparations of Gr-1^{bright} cells isolated by fluorescence-activated cell sorting of lung digests of mice on D5+7 (>95% pure neutrophils as judged by standard cytological criteria). **(d)** Representative hematoxylin and eosin (H&E)-stained histological cross-sections from mouse lungs on D5+7, and **(e)** D5+7 showing severe neutrophilic inflammation and an inflammatory exudate in the lumens in heterologously-infected mice. Images were obtained at 200x magnification and inserts at 400x magnification. **(f)** Broncho-alveolar lavage inflammation, showing increased total cells and neutrophils (PMNs) in heterologously-infected mice on D5+7 (upper panel), and total cells and mononuclear cells (MNCs) on D5+14 (lower panel) compared to mice given *B. parapertussis* or influenza virus alone. Insert in the centre lower panel shows the same data displayed with an expanded scale. Data are expressed as the means ± SEMs and are analysed by 2-way ANOVA. n= 3-4 per group. *, †, and ‡ denote a significant difference at $p<0.05$ compared to PBS+PBS, PBS+*B. parapertussis*, and influenza virus+PBS-exposed mice, respectively. 2 icons denote $p<0.01$; 3 icons denote $p<0.001$. Data represent two independent experiments.

Figure 5

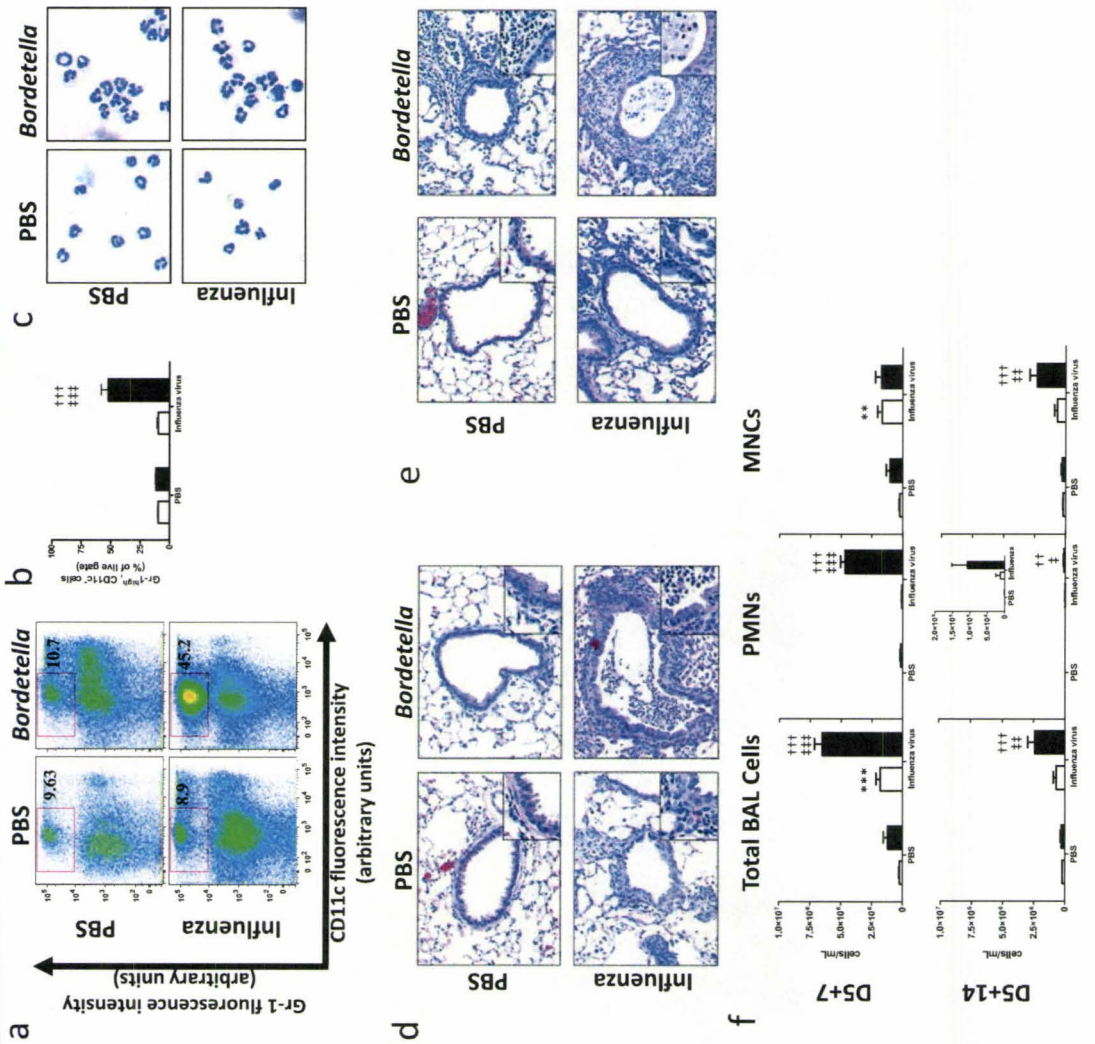
a
PBS
Bordetella
Influenza
9.63
10.7
8.9
45.2
Gr-1 fluorescence intensity (arbitrary units)
CD11c fluorescence intensity (arbitrary units)
b
Gr-1high, CD11c+ cells (% of live gate)
PBS
Influenza virus
c
PBS
Bordetella
Influenza
d
PBS
Bordetella
Influenza
e
PBS
Bordetella
Influenza
f
Total BAL Cells
PMNs
MNCs
D5+7
D5+14
cells/mL
PBS
Influenza virus

Figure 6: Increased inflammation is independent of pathogen burden in heterologous infection. Mice were given sterile PBS or influenza virus intranasally, and then 5 days later sterile PBS (open bars) or *B. parapertussis* (filled bars). **(a)** Broncho-alveolar lavage inflammation in mice given an intranasal administration of PBS or influenza virus as indicated, challenged intranasally with PBS (open bars) or *B. parapertussis* (filled bars) 5 days later, and then sacrificed 1 (upper panel) or **(b)** 3 (lower panel) days after challenge. n = 4 mice per group. Insert in the centre upper panel re-presents the same data displayed with an expanded scale. **(c)** bacterial, and **(d)** viral burdens in the lungs of the same mice, showing unchanged pathogen loads on both days 5+1 and 5+3. **(e)** Type-I interferon production was determined in the BAL of heterologously-infected (filled bars) and mice given influenza virus alone (open bars) on days 5+1 and 5+3 by a vesicular stomatitis virus-green fluorescent protein (VSV-GFP) plaque reduction assay, revealing reduced Type-I interferon expression in heterologously-infected mice. GFP intensity was calculated as a percentage of the mean signal observed in non-protected (operationally termed "mock infected"), VSV-GFP infected cells (arbitrarily set at 100% intensity). Data are expressed as the means ± SEMs and were analysed by 2-way ANOVA. n = 4 per group. *, †, and ‡ denote a significant difference at $p<0.05$ compared to PBS+PBS, PBS+*B. parapertussis*, and influenza virus+PBS-exposed mice, respectively. 2 icons denote $p<0.01$; 3 icons denote $p<0.001$. Data are representative of two independent experiments.

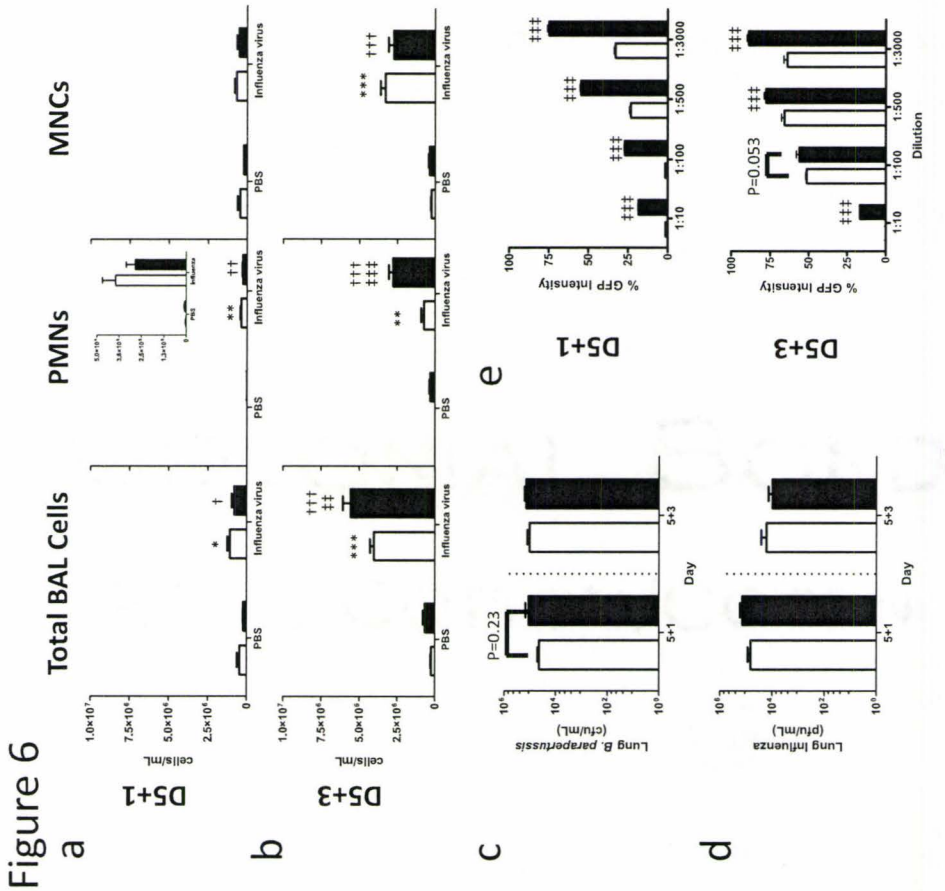
Figure 6
a
b
c
d
e
Total BAL Cells
PMNs
MNCs
D5+1
D5+3
cells/mL
PBS
Influenza virus
Lung B. parapertussis (cfu/mL)
Lung Influenza (pfu/mL)
P=0.23
P=0.053
Day
5+1
5+3
% GFP Intensity
Dilution
1:10
1:100
1:500
1:3000

Figure 7: Neutrophil apoptosis is not impacted by heterologous infection. (a) Apoptosis was measured by TUNEL-staining using flow cytometric analysis of Gr-1^{bright} neutrophils from lung digests of mice given an intranasal administration of PBS or influenza virus as indicated, challenged 5 days later with PBS (open bars) or *B. parapertussis* (filled bars), and then sacrificed 1, 3, or 7 days later. **(b)** Neutrophil death was determined by 7AAD-staining and flow cytometry. n=4 per group. **(c)** Myeloperoxidase (MPO) activity was determined in lung homogenates on D5+7. n= 8-9 per group. Data are expressed as the means ± SEMs and were analysed by 2-way ANOVA. *, †, and ‡ denote a significant difference at $p<0.05$ compared to PBS+PBS, PBS+*B. parapertussis*, and influenza virus+PBS-exposed mice, respectively. 2 icons denote $p<0.01$; 3 icons denote $p<0.001$.

Figure 7

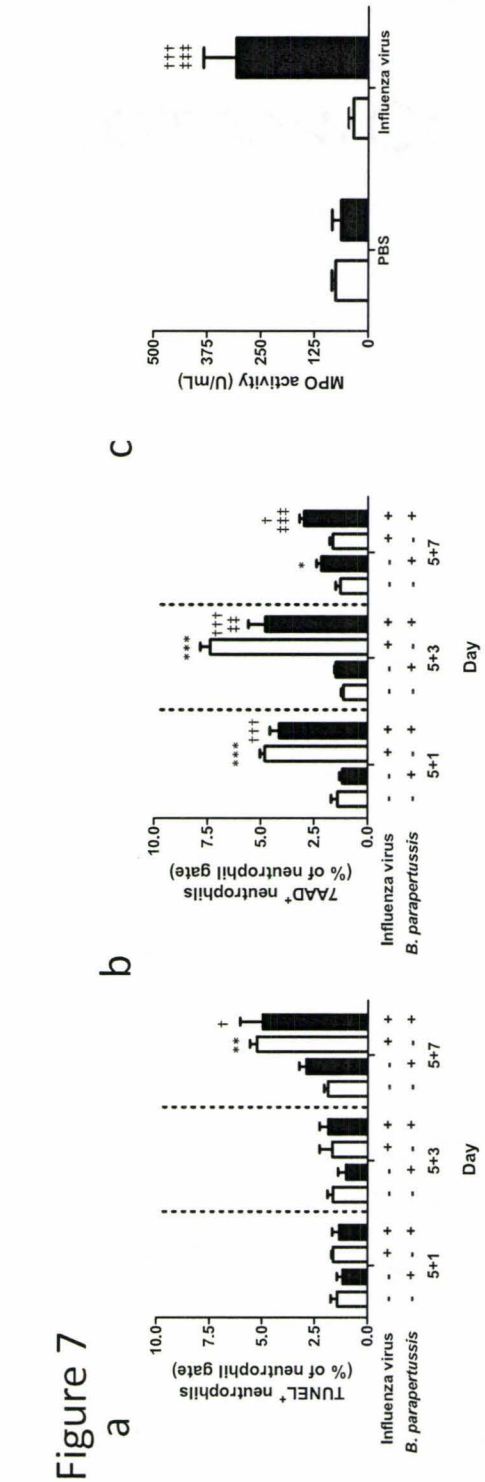
a
TUNEL+ neutrophils (% of neutrophil gate)
10.0
7.5
5.0
2.5
0.0
Influenza virus - - + + - - + + -
B. parapertussis - + - + - + - + +
5+1 5+3 5+7
Day
b
7AAD+ neutrophils (% of neutrophil gate)
10.0
7.5
5.0
2.5
0.0
Influenza virus - - + + - - + + -
B. parapertussis - + - + - + - + +
5+1 5+3 5+7
Day
c
MPO activity (U/mL)
500
375
250
125
0
PBS
Influenza virus

Figure 8: Increased chemokine expression in the lungs of heterologously-infected mice. Mice were given an intranasal administration of PBS or influenza virus as indicated, challenged intranasally with PBS or *B. parapertussis* 5 days later, and sacrificed 1, 3, 7, and 14 days later. **(a)** Heatmap of bead-array analyses of cytokines in lung homogenates of animals given treatments and at timepoints indicated. Blue cells denote low concentrations of given cytokine, and red denote high concentrations, with gradations through black indicating intermediate concentrations. Cytokines are sorted from greatest increase in expression between heterologous- and influenza virus-only infected mice on day 5+7 to greatest decrease in expression. Each cell represents the mean of homogenates obtained from 4 independent animals. **(b)** Expression of KC (top) and MIP-2 (bottom) in lung homogenates as confirmed by ELISA on days 5+1, 5+3, and 5+7 (left to right) in mice given PBS or influenza virus as indicated, then challenged 5 days later with PBS (open bars) or *B. parapertussis* (filled bars). **(c)** Levels of KC (left) and MIP-2 (right) in the BAL 7 days post-challenge. n= 3-4 per group. **(d)** KC expression in the sera 7 days post-challenge; (n=3-4 per group, MIP-2 expression was below the limit of detection). Data are expressed as the means ± SEMs and were analysed by 2-way ANOVA. *, †, and ‡ denote a significant difference at $p<0.05$ compared to PBS+PBS, PBS+*B. parapertussis*, and influenza virus+PBS-exposed mice, respectively. 2 icons denote $p<0.01$; 3 icons denote $p<0.001$. ELISA data are representative of at least two independent experiments.

Figure 8

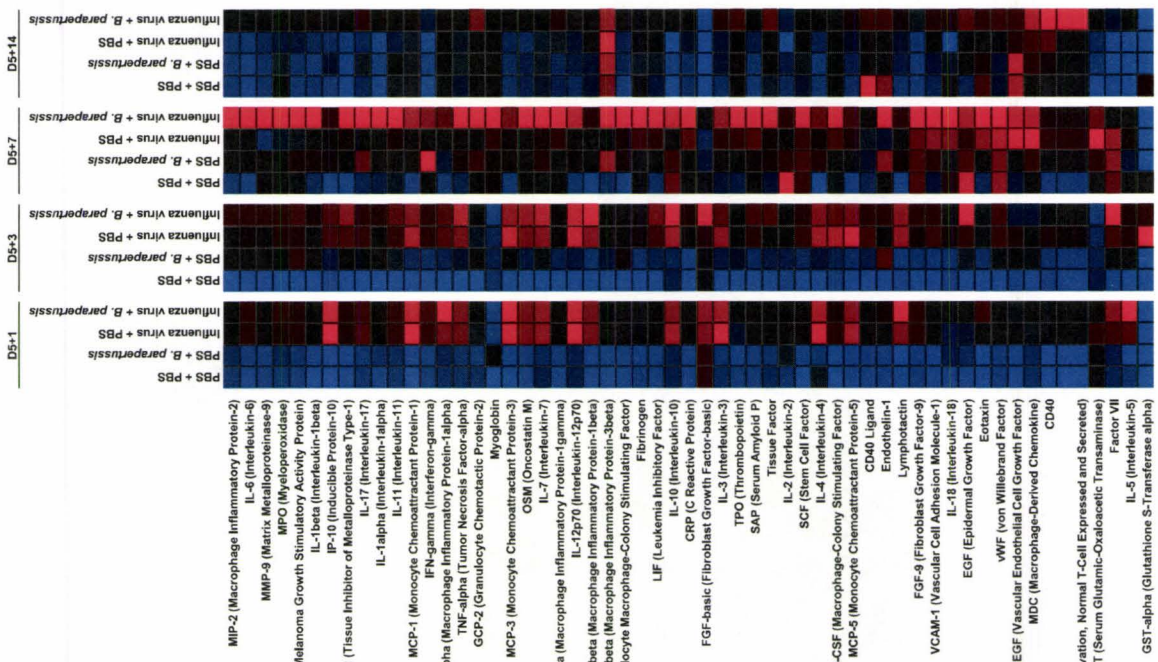
a
D5+1
D5+3
D5+7
D5+14
PBS + PBS
PBS + B. parapertussis
Influenza virus + PBS
Influenza virus + B. parapertussis
MIP-2 (Macrophage Inflammatory Protein-2)
IL-6 (Interleukin-6)
MMP-9 (Matrix Metalloproteinase-9)
MPO (Myeloperoxidase)
KC/GROalpha (Melanoma Growth Stimulatory Activity Protein)
IL-1beta (Interleukin-1beta)
IP-10 (Inducible Protein-10)
TIMP-1 (Tissue Inhibitor of Metalloproteinase Type-1)
IL-17 (Interleukin-17)
IL-1alpha (Interleukin-1alpha)
IL-11 (Interleukin-11)
MCP-1 (Monocyte Chemoattractant Protein-1)
IFN-gamma (Interferon-gamma)
MIP-1alpha (Macrophage Inflammatory Protein-1alpha)
TNF-alpha (Tumor Necrosis Factor-alpha)
GCP-2 (Granulocyte Chemotactic Protein-2)
Myoglobin
MCP-3 (Monocyte Chemoattractant Protein-3)
OSM (Oncostatin M)
IL-7 (Interleukin-7)
MIP-1gamma (Macrophage Inflammatory Protein-1gamma)
IL-12p70 (Interleukin-12p70)
MIP-1beta (Macrophage Inflammatory Protein-1beta)
MIP-3beta (Macrophage Inflammatory Protein-3beta)
GM-CSF (Granulocyte Macrophage-Colony Stimulating Factor)
Fibrinogen
LIF (Leukemia Inhibitory Factor)
IL-10 (Interleukin-10)
CRP (C Reactive Protein)
FGF-basic (Fibroblast Growth Factor-basic)
IL-3 (Interleukin-3)
TPO (Thrombopoietin)
SAP (Serum Amyloid P)
Tissue Factor
IL-2 (Interleukin-2)
SCF (Stem Cell Factor)
IL-4 (Interleukin-4)
M-CSF (Macrophage-Colony Stimulating Factor)
MCP-5 (Monocyte Chemoattractant Protein-5)
CD40 Ligand
Endothelin-1
Lymphotactin
FGF-9 (Fibroblast Growth Factor-9)
VCAM-1 (Vascular Cell Adhesion Molecule-1)
IL-18 (Interleukin-18)
EGF (Epidermal Growth Factor)
Eotaxin
vWF (von Willebrand Factor)
VEGF (Vascular Endothelial Cell Growth Factor)
MDC (Macrophage-Derived Chemokine)
CD40
RANTES (Regulation Upon Activation, Normal T-Cell Expressed and Secreted)
SGOT (Serum Glutamic-Oxaloacetic Transaminase)
Factor VII
IL-5 (Interleukin-5)
GST-alpha (Glutathione S-Transferase alpha)
b
D5+1
D5+3
D5+7
KC (pg/mL)
MIP-2 (pg/mL)
PBS
Influenza virus
c
KC (pg/mL)
MIP-2 (pg/mL)
d
KC (pg/mL)

Figure 9: Therapeutic neutralization of MIP-2 reduces pulmonary neutrophilia, improves clinical presentation and lessens weight loss in heterologously-infected mice. (a) Symptom scores on Day 5+7 for mice given an intranasal administration of influenza virus, and then challenged intranasally 5 days later with *B. parapertussis,* and treated beginning on Day 5+3 with a daily i.p. injection of control rabbit (rbt) IgG (black icons) or anti-MIP-2 (grey icons). Mice were scored by a blinded investigator on a scale from 0 (no distress) to 8 (severe distress). Each icon represents an individual animal. **(b)** Body weight change at the time of sacrifice on Day 5+7 for heterologously-infected mice given rabbit IgG i.p (black hatched boxes) or anti-MIP-2 antibodies (grey hatched boxes) commencing on D5+3; n = 15 and 17 mice, respectively. Lines within boxplots denote means, with whiskers denoting the 90% confidence intervals. **(c)** Equivalent lung bacterial burdens on D5+7 in heterologously-infected mice treated with IgG (black hatched bars) or anti-MIP-2 antibodies (grey hatched bars). n=6 and 7 mice, respectively. **(d)** Reduced neutrophilia on D5+7 in the lungs of mice treated with anti-MIP-2 compared to treatment with control IgG; n=14 and 17 mice, respectively. Data are representative of at least two independent experiments. Data are expressed as the means ± SEMs and were analysed by 2-way ANOVA. § denotes a statistically significant difference at $p<0.05$ compared to influenza virus+*B. parapertussis*-exposed mice. 2 icons denote $p<0.01$; 3 icons denote $p<0.001$.

Figure 9

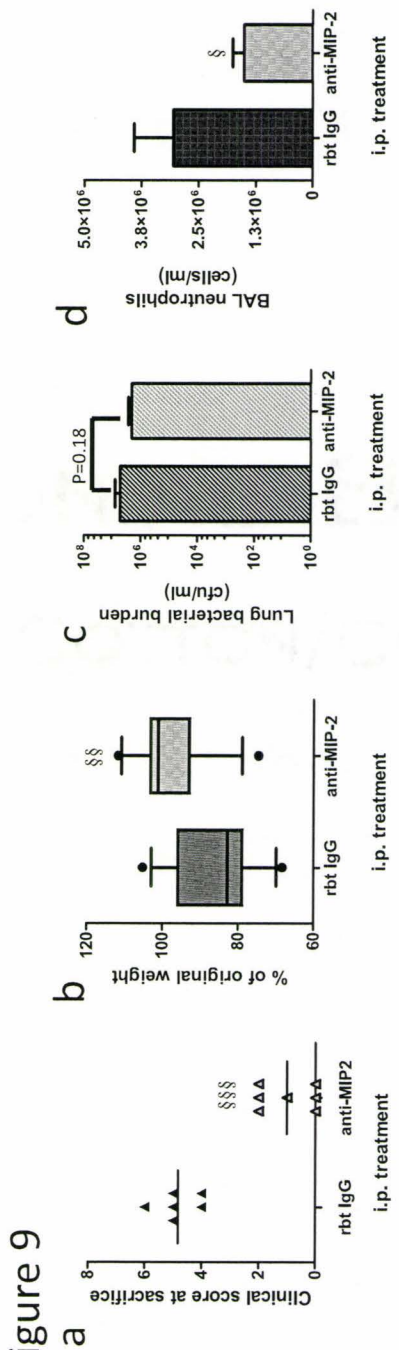
a
Clinical score at sacrifice
rbt IgG
anti-MIP2
i.p. treatment
b
% of original weight
rbt IgG
anti-MIP-2
i.p. treatment
c
Lung bacterial burden (cfu/ml)
P=0.18
rbt IgG
anti-MIP-2
i.p. treatment
d
BAL neutrophils (cells/ml)
rbt IgG
anti-MIP-2
i.p. treatment

Figure 10: Immunoblockade of CXCR2 impairs clinical performance and antibacterial immunity during heterologous infection. Mice were given an intranasal administration of influenza virus, then challenged intranasally 5 days later with *B. parapertussis,* and treated i.p. with normal goat sera (black icons) or anti-CXCR2 hyperimmune antisera (grey). **(a)** Increased weight loss and **(b)** bacterial burden at the time of sacrifice (day 5+7) in mice treated with a daily administration of anti-CXCR2 hyperimmune antisera commencing on D5+3. n= 10 mice per group. Data are expressed as the means ± SEMs and are analysed by 2-way ANOVA. §§ denotes $p<0.01$ compared to influenza virus+*B. parapertussis*-exposed mice.

Figure 10

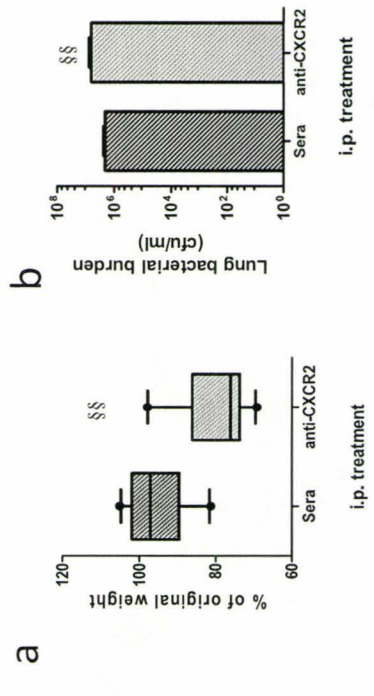
a
% of original weight
120
100
80
60
§§
Sera
anti-CXCR2
i.p. treatment
b
Lung bacterial burden
(cfu/ml)
10^8
10^6
10^4
10^2
10^0
§§
Sera
anti-CXCR2
i.p. treatment

Figure 11: Influenza virus infection attenuates alveolar macrophage Responses to lipopolysaccharide. Mice were given an intranasal administration of $2.5x10^5$ pfu of influenza virus (filled bars) or sterile PBS (open bars). Five (5), 14, and 84 days (d) later, alveolar macrophages were collected, and cultured in the presence of sterile media only (cRPMI), 1μg/ml LPS, 10 μg/ml poly (I:C) for 6 or 24 hours as indicated. Levels of the inflammatory mediators **(a)** TNFα, **(b)** MIP-1α, **(c)** KC, and **(d)** MIP-2 were measured in culture supernatants by ELISA. Cultures were performed in triplicate; n= 4-10 mice per group. Data are expressed as the means of individual animals ± SEMs and were analysed by 2-way ANOVA. * denotes a significant difference at $p<0.05$ compared to cells from PBS-exposed mice stimulated with the same ligand. 2 icons denote $p<0.01$; 3 icons denote $p<0.001$.

Figure 11

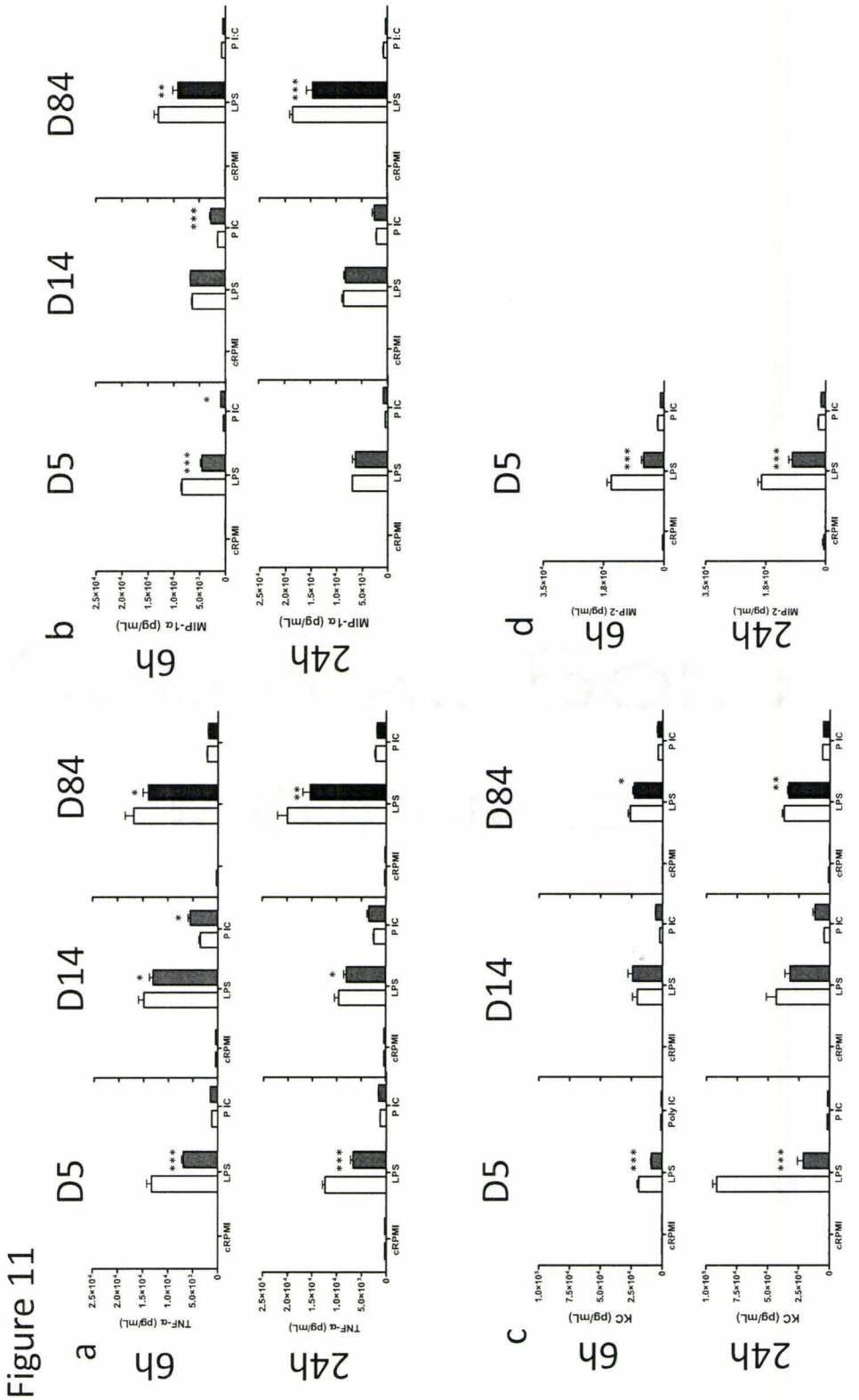
a
b
c
d
6h
24h
D5
D14
D84
TNF-α (pg/mL)
MIP-1α (pg/mL)
KC (pg/mL)
MIP-2 (pg/mL)
cRPMI
LPS
P:IC
Poly IC

Figure 12: A delay in bacterial challenge attenuates the severity of heterologous infection-related inflammation. Mice were given sterile PBS or influenza virus intranasally, and challenged with sterile PBS (open bars) or *B. parapertussis* (filled bars) 14 days later. Broncho-alveolar lavage inflammation was assessed in terms of the total BAL cell number (TCN), number of neutrophils (PMNs), and mononuclear cells (MNCs) 1 (upper panel), 3 (middle panel), and 7 (lower panel) days post-challenge. n=3-5 mice per group. Data are expressed as the means ± SEMs and were analysed by 2-way ANOVA. *, †, and ‡ denote a statistically significant difference at $p<0.05$ compared to PBS+PBS, PBS+*B. parapertussis*, and influenza virus+PBS-exposed mice, respectively. 2 icons denote $p<0.01$; 3 icons denote $p<0.001$.

Figure 12

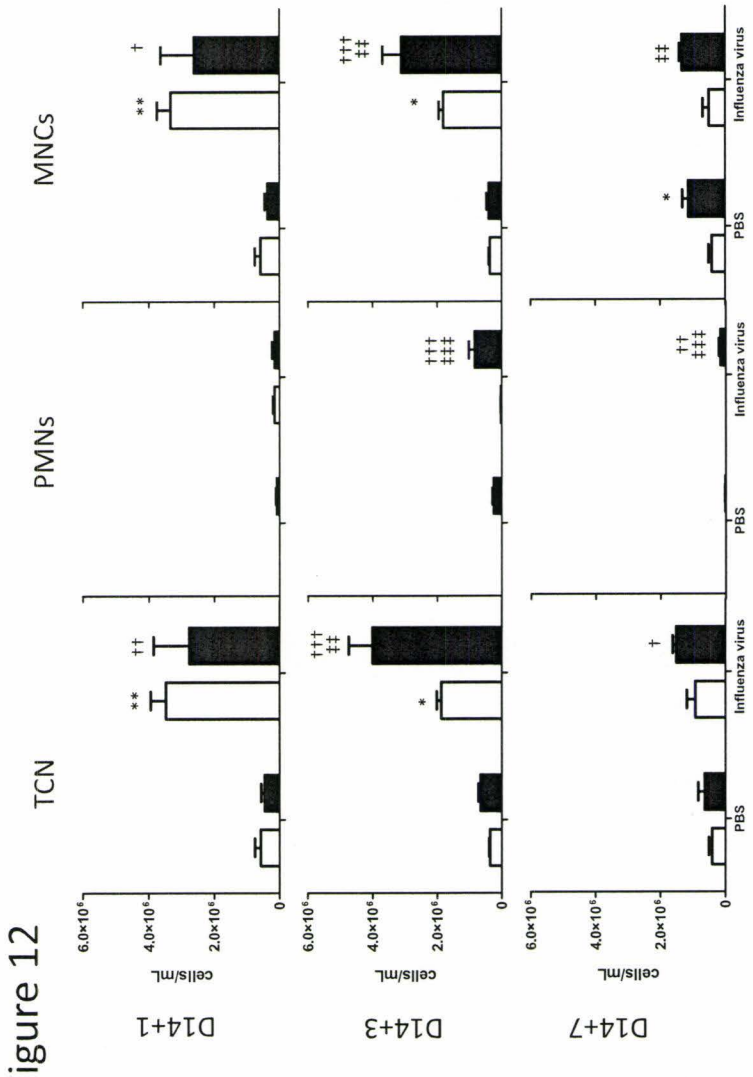
TCN
PMNs
MNCs
D14+1
D14+3
D14+7
cells/mL
6.0×10⁶
4.0×10⁶
2.0×10⁶
0
PBS
Influenza virus
PBS
Influenza virus
PBS
Influenza virus

Figure 13: Long-lived impact of influenza virus infection on antibacterial responses. Mice were given sterile PBS or influenza virus intranasally, then challenged with sterile PBS (open bars) or *B. parapertussis* (filled bars) 90 days (D) later. **(a)** Broncho-alveolar lavage inflammation was assessed in terms of the total BAL cell number (TCN), number of neutrophils (PMNs), and mononuclear cells (MNCs) 1 (upper panels), 3 (middle panels), and 7 days later (lower panels). n=3-5 mice per group. **(b)** Bacterial burdens were assessed in lung homogenates at the same timepoints (n=4 per group). Data are expressed as the means ± SEMs and were analysed by 2-way ANOVA. *, †, and ‡ denote a statistically significant difference at $p<0.05$ compared to PBS+PBS, PBS+*B. parapertussis*, and influenza virus+PBS-exposed mice, respectively. 2 icons denote $p<0.01$; 3 icons denote $p<0.001$.

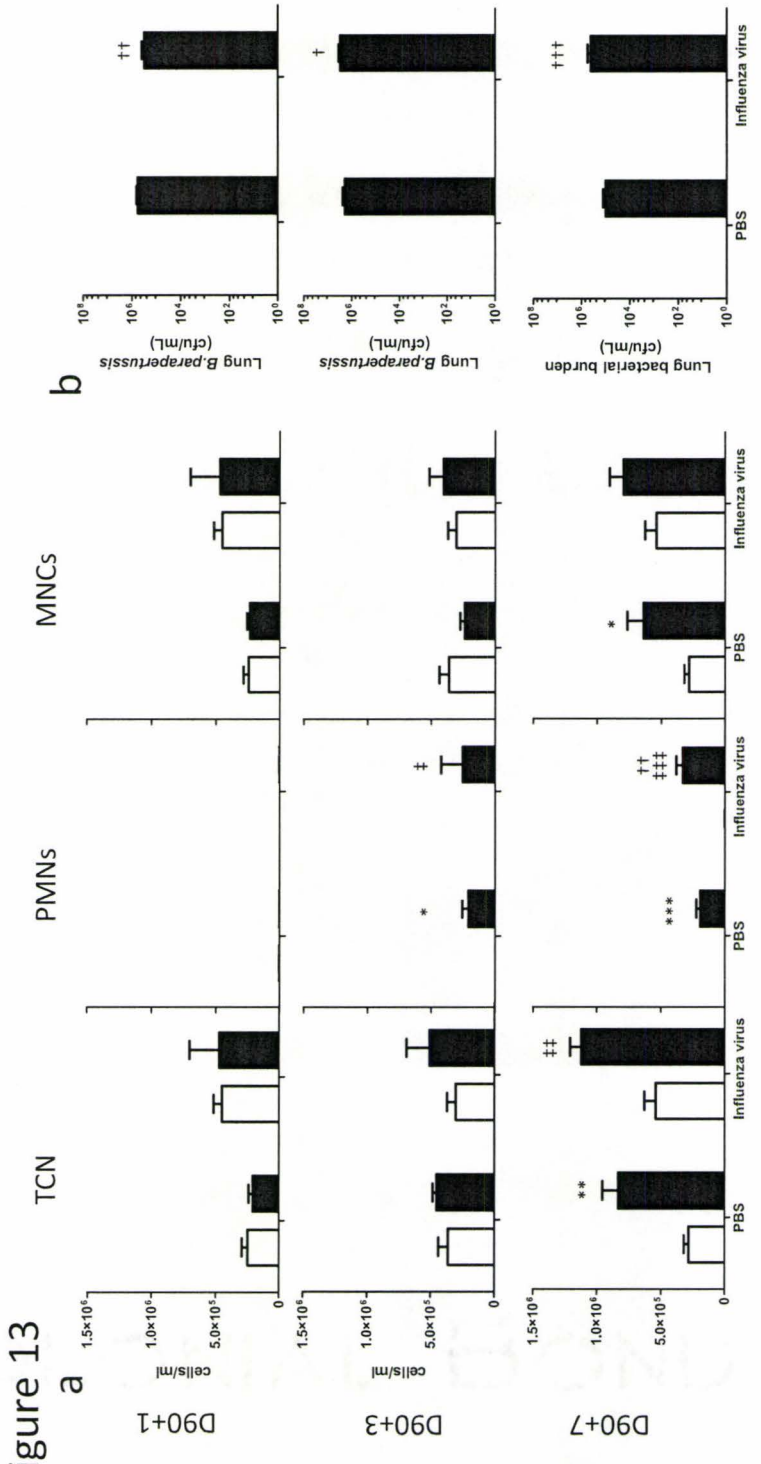
Figure 13
a
TCN
PMNs
MNCs
D90+1
D90+3
D90+7
cells/ml
PBS
Influenza virus
b
Lung B.parapertussis (cfu/mL)
Lung bacterial burden (cfu/mL)

Figure 14: Pathogen sequence plays a role in determining the outcome of heterologous infection. Mice were given $5x10^5$ cfu of *B. parapertussis* (triangles) or sterile PBS (squares) i.n., then challenged 7 days later with $2.5x10^5$ pfu of influenza virus (black icons) or sterile PBS (grey icons). **(a)** On D7+5, weight loss was assessed, **(b)** and broncho-alveolar lavage inflammation was quantified in terms of total cells (TCN), neutrophils (PMNs), and mononuclear cells (MNCs). Filled bars represent B. parapertussis-infected groups, while open bars represent groups given sterile PBS. Data are expressed as the means ± SEMs and were analysed by 2-way ANOVA. *, †, and ‡ denote a significant difference at $p<0.05$ compared to PBS+PBS, PBS+*B. parapertussis*, and influenza virus+PBS-exposed mice, respectively. 2 icons denote $p<0.01$; 3 icons denote $p<0.001$.

Figure 14

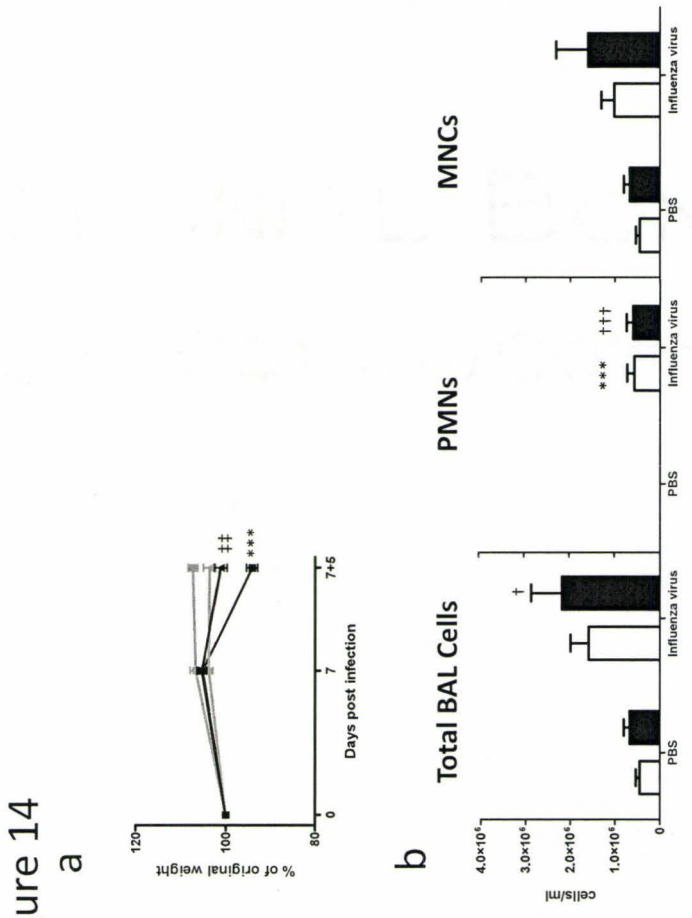
a
% of original weight
120
100
80
0
7
7+6
Days post infection
***
‡‡
b
Total BAL Cells
PMNs
MNCs
cells/ml
4.0×10⁶
3.0×10⁶
2.0×10⁶
1.0×10⁶
0
PBS
Influenza virus
†
***
†††

Figure 15: Impact of *B. parapertussis* infection on *ex vivo* alveolar macrophage (AM) responses. Mice were given an intranasal administration of $5x10^5$ cfu *B. parapertussis* (filled bars) or sterile PBS (open bars). Seven (7), 21, and 84 days later AMs were collected and cultured in the presence of 1μg/ml LPS or 10 μg/ml poly (I:C) for 6 or 24 hours as indicated. Levels of the inflammatory mediators **(a)** TNFα, **(b)** MIP-1α, **(c)** KC, and **(d)** MIP-2 were measured in culture supernatants by ELISA. Cultures were performed in triplicate, and n= 4-10 mice per group. Data are expressed as the means of individual animals ± SEMs and were analysed by 2-way ANOVA. * denotes a statistically significant difference at $p<0.05$ compared to cells from PBS-exposed mice stimulated with the same ligand. 2 icons denote $p<0.01$; 3 icons denote $p<0.001$.

Figure 15

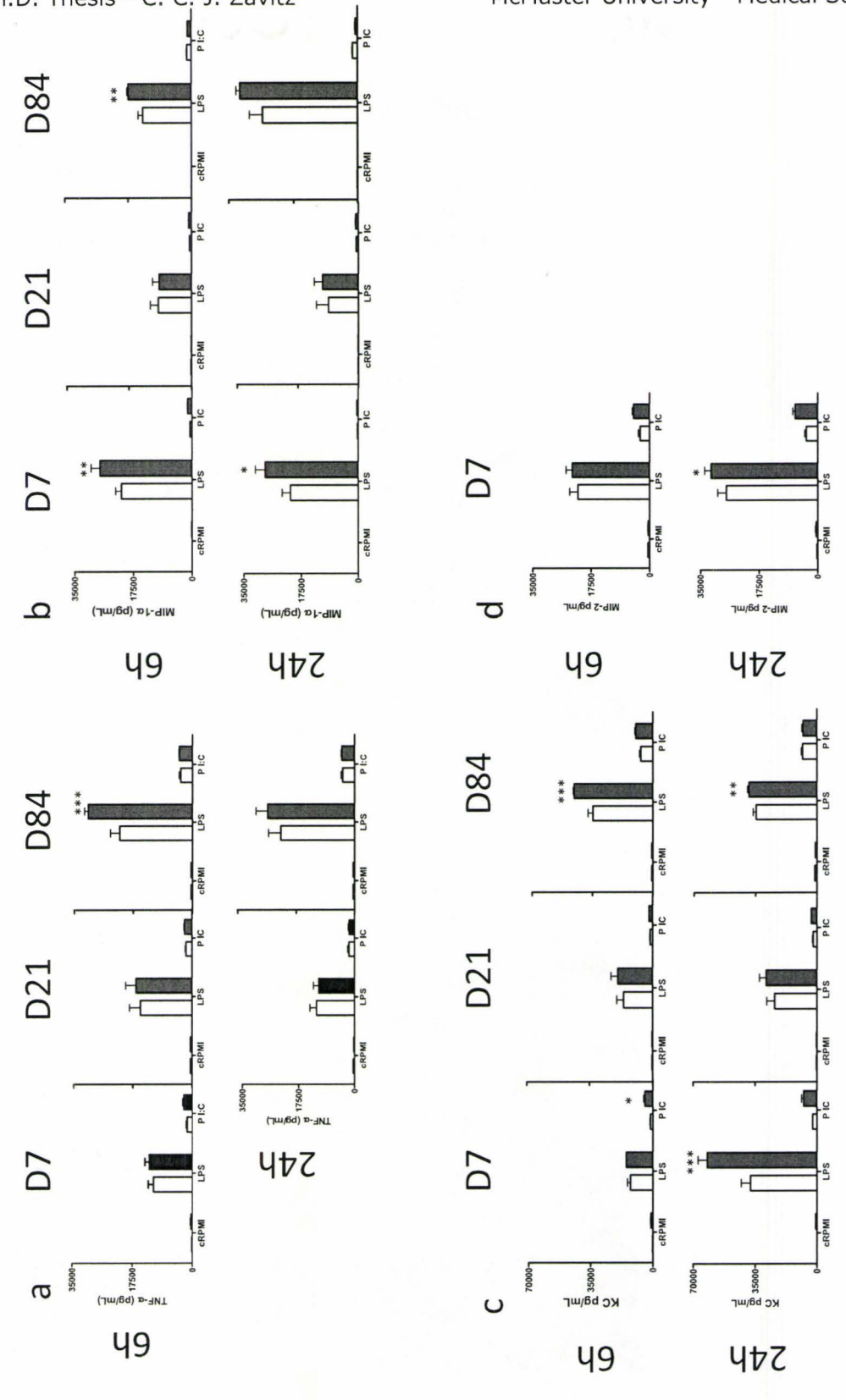
a
b
c
d
D7
D21
D84
6h
24h
cRPMI
LPS
P:IC
TNF-α (pg/mL)
MIP-1α (pg/mL)
KC pg/mL
MIP-2 pg/mL
35000
17500
0
70000

Figure 16: Functional equivalence of B cells from smoke- and sham-exposed animals *ex vivo*. (a, b) Splenocytes from animals exposed to the mainstream smoke of 2 or **(c-f)** 4 cigarettes per day (filled bars) or sham-exposed controls (open bars) were cultured in the presence of 20 µg/ml anti-IgM $f(ab')_2$ or 20 µg/ml anti-CD40 antibodies. **(a-d)** Proliferation was determined by $[^3H]$-thymidine incorporation after 72h of culture. Background proliferation calculated in unstimulated wells was subtracted from stimulated wells in order to determine delta counts per minute (CPMs) from triplicate cultures. **(e, f)** IgG secretion was determined in pooled supernatants from triplicate wells after 7 days of culture by ELISA. Data represent means ± SEMs, n = 4-5 per group, with one representative experiment of three shown. Data were analysed by 1-way ANOVA, and * denotes a statistically significant difference at $p<0.05$ compared to supernatants from cells cultured in cRPMI only.

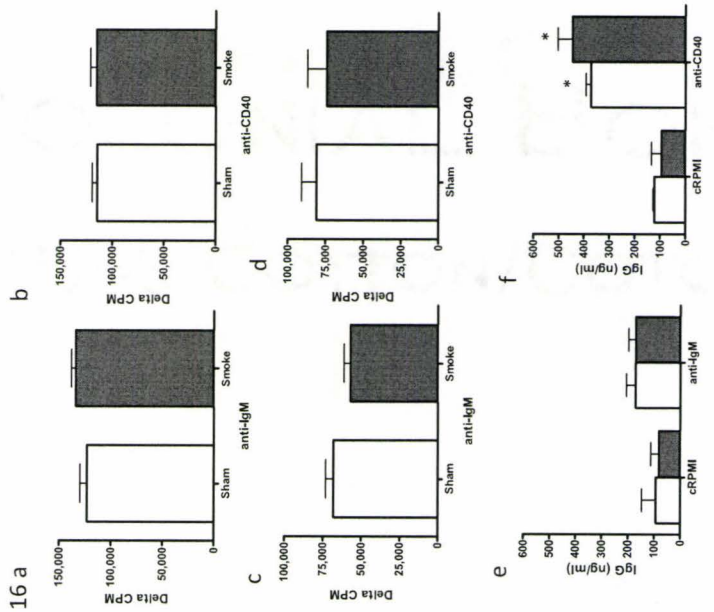
a
b
c
d
e
f
Delta CPM
150,000
100,000
50,000
0
Sham
Smoke
anti-IgM
anti-CD40
100,000
75,000
50,000
25,000
IgG (ng/ml)
600
500
400
300
200
100
cRPMI
*

Figure 16

Figure 17: Equivalent B-cell populations and *ex vivo* function in smoke- and sham-exposed animals. Splenocytes from smoke (filled bars)- and sham-exposed (white bars) animals were analyzed by flow cytometry. **(a)** representative plots, and **(b)** aggregate data are presented. **(c)** Splenic B-cells were magnetically purified by negative selection from smoke- and sham-exposed animals' spleens, and cultured in the presence of 20 μg/ml anti-IgM $f(ab')_2$ or 20 μg/ml anti-CD40. Proliferation was determined by $[^3H]$-Thymidine incorporation following 72 hours of culture and **(d)** secretion of IgG in day 6 cultures was assayed by ELISA. Flow cytometry data are shown as means ± SEMs, n = 3-5 per group, with one representative experiment of 2 shown. Cell culture data represent means ± SEMs, n = 5 per group, with one representative experiment of 2 shown. Data were analysed by 1-way ANOVA, and * denotes a statistically significant difference at $p<0.05$ compared to supernatants from cells cultured in cRPMI only.

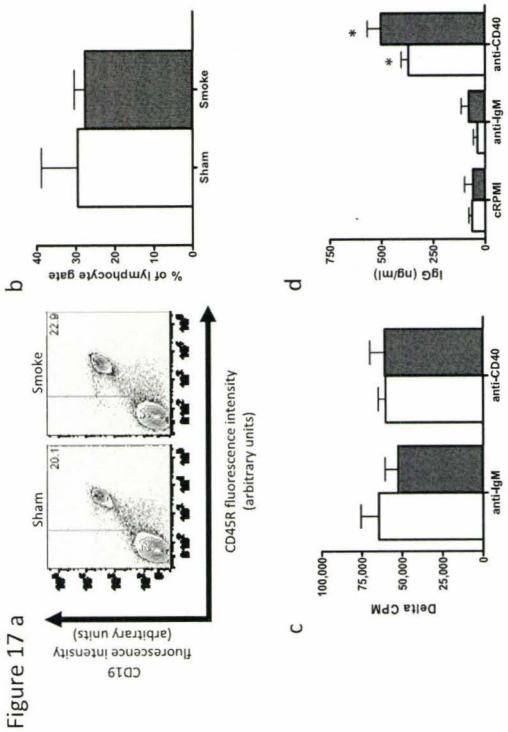
a
CD19
fluorescence intensity
(arbitrary units)
Sham
20.1
Smoke
22.9
CD45R fluorescence intensity
(arbitrary units)
b
% of lymphocyte gate
40
30
20
10
0
Sham
Smoke
c
Delta CPM
100,000
75,000
50,000
25,000
0
anti-IgM
anti-CD40
d
IgG (ng/ml)
750
500
250
0
cRPMI
anti-IgM
anti-CD40
*
*

Figure 17

Figure 18: Equivalent T cell function in smoke- and sham- exposed animals. Splenocytes and magnetically enriched T-cells from smoke- (filled bars) and sham-exposed animals (open bars) were cultured in the presence of 10 μg/ml anti-CD3 antibodies. **(a)** Proliferation was assayed by [^{3}H]-thymidine incorporation following 72 hours of culture. **(b)** IFNγ concentrations in culture supernatants at day 6 were assayed by ELISA. Data are shown as means from pooled triplicate cultures, ± SEMs. n = 4-5 per group, with one representative experiment of 2 shown. Data were analysed by 1-way ANOVA, and * denotes a statistically significant difference at $p<0.05$ compared to supernatants from cells cultured in cRPMI only.

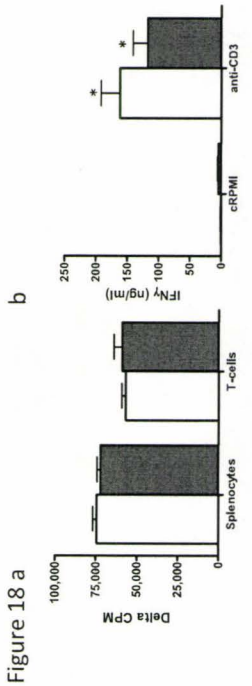
Delta CPM
100,000
75,000
50,000
25,000
0
Splenocytes
T-cells
b
IFNγ (ng/ml)
250
200
150
100
50
0
cRPMI
anti-CD3
*
*

Figure 18 a

Figure 19: Calcium fluxing in cells from smoke- and sham-exposed animals. Splenocytes from smoke- and sham-exposed mice were incubated with the calcium binding dye Fluo-4 and stained for flow cytometric analyses with fluorescent anti-CD3, -CD4, and -CD8, or anti-CD19 antibodies. Cells were acquired by flow cytometry for 30 seconds, then stimulated with anti-Armenian hamster antibodies to cross-link CD3, or stimulated with anti-mouse IgM antibodies to cross-link the B-cell receptor. Calcium flux was monitored over time in order to compare kinetics between smoke- and sham-derived cells. Ionomycin was added at the end of each experiment in order to demonstrate equal fluorophore accumulation in smoke- and sham-derived cells. Flow cytometry plots of **(a)** anti-CD3-induced calcium fluxing in CD4 (upper panel) and CD8 (lower panel) T-cells, and **(b)** anti-IgM induced calcium fluxing in B-cells. Plots are representative of 3-4 experiments.

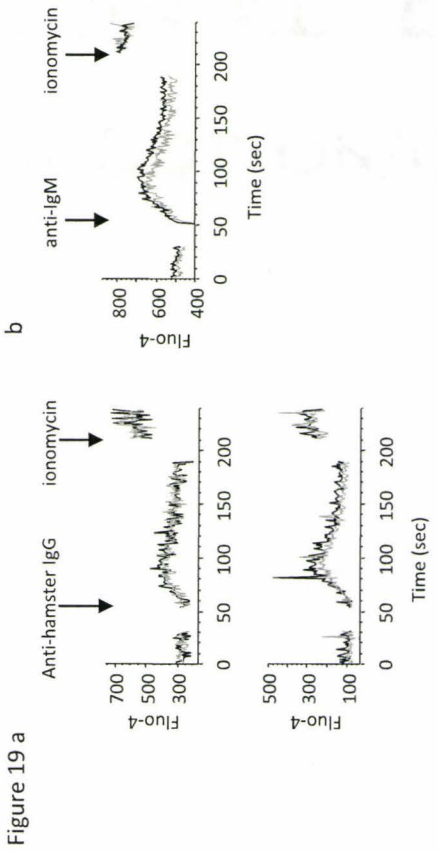
b
anti-IgM
ionomycin
Fluo-4
800
600
400
0 50 100 150 200
Time (sec)
Anti-hamster IgG
ionomycin
Fluo-4
700
500
300
0 50 100 150 200
Fluo-4
500
300
100
0 50 100 150 200
Time (sec)

Figure 19 a

Figure 20: Equivalent proliferation of regional and local lymphocytes from smoke- and sham-exposed animals. (a) Lymphocytes isolated from cervical lymph nodes **(b)** and lung mononuclear cells from smoke- (filled bars) and sham-exposed (open bars) were cultured with 20 µg/ml anti-IgM $f(ab')_2$, 20 µg/ml anti-CD40, or 10 ug/ml anti-CD3 antibodies for 72 hours and proliferation was determined by $[^3H]$-Thymidine incorporation. Data are shown as means from pooled triplicate cultures, ± SEMs. n = 3-5 per group, with one representative experiment of 2 shown.

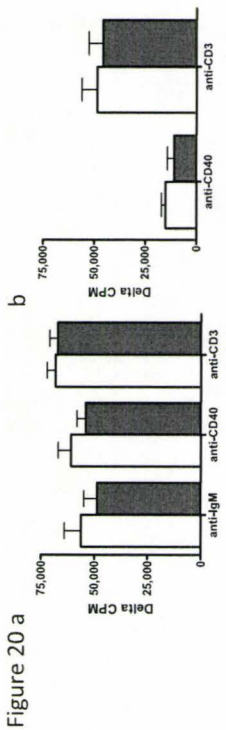
b
Delta CPM
75,000
50,000
25,000
0
anti-CD40
anti-CD3
Delta CPM
75,000
50,000
25,000
0
anti-IgM
anti-CD40
anti-CD3

Figure 20 a

Figure 21: **PBMCs from human smokers are not unresponsive to stimulation**. PBMCs from human smokers (filled bars) and never-smokers were cultured in the presence of 40 μg/ml anti-IgM, 1 μg/ml CD154 + 10 ng/ml IL4, or 10 μg/ml anti-CD3 and proliferation was determined by [3H] thymidine incorporation following 72 hours of culture. Data are shown as means from pooled duplicate cultures, ± SEMs. n=8 per group, pooled from two experiments.

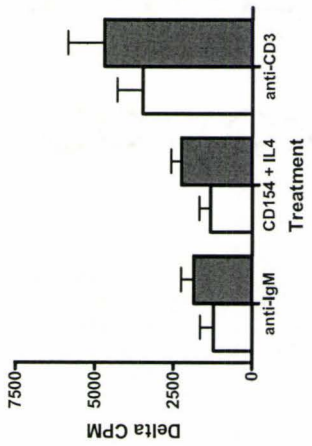
Delta CPM
7500
5000
2500
0
anti-IgM
CD154 + IL4
anti-CD3
Treatment

Figure 21

Table 7: Flow cytometric analyses of lymphocyte subsets in the lungs

	Sham (% of indicated gate)	Smoke
T-cells		
CD4+	54.9	52.7
CD25+	12.7	11.1
CD69+	15.4	13.4
CD8+	37.8	41.8
CD25+	4.1	2
CD69+	5.1	5.4
B-cells		
CD69+	1.16	1.56

Flow cytometric analyses of splenocytes isolated from sham-exposed mice or those exposed to smoke for a minimum of 8 weeks. Data are expressed as means of 5 mice. Data were analysed by students' T-test, and cell percentages were not significantly different between smoke- and sham-exposed mice.

Table 6: Bead-array cytokine analyses in the lung on day 5+14

	Concentration	Limit of Detection	PBS + PBS	PBS + *B. parapertussis*	Influenza + PBS	Influenza + *B. parapertussis*
CD40	pg/mL	2.4	946 ± 89.7	1103 ± 135	1670 ± 413 **	2355 ± 308 †††,‡‡
CD40 Ligand	pg/mL	18	981 ± 522	581 ± 205	593 ± 154	732 ± 246
CRP (C Reactive Protein)	ug/mL	0.0042	0.06 ± 0.02	0.06 ± 0.01	0.08 ± 0.02	0.16 ± 0.09 †,‡
EGF (Epidermal Growth Factor)	pg/mL	7.8	3.66 ± 0.24	4.23 ± 0.46	4.07 ± 0.69	5.04 ± 0.57 †,‡
Endothelin-1	pg/mL	13	6.59 ± 2.32	5.47 ± 1.08	5.37 ± 0.49	6.19 ± 0.23
Eotaxin	pg/mL	2.5	239 ± 29.3	193 ± 44	165 ± 37.1 *	221 ± 22.6 ‡‡
Factor VII	ng/mL	0.19	2.96 ± 0.16	2.9 ± 0.52	2.94 ± 0.18	4.02 ± 0.52 ††,‡‡
FGF-9 (Fibroblast Growth Factor-9)	ng/mL	0.20	0.38 ± 0.04	0.38 ± 0.1	0.4 ± 0.1	0.78 ± 0.31 ††,‡‡
FGF-basic (Fibroblast Growth Factor-basic)	ng/mL	0.12	6.68 ± 1.13	5.92 ± 2.72	5.83 ± 1.95	8.75 ± 2.83
Fibrinogen	ug/mL	0.85	105 ± 26.7	84.8 ± 6.33	103 ± 8.33	136 ± 33.7 ††
GCP-2 (Granulocyte Chemotactic Protein-2)	ng/mL	0.0049	1.52 ± 0.37	1.53 ± 0.23	1.66 ± 0.33	5.31 ± 2.93 ††,‡‡
GM-CSF (Granulocyte Macrophage-Colony Stimulating Factor)	pg/mL	1.7	2.3 ± 0.17	4.31 ± 1 *	4.62 ± 0.99 **	9.29 ± 1.32 †††,‡‡‡
GST-alpha (Glutathione S-Transferase alpha)	ng/mL	0.084	0 ± 0.01	0 ± 0	0 ± 0	0 ± 0
IFN-gamma (Interferon-gamma)	pg/mL	14	2.07 ± 0.41	2.98 ± 1.73	2.26 ± 0.86	6.64 ± 3.79 †,‡
IL-10 (Interleukin-10)	pg/mL	22	91.5 ± 11.9	98.6 ± 12.2	89.8 ± 4.05	170 ± 54.2 ††,‡‡
IL-11 (Interleukin-11)	pg/mL	17	8.49 ± 1.6	8.81 ± 2.14	6.86 ± 1.77	12.4 ± 5.82
IL-12p70 (Interleukin-12p70)	ng/mL	0.11	0.03 ± 0.01	0.04 ± 0.01	0.04 ± 0.01	0.06 ± 0.02 †,‡
IL-17 (Interleukin-17)	ng/mL	0.030	0 ± 0	0 ± 0	0 ± 0	0.01 ± 0 †††,‡‡‡
IL-18 (Interleukin-18)	ng/mL	0.13	3.02 ± 0.78	2.52 ± 0.54	1.66 ± 0.25 *	3.52 ± 1.12 ‡‡
IL-1alpha (Interleukin-1alpha)	pg/mL	9.0	170 ± 16	197 ± 55.8	166 ± 21.1	550 ± 180 †††,‡‡‡
IL-1beta (Interleukin-1beta)	ng/mL	0.089	2.8 ± 0.55	2.62 ± 0.31	3.04 ± 0.4	8.83 ± 5.08 †,‡‡
IL-2 (Interleukin-2)	pg/mL	13	8.09 ± 3.04	9.83 ± 6.67	4.54 ± 1.7	10.1 ± 4.23
IL-3 (Interleukin-3)	pg/mL	4.3	0.38 ± 0.07	0.7 ± 0.12	0.7 ± 0.12	1.71 ± 0.84 †,‡‡
IL-4 (Interleukin-4)	pg/mL	15	8.91 ± 1.68	8.56 ± 2.81	9.9 ± 1.87	15 ± 3.33 †,‡
IL-5 (Interleukin-5)	ng/mL	0.039	0 ± 0	0 ± 0	0 ± 0	0.02 ± 0.03
IL-6 (Interleukin-6)	pg/mL	2.8	2.29 ± 0.22	2.96 ± 0.67	4.09 ± 0.84	11.3 ± 5.35 †,‡‡
IL-7 (Interleukin-7)	ng/mL	0.062	0.03 ± 0.01	0.03 ± 0	0.03 ± 0.01	0.04 ± 0.01
IP-10 (Inducible Protein-10)	pg/mL	8.1	49.7 ± 8.3	96.5 ± 55.8	66.3 ± 6.15	226 ± 175 ‡
KC/GROalpha (Melanoma Growth Stimulatory Activity Protein)	ng/mL	0.035	0.02 ± 0	0.03 ± 0	0.04 ± 0.01	0.08 ± 0.03 ††,‡
LIF (Leukemia Inhibitory Factor)	pg/mL	8.7	328 ± 21.4	352 ± 37.6	380 ± 24.6	528 ± 122 ††,‡‡
Lymphotactin	pg/mL	17	61.7 ± 1.82	98.4 ± 28	113 ± 22	223 ± 83.6 ††,‡‡
MCP-1 (Monocyte Chemoattractant Protein-1)	pg/mL	3.4	103 ± 18.6	102 ± 24.2	98.2 ± 24.7	154 ± 60.4
MCP-3 (Monocyte Chemoattractant Protein-3)	pg/mL	6.3	54.4 ± 3.94	59.3 ± 13	65.1 ± 11.2	141 ± 64.7 ††,‡‡
MCP-5 (Monocyte Chemoattractant Protein-5)	pg/mL	9.3	17.3 ± 2.26	26.2 ± 7.55	34.9 ± 9.94	92.8 ± 38.9 †††,‡‡
M-CSF (Macrophage-Colony Stimulating Factor)	ng/mL	0.0036	0.37 ± 0.05	0.35 ± 0.02	0.37 ± 0.05	0.37 ± 0.07
MDC (Macrophage-Derived Chemokine)	pg/mL	4.4	207 ± 5.92	316 ± 75.6	397 ± 44	670 ± 325 †,‡
MIP-1alpha (Macrophage Inflammatory Protein-1alpha)	ng/mL	0.045	0.27 ± 0.04	0.27 ± 0.02	0.33 ± 0.03	0.48 ± 0.12 †††,‡‡
MIP-1beta (Macrophage Inflammatory Protein-1beta)	pg/mL	16	177 ± 14.7	174 ± 44	247 ± 41.3	513 ± 231 ††,‡‡
MIP-1gamma (Macrophage Inflammatory Protein-1gamma)	ng/mL	0.015	0.9 ± 0.13	0.83 ± 0.14	1.12 ± 0.12	3.26 ± 2.41 †,‡
MIP-2 (Macrophage Inflammatory Protein-2)	pg/mL	1.4	9.3 ± 0.92	9.41 ± 0.88	10.1 ± 1.03	21.9 ± 9.85 ††,‡‡
MIP-3beta (Macrophage Inflammatory Protein-3beta)	ng/mL	0.093	1.82 ± 0.07	2.05 ± 0.34	2.17 ± 0.29	1.98 ± 0.36
MMP-9 (Matrix Metalloproteinase-9)	ng/mL	0.10	78 ± 11.2	79.4 ± 20.4	97.2 ± 12.7	159 ± 94.3
MPO (Myeloperoxidase)	ng/mL	0.19	275 ± 74.7	223 ± 119	194 ± 91.1	436 ± 411
Myoglobin	ng/mL	0.24	40.5 ± 21	37 ± 12	47.4 ± 35.5	45.8 ± 21.6
OSM (Oncostatin M)	ng/mL	0.026	0.04 ± 0	0.04 ± 0.01	0.04 ± 0	0.06 ± 0.01 †,‡‡
RANTES (Regulation Upon Activation, Normal T-Cell Expressed and Secreted)	pg/mL	9.6	11.5 ± 2.83	11.9 ± 4.45	19.2 ± 3.68	88.9 ± 102
SAP (Serum Amyloid P)	ug/mL	0.027	0.16 ± 0.03	0.17 ± 0.02	0.22 ± 0.03	0.32 ± 0.07 †††,‡‡
SCF (Stem Cell Factor)	pg/mL	15	218 ± 13	235 ± 27.2	243 ± 37.6	248 ± 34.6
SGOT (Serum Glutamic-Oxaloacetic Transaminase)	ug/mL	0.37	1.56 ± 3.11	2.71 ± 1.82	3.35 ± 2.25	6.03 ± 4.4
TIMP-1 (Tissue Inhibitor of Metalloproteinase Type-1)	ng/mL	0.036	0.31 ± 0.03	0.45 ± 0.09	0.66 ± 0.18	2.69 ± 2.68
Tissue Factor	ng/mL	0.10	2.2 ± 0.15	2.62 ± 0.71	2.53 ± 0.39	3.55 ± 0.82 †,‡
TNF-alpha (Tumor Necrosis Factor-alpha)	ng/mL	0.027	0.03 ± 0	0.03 ± 0.01	0.03 ± 0.01	0.05 ± 0.02 †,‡
TPO (Thrombopoietin)	ng/mL	0.53	11.1 ± 0.78	11.6 ± 1.55	11.1 ± 1.61	15.3 ± 2.44 ††,‡‡
VCAM-1 (Vascular Cell Adhesion Molecule-1)	ng/mL	0.19	23.9 ± 1.52	29.3 ± 5.33	37.3 ± 8.63	82.8 ± 38.3 ††,‡‡
VEGF (Vascular Endothelial Cell Growth Factor)	pg/mL	7.6	4070 ± 297	4180 ± 297	3215 ± 395 **	3385 ± 420 ††
vWF (von Willebrand Factor)	ng/mL	0.99	4.92 ± 0.53	4.85 ± 1.45	5.31 ± 1.04	8.15 ± 3.42

Tabular presentation of bead-array cytokine analysis in lung homogenates of animals given PBS or influenza virus intranasally on day 0, challenged with PBS or *B. parapertussis* on day 5, and sacrificed 14 days later. Data are presented as means ± SEMs, organized alphabetically by molecule name. n=4 per group. *, †, and ‡ denote a statistically significant difference at $p<0.05$ by 2-way ANOVA compared to PBS+PBS, PBS+*B. parapertussis*, and influenza virus+PBS-exposed mice, respectively. 2 icons denote $p<0.01$; 3 icons denote $p<0.001$.

Table 5: Bead-array cytokine analyses in the lung on day 5+7

	Concentration	Limit of Detection	PBS + PBS	PBS + *B. parapertussis*	Influenza + PBS	Influenza + *B. parapertussis*
CD40	pg/mL	2.4	359 ± 74.7	765 ± 162	1338 ± 184 ***	1120 ± 403
CD40 Ligand	pg/mL	18	317 ± 180	404 ± 121	439 ± 77	616 ± 188
CRP (C Reactive Protein)	ug/mL	0.0042	0.11 ± 0.04	0.23 ± 0.03	0.86 ± 0.14 *	1.6 ± 0.64 ††, ‡
EGF (Epidermal Growth Factor)	pg/mL	7.8	5.6 ± 1.17	4.92 ± 0.68	4.72 ± 0.28	5.49 ± 0.32
Endothelin-1	pg/mL	13	5.56 ± 1.15	6.65 ± 0.83	5.12 ± 0.75	6.97 ± 1.34 ‡
Eotaxin	pg/mL	2.5	99.3 ± 28.2	155 ± 8.89	307 ± 48 ***	349 ± 91.8 ††
Factor VII	ng/mL	0.19	6.01 ± 1.81	6.47 ± 0.98	6.58 ± 0.24	4.68 ± 0.38
FGF-9 (Fibroblast Growth Factor-9)	ng/mL	0.20	1.4 ± 0.67	1.4 ± 0.78	1.52 ± 0.38	1.91 ± 0.61
FGF-basic (Fibroblast Growth Factor-basic)	ng/mL	0.12	58.1 ± 11.2	40.1 ± 7.26	32 ± 19.5 *	59.1 ± 17.7 ‡
Fibrinogen	ug/mL	0.85	116 ± 31.6	168 ± 38.6	393 ± 44.3	818 ± 485 ††, ‡
GCP-2 (Granulocyte Chemotactic Protein-2)	ng/mL	0.0049	1.36 ± 0.31	3.63 ± 0.5 *	2.19 ± 0.4	7.75 ± 1.96 †††, ‡‡‡
GM-CSF (Granulocyte Macrophage-Colony Stimulating Factor)	pg/mL	1.7	2.08 ± 0.68	10.5 ± 2.17 **	10.8 ± 1.45 ***	22.5 ± 4.04 †††, ‡‡‡
GST-alpha (Glutathione S-Transferase alpha)	ng/mL	0.084	0 ± 0	0 ± 0	0 ± 0	0 ± 0
IFN-gamma (Interferon-gamma)	pg/mL	14	14.7 ± 14.8	60.3 ± 44.8	12.4 ± 3.17	46.3 ± 42.6
IL-10 (Interleukin-10)	pg/mL	22	276 ± 26.5	240 ± 46.7	172 ± 23.9 **	347 ± 53.2 ††, ‡‡
IL-11 (Interleukin-11)	pg/mL	17	7.98 ± 2.97	20.2 ± 6.45	39.4 ± 2.98	164 ± 140 †, ‡
IL-12p70 (Interleukin-12p70)	ng/mL	0.11	0.02 ± 0.01	0.07 ± 0.03	0.06 ± 0.02	0.15 ± 0.03 †††, ‡‡‡
IL-17 (Interleukin-17)	ng/mL	0.030	0 ± 0	0.01 ± 0.01 *	0 ± 0	0.02 ± 0.01 ‡‡
IL-18 (Interleukin-18)	ng/mL	0.13	3.53 ± 0.61	3.01 ± 0.2	5.05 ± 0.35 ***	5.98 ± 0.52 †††, ‡
IL-1alpha (Interleukin-1alpha)	pg/mL	9.0	327 ± 166	604 ± 136	440 ± 20.8	2168 ± 750 †††, ‡‡‡
IL-1beta (Interleukin-1beta)	ng/mL	0.089	3 ± 0.87	9.77 ± 4.78	6.5 ± 1.9	37.5 ± 16.6 ††, ‡‡‡
IL-2 (Interleukin-2)	pg/mL	13	88.8 ± 101	36.8 ± 30.5	22 ± 9.37	34.5 ± 9.23
IL-3 (Interleukin-3)	pg/mL	4.3	0.66 ± 0.21	1.41 ± 0.53	1.82 ± 0.39	3.21 ± 1.38 †, ‡
IL-4 (Interleukin-4)	pg/mL	15	7.22 ± 2.52	18 ± 5.01 **	16.6 ± 2.81 **	24.5 ± 4.63 †, ‡
IL-5 (Interleukin-5)	ng/mL	0.039	0.02 ± 0.05	0.01 ± 0.03	0.18 ± 0.12 *	0.11 ± 0.05
IL-6 (Interleukin-6)	ng/mL	2.8	3.38 ± 2.86	16.5 ± 2.97	17.4 ± 2.17	294 ± 395
IL-7 (Interleukin-7)	ng/mL	0.062	0.03 ± 0	0.06 ± 0.01 *	0.06 ± 0.01	0.16 ± 0.03 †††, ‡‡‡
IP-10 (Inducible Protein-10)	pg/mL	8.1	34.4 ± 11.2	659 ± 161 *	171 ± 30.3	981 ± 663 ‡‡
KC/GROalpha (Melanoma Growth Stimulatory Activity Protein)	ng/mL	0.035	0.05 ± 0.09	0.15 ± 0.02	0.05 ± 0.01	0.48 ± 0.12 †††, ‡‡‡
LIF (Leukemia Inhibitory Factor)	pg/mL	8.7	277 ± 30.9	423 ± 49	803 ± 12.8	1662 ± 1258 †
Lymphotactin	pg/mL	17	30.4 ± 7.34	223 ± 58.7 ***	198 ± 39.4 ***	261 ± 75.1
MCP-1 (Monocyte Chemoattractant Protein-1)	pg/mL	3.4	33.7 ± 32.3	194 ± 28.6	237 ± 51.8	971 ± 321 †††, ‡‡‡
MCP-3 (Monocyte Chemoattractant Protein-3)	pg/mL	6.3	42.4 ± 36	299 ± 42.6 *	306 ± 54.3 **	925 ± 163 †††, ‡‡‡
MCP-5 (Monocyte Chemoattractant Protein-5)	pg/mL	9.3	8.37 ± 6.79	62.7 ± 13.9 ***	106 ± 9.7 ***	154 ± 16.2 †††, ‡‡‡
M-CSF (Macrophage-Colony Stimulating Factor)	ng/mL	0.0036	0.32 ± 0.05	0.42 ± 0.04	0.6 ± 0.02 **	0.89 ± 0.2 †††, ‡‡
MDC (Macrophage-Derived Chemokine)	pg/mL	4.4	163 ± 19.5	355 ± 130	716 ± 110 ***	673 ± 186 †
MIP-1alpha (Macrophage Inflammatory Protein-1alpha)	ng/mL	0.045	0.18 ± 0.03	0.23 ± 0.03	0.3 ± 0.02 *	1.07 ± 0.12 †††, ‡‡‡
MIP-1beta (Macrophage Inflammatory Protein-1beta)	pg/mL	16	54.6 ± 16.6	249 ± 49.5 *	327 ± 73.5 **	773 ± 156 †††, ‡‡‡
MIP-1gamma (Macrophage Inflammatory Protein-1gamma)	ng/mL	0.015	1.4 ± 0.82	1.83 ± 0.34	4.11 ± 0.63	10.4 ± 4.32 †††, ‡‡
MIP-2 (Macrophage Inflammatory Protein-2)	pg/mL	1.4	9.95 ± 10.3	37.7 ± 9.97	26.7 ± 1.57	874 ± 361 †††, ‡‡‡
MIP-3beta (Macrophage Inflammatory Protein-3beta)	ng/mL	0.093	0.74 ± 0.11	1.99 ± 0.27 **	1.02 ± 0.13	2.19 ± 0.83 ‡‡
MMP-9 (Matrix Metalloproteinase-9)	ng/mL	0.10	193 ± 169	275 ± 82.2	82.7 ± 21.5	958 ± 265 †††, ‡‡‡
MPO (Myeloperoxidase)	ng/mL	0.19	366 ± 403	285 ± 164	213 ± 107	2241 ± 1484 ††, ‡‡
Myoglobin	ng/mL	0.24	170 ± 147	173 ± 151	305 ± 152	965 ± 1266
OSM (Oncostatin M)	ng/mL	0.026	0.06 ± 0.01	0.07 ± 0.01	0.07 ± 0	0.19 ± 0.04 †††, ‡‡‡
RANTES (Regulation Upon Activation, Normal T-Cell Expressed and Secreted)	pg/mL	9.6	4.88 ± 1.61	21.6 ± 4.58 **	32.4 ± 5.25 ***	25 ± 8.69
SAP (Serum Amyloid P)	ug/mL	0.027	0.28 ± 0.14	0.43 ± 0.09	0.74 ± 0.07 **	1.2 ± 0.31 †††, ‡‡
SCF (Stem Cell Factor)	pg/mL	15	390 ± 37.5	406 ± 35	384 ± 14.8	581 ± 178
SGOT (Serum Glutamic-Oxaloacetic Transaminase)	ug/mL	0.37	6.51 ± 4.05	11.9 ± 3.53	23.8 ± 6.37 ***	17.1 ± 4.63
TIMP-1 (Tissue Inhibitor of Metalloproteinase Type-1)	ng/mL	0.036	0.44 ± 0.21	8.72 ± 0.59	12.5 ± 1.61 ***	67.7 ± 74.2
Tissue Factor	ng/mL	0.10	2.07 ± 0.4	2.89 ± 0.33	2.82 ± 0.4	4.5 ± 0.88 ††, ‡‡
TNF-alpha (Tumor Necrosis Factor-alpha)	ng/mL	0.027	0.02 ± 0.01	0.08 ± 0.02 **	0.07 ± 0.01 **	0.25 ± 0.03 †††, ‡‡‡
TPO (Thrombopoietin)	ng/mL	0.53	7.28 ± 1.52	10.5 ± 1.11	14.7 ± 1.36 ***	23.9 ± 3.75 †††, ‡‡‡
VCAM-1 (Vascular Cell Adhesion Molecule-1)	ng/mL	0.19	28.9 ± 5.85	90 ± 14 *	176 ± 25.4 ***	217 ± 45.4 †††
VEGF (Vascular Endothelial Cell Growth Factor)	pg/mL	7.6	2415 ± 631	2780 ± 233	4220 ± 1080 *	4155 ± 1591
vWF (von Willebrand Factor)	ng/mL	0.99	10.5 ± 2.91	9.7 ± 2.68	11.2 ± 1.36	11.6 ± 2.13

Tabular presentation of bead-array cytokine analysis in lung homogenates of animals given PBS or influenza virus intranasally on day 0, challenged with PBS or *B. parapertussis* on day 5, and sacrificed 7 days later. Data are presented as means ± SEMs, organized alphabetically by molecule name. n=4 per group. *, †, and ‡ denote a statistically significant difference at $p<0.05$ by 2-way ANOVA compared to PBS+PBS, PBS+*B. parapertussis*, and influenza virus+PBS-exposed mice, respectively. 2 icons denote $p<0.01$; 3 icons denote $p<0.001$.

Table 4: Bead-array cytokine analyses in the lung on day 5+3

	Concentration	Limit of Detection	PBS + PBS		PBS + *B. parapertussis*		Influenza + PBS		Influenza + *B. parapertussis*	
CD40	pg/mL	2.4	325 ± 325		410 ± 63.6		1154 ± 204	***	761 ± 222	†, ‡
CD40 Ligand	pg/mL	18	91 ± 91		328 ± 140		742 ± 59.7	***	686 ± 53.4	†††
CRP (C Reactive Protein)	ug/mL	0.0042	0.03 ± 0.03		0.04 ± 0		0.29 ± 0.06	***	0.42 ± 0.06	†††, ‡
EGF (Epidermal Growth Factor)	pg/mL	7.8	3.12 ± 3.12		3.99 ± 0.92		4.77 ± 0.64	**	5.66 ± 0	††
Endothelin-1	pg/mL	13	4.04 ± 4.04		6.34 ± 0.86	***	5.81 ± 0.69	**	6.06 ± 0.29	
Eotaxin	pg/mL	2.5	58.2 ± 58.2		86.6 ± 15.9	*	136 ± 17	***	135 ± 26.7	††
Factor VII	ng/mL	0.19	3.03 ± 3.03		4.51 ± 1.01	*	5.71 ± 0.91	*	7.02 ± 1.29	††
FGF-9 (Fibroblast Growth Factor-9)	ng/mL	0.20	0.25 ± 0.25		0.43 ± 0.17		1.12 ± 0.14	***	1.22 ± 0.3	†††
FGF-basic (Fibroblast Growth Factor-basic)	ng/mL	0.12	59.4 ± 59.4		59.7 ± 31		113 ± 74.8		278 ± 99.3	†††, ‡‡
Fibrinogen	ug/mL	0.85	26.6 ± 26.6		50.1 ± 8.59		218 ± 65.9	***	205 ± 97.1	††
GCP-2 (Granulocyte Chemotactic Protein-2)	ng/mL	0.0049	0.52 ± 0.52		1.54 ± 0.22	***	1.24 ± 0.27	***	1.62 ± 0.14	‡
GM-CSF (Granulocyte Macrophage-Colony Stimulating Factor)	pg/mL	1.7	1.22 ± 1.22		10.3 ± 3.2	***	8.02 ± 1.07	***	8 ± 1.98	
GST-alpha (Glutathione S-Transferase alpha)	ng/mL	0.084	0 ± 0		0 ± 0		0.02 ± 0.02	**	0.01 ± 0.01	
IFN-gamma (Interferon-gamma)	pg/mL	14	1.71 ± 1.71		4.35 ± 2.33		23.6 ± 3.54	***	22.6 ± 6.98	†††
IL-10 (Interleukin-10)	pg/mL	22	135 ± 135		126 ± 6.5		328 ± 41	***	353 ± 95	†††
IL-11 (Interleukin-11)	pg/mL	17	1.16 ± 1.16		8.12 ± 4.83		64.3 ± 8.87	***	90.2 ± 28.2	†††, ‡
IL-12p70 (Interleukin-12p70)	ng/mL	0.11	0.01 ± 0.01		0.03 ± 0.01		0.16 ± 0.01	***	0.16 ± 0.05	†††
IL-17 (Interleukin-17)	ng/mL	0.030	0 ± 0		0 ± 0		0.01 ± 0	***	0.01 ± 0	†††
IL-18 (Interleukin-18)	ng/mL	0.13	1.81 ± 1.81		1.96 ± 0.44		3.42 ± 0.4	***	3.05 ± 0.28	†
IL-1alpha (Interleukin-1alpha)	pg/mL	9.0	137 ± 137		535 ± 243	**	495 ± 82.5	**	845 ± 130	†, ‡‡
IL-1beta (Interleukin-1beta)	ng/mL	0.089	2.06 ± 2.06		7.62 ± 2.31	**	5.28 ± 0.27		10.5 ± 3.94	‡‡
IL-2 (Interleukin-2)	pg/mL	13	5.8 ± 5.8		9.63 ± 4.91		16.4 ± 2.24	**	18.4 ± 5.46	††
IL-3 (Interleukin-3)	pg/mL	4.3	0 ± 0		0.6 ± 0.24		3.21 ± 0.11	***	2.44 ± 0.85	†††, ‡
IL-4 (Interleukin-4)	pg/mL	15	7.2 ± 7.2		11 ± 1.4		30 ± 2.37	***	27.7 ± 6.32	†††
IL-5 (Interleukin-5)	ng/mL	0.039	0 ± 0		0.05 ± 0.05		0.3 ± 0.07	**	0.25 ± 0.24	
IL-6 (Interleukin-6)	pg/mL	2.8	0.76 ± 0.76		35.1 ± 20.5		57.4 ± 9.74		105 ± 70.9	†
IL-7 (Interleukin-7)	ng/mL	0.062	0.01 ± 0.01		0.03 ± 0.01		0.13 ± 0.02	***	0.15 ± 0.03	†††
IP-10 (Inducible Protein-10)	pg/mL	8.1	32.5 ± 32.5		90.7 ± 52.1		1613 ± 242	***	1777 ± 822	†††
KC/GROalpha (Melanoma Growth Stimulatory Activity Protein)	ng/mL	0.035	0.01 ± 0.01		0.2 ± 0.08	***	0.16 ± 0.04	**	0.24 ± 0.07	
LIF (Leukemia Inhibitory Factor)	pg/mL	8.7	214 ± 214		302 ± 30.6		914 ± 159	**	1250 ± 573	†††
Lymphotactin	pg/mL	17	28.6 ± 28.6		43.2 ± 14.6		468 ± 134	***	457 ± 69.9	†††
MCP-1 (Monocyte Chemoattractant Protein-1)	pg/mL	3.4	13.2 ± 13.2		63.1 ± 31.5		1010 ± 142	***	861 ± 316	†††
MCP-3 (Monocyte Chemoattractant Protein-3)	pg/mL	6.3	17.2 ± 17.2		106 ± 43.9		1285 ± 79.4	***	1106 ± 332	†††
MCP-5 (Monocyte Chemoattractant Protein-5)	pg/mL	9.3	3.6 ± 3.6		16.9 ± 5.22		303 ± 17.8	***	225 ± 118	†††
M-CSF (Macrophage-Colony Stimulating Factor)	ng/mL	0.0036	0.15 ± 0.15		0.23 ± 0.05		0.84 ± 0.09	***	0.66 ± 0.11	†††, ‡‡
MDC (Macrophage-Derived Chemokine)	pg/mL	4.4	64.4 ± 64.4		143 ± 49.1	**	148 ± 38.5	*	128 ± 32.2	
MIP-1alpha (Macrophage Inflammatory Protein-1alpha)	ng/mL	0.045	0.14 ± 0.14		0.21 ± 0.03		1.03 ± 0.29	***	1.02 ± 0.33	†††
MIP-1beta (Macrophage Inflammatory Protein-1beta)	pg/mL	16	34.7 ± 34.7		88.5 ± 37.9		1928 ± 595	***	2425 ± 978	†††
MIP-1gamma (Macrophage Inflammatory Protein-1gamma)	ng/mL	0.015	0.4 ± 0.4		0.87 ± 0.26		2.08 ± 0.61	**	2.46 ± 0.86	††
MIP-2 (Macrophage Inflammatory Protein-2)	pg/mL	1.4	3.59 ± 3.59		80.5 ± 34.9	*	82.5 ± 13.5	*	292 ± 84.5	†††, ‡‡‡
MIP-3beta (Macrophage Inflammatory Protein-3beta)	ng/mL	0.093	0.53 ± 0.53		0.86 ± 0.17	*	1.14 ± 0.17	***	1.05 ± 0.21	
MMP-9 (Matrix Metalloproteinase-9)	ng/mL	0.10	34.6 ± 34.6		192 ± 40.1	**	218 ± 49.6	**	396 ± 127	†††, ‡‡
MPO (Myeloperoxidase)	ng/mL	0.19	53.2 ± 53.2		242 ± 136		755 ± 326	**	871 ± 283	††
Myoglobin	ng/mL	0.24	17.6 ± 17.6		21.7 ± 5.42		19.8 ± 4.88		12.8 ± 8.4	
OSM (Oncostatin M)	ng/mL	0.026	0.02 ± 0.02		0.04 ± 0.01		0.15 ± 0.01	***	0.17 ± 0.04	†††
RANTES (Regulation Upon Activation, Normal T-Cell Expressed and Secreted)	pg/mL	9.6	3.04 ± 3.04		4.48 ± 1.97		24.9 ± 6.87	***	15.7 ± 3.13	†, ‡‡
SAP (Serum Amyloid P)	ug/mL	0.027	0.12 ± 0.12		0.18 ± 0.02	*	0.55 ± 0.04	***	0.68 ± 0.07	†††, ‡‡‡
SCF (Stem Cell Factor)	pg/mL	15	105 ± 105		170 ± 38.6	*	384 ± 37.8	***	352 ± 38	†††
SGOT (Serum Glutamic-Oxaloacetic Transaminase)	ug/mL	0.37	4.16 ± 4.16		3.83 ± 1.82		3.43 ± 4.32		2.65 ± 5.3	
TIMP-1 (Tissue Inhibitor of Metalloproteinase Type-1)	ng/mL	0.036	0.18 ± 0.18		2.42 ± 1.17		31.4 ± 8.54	**	51.6 ± 25.9	†††
Tissue Factor	ng/mL	0.10	1.34 ± 1.34		1.99 ± 0.45	*	2.65 ± 0.52	***	3.41 ± 0.31	†††, ‡
TNF-alpha (Tumor Necrosis Factor-alpha)	ng/mL	0.027	0 ± 0		0.03 ± 0.01		0.18 ± 0.03	***	0.23 ± 0.06	†††
TPO (Thrombopoietin)	ng/mL	0.53	4.36 ± 4.36		7.87 ± 0.86	**	8.91 ± 1.28	***	10.2 ± 1.64	†
VCAM-1 (Vascular Cell Adhesion Molecule-1)	ng/mL	0.19	9.33 ± 9.33		15.3 ± 2.8		112 ± 17.7	***	96.3 ± 15.5	†††
VEGF (Vascular Endothelial Cell Growth Factor)	pg/mL	7.6	1753 ± 1753		2713 ± 667		3143 ± 1097	*	2418 ± 742	
vWF (von Willebrand Factor)	ng/mL	0.99	3.21 ± 3.21		5.26 ± 0.67	*	8.05 ± 1.3	***	8.22 ± 1.61	††

Tabular presentation of bead-array cytokine analysis in lung homogenates of animals given PBS or influenza virus intranasally on day 0, challenged with PBS or *B. parapertussis* on day 5, and sacrificed 3 days later. Data are presented as means ± SEMs, organized alphabetically by molecule name. n=4 per group. *, †, and ‡ denote a statistically significant difference at $p<0.05$ by 2-way ANOVA compared to PBS+PBS, PBS+*B. parapertussis*, and influenza virus+PBS-exposed mice, respectively. 2 icons denote $p<0.01$; 3 icons denote $p<0.001$.

Table 3: Bead-array cytokine analyses in the lung on day 5+1

	Concentration	Limit of Detection	PBS + PBS	PBS + *B. parapertussis*	Influenza + PBS		Influenza + *B. parapertussis*	
CD40	pg/mL	2.4	251 ± 42.9	241 ± 62.2	903 ± 306	***	803 ± 174	†††
CD40 Ligand	pg/mL	18	145 ± 60.7	165 ± 46.6	557 ± 77.3	***	598 ± 72.4	†††
CRP (C Reactive Protein)	ug/mL	0.0042	0.04 ± 0.01	0.04 ± 0.01	0.1 ± 0.03	***	0.11 ± 0.02	†††
EGF (Epidermal Growth Factor)	pg/mL	7.8	3.22 ± 0.35	3.58 ± 0.18	3.9 ± 0.54	*	4.36 ± 0.43	†
Endothelin-1	pg/mL	13	4.3 ± 1.27	4.29 ± 1.36	5.48 ± 0.67		5.91 ± 1.31	
Eotaxin	pg/mL	2.5	60.6 ± 13.5	58.9 ± 11	157 ± 55.5	*	231 ± 73.9	†††,‡
Factor VII	ng/mL	0.19	3.66 ± 1.06	3.8 ± 0.57	5.64 ± 0.72	**	6.47 ± 0.68	†††
FGF-9 (Fibroblast Growth Factor-9)	ng/mL	0.20	0.39 ± 0.13	0.37 ± 0.15	1.23 ± 0.46	**	1.23 ± 0.28	††
FGF-basic (Fibroblast Growth Factor-basic)	ng/mL	0.12	117 ± 43.5	130 ± 30.7	222 ± 56.8	**	232 ± 33.7	††
Fibrinogen	ug/mL	0.85	44.3 ± 31	36.3 ± 8.4	91.2 ± 24.3	*	104 ± 17.6	††
GCP-2 (Granulocyte Chemotactic Protein-2)	ng/mL	0.0049	0.9 ± 0.43	0.76 ± 0.21	1.29 ± 0.25		1.38 ± 0.17	††
GM-CSF (Granulocyte Macrophage-Colony Stimulating Factor)	pg/mL	1.7	1.79 ± 0.46	2.18 ± 0.72	8.45 ± 2.44	***	9.3 ± 0.6	†††
GST-alpha (Glutathione S-Transferase alpha)	ng/mL	0.084	0 ± 0	0 ± 0	0 ± 0		0 ± 0	
IFN-gamma (Interferon-gamma)	pg/mL	14	3.1 ± 1.33	2.79 ± 1.85	26.5 ± 10.8	***	30.2 ± 9.31	†††
IL-10 (Interleukin-10)	pg/mL	22	130 ± 35.2	132 ± 12	330 ± 86.3	***	308 ± 61.8	†††
IL-11 (Interleukin-11)	pg/mL	17	4.2 ± 0.75	4.74 ± 0.57	59.1 ± 22.6	***	63 ± 15.3	†††
IL-12p70 (Interleukin-12p70)	ng/mL	0.11	0.03 ± 0.01	0.03 ± 0.01	0.16 ± 0.06	***	0.16 ± 0.03	†††
IL-17 (Interleukin-17)	ng/mL	0.030	0 ± 0	0 ± 0	0.01 ± 0	***	0.01 ± 0	†††
IL-18 (Interleukin-18)	ng/mL	0.13	1.79 ± 0.65	2.29 ± 0.71	2.35 ± 0.23		2.65 ± 0.19	
IL-1alpha (Interleukin-1alpha)	pg/mL	9.0	175 ± 63.9	252 ± 109	525 ± 137	***	661 ± 84	†††
IL-1beta (Interleukin-1beta)	ng/mL	0.089	2.09 ± 0.27	2.26 ± 0.48	3.88 ± 0.95	**	4.7 ± 0.77	†††
IL-2 (Interleukin-2)	pg/mL	13	7.29 ± 3.66	11.6 ± 9.34	18.4 ± 7.04	*	19.9 ± 3.77	
IL-3 (Interleukin-3)	pg/mL	4.3	0.41 ± 0.04	0.27 ± 0.31	3.76 ± 1.74	***	3.39 ± 0.81	†††
IL-4 (Interleukin-4)	pg/mL	15	12 ± 4.03	8.69 ± 7.02	32.2 ± 6.26	***	30.2 ± 3.6	†††
IL-5 (Interleukin-5)	ng/mL	0.039	0.01 ± 0.01	0 ± 0	0.58 ± 0.37	**	1.06 ± 0.33	†††,‡
IL-6 (Interleukin-6)	pg/mL	2.8	1.62 ± 0.74	3.15 ± 2.07	86 ± 44.4	**	95.7 ± 31.3	†††
IL-7 (Interleukin-7)	ng/mL	0.062	0.02 ± 0.01	0.02 ± 0.01	0.13 ± 0.04	***	0.13 ± 0.02	†††
IP-10 (Inducible Protein-10)	pg/mL	8.1	21.3 ± 6.98	25.9 ± 8.24	3655 ± 1482	***	3555 ± 853	†††
KC/GROalpha (Melanoma Growth Stimulatory Activity Protein)	ng/mL	0.035	0.02 ± 0.01	0.02 ± 0.02	0.16 ± 0.07	***	0.16 ± 0.03	†††
LIF (Leukemia Inhibitory Factor)	pg/mL	8.7	238 ± 25.4	238 ± 6.5	525 ± 170	**	553 ± 123	††
Lymphotactin	pg/mL	17	30.4 ± 7.18	24.5 ± 4.84	433 ± 210	**	532 ± 193	†††
MCP-1 (Monocyte Chemoattractant Protein-1)	pg/mL	3.4	14.2 ± 3.37	19.2 ± 6.68	1122 ± 492	***	1062 ± 192	†††
MCP-3 (Monocyte Chemoattractant Protein-3)	pg/mL	6.3	18.5 ± 4.99	23.4 ± 8.86	1335 ± 531	***	1343 ± 165	†††
MCP-5 (Monocyte Chemoattractant Protein-5)	pg/mL	9.3	6.54 ± 2.68	7.44 ± 2.96	274 ± 110	***	247 ± 69.9	†††
M-CSF (Macrophage-Colony Stimulating Factor)	ng/mL	0.0036	0.12 ± 0.01	0.12 ± 0.02	0.52 ± 0.15	***	0.48 ± 0.08	†††
MDC (Macrophage-Derived Chemokine)	pg/mL	4.4	101 ± 37.2	105 ± 29.3	143 ± 43.2		167 ± 27.1	†
MIP-1alpha (Macrophage Inflammatory Protein-1alpha)	ng/mL	0.045	0.2 ± 0.07	0.21 ± 0.05	1.3 ± 0.77	*	1.79 ± 0.87	††
MIP-1beta (Macrophage Inflammatory Protein-1beta)	pg/mL	16	50.2 ± 14.6	45.2 ± 5.7	1756 ± 1056	**	1725 ± 785	††
MIP-1gamma (Macrophage Inflammatory Protein-1gamma)	ng/mL	0.015	0.49 ± 0.14	0.58 ± 0.1	1.33 ± 0.31	**	1.86 ± 0.5	†††,‡
MIP-2 (Macrophage Inflammatory Protein-2)	pg/mL	1.4	10.2 ± 8.18	12.7 ± 7.45	68.1 ± 23.9	***	86.8 ± 25.8	†††
MIP-3beta (Macrophage Inflammatory Protein-3beta)	ng/mL	0.093	0.55 ± 0.16	0.58 ± 0.15	1.1 ± 0.19	***	1.03 ± 0.06	††
MMP-9 (Matrix Metalloproteinase-9)	ng/mL	0.10	56.8 ± 15.3	56.5 ± 16.9	216 ± 38.1	***	267 ± 54.1	†††
MPO (Myeloperoxidase)	ng/mL	0.19	113 ± 46.8	157 ± 39	707 ± 278	**	836 ± 414	††
Myoglobin	ng/mL	0.24	8.74 ± 4.36	30.8 ± 33.1	13.3 ± 5		12.1 ± 8.12	
OSM (Oncostatin M)	ng/mL	0.026	0.03 ± 0.01	0.03 ± 0	0.15 ± 0.05	***	0.15 ± 0.02	†††
RANTES (Regulation Upon Activation, Normal T-Cell Expressed and Secreted)	pg/mL	9.6	2.52 ± 1	2.89 ± 0.86	13 ± 4.6	***	13.1 ± 2.01	†††
SAP (Serum Amyloid P)	ug/mL	0.027	0.15 ± 0.04	0.15 ± 0.02	0.34 ± 0.06	***	0.4 ± 0.05	†††
SCF (Stem Cell Factor)	pg/mL	15	102 ± 19.1	118 ± 29.2	310 ± 68.9	***	304 ± 38.8	†††
SGOT (Serum Glutamic-Oxaloacetic Transaminase)	ug/mL	0.37	7.52 ± 5.22	7.97 ± 3.84	12.4 ± 6.2		8.48 ± 2.91	
TIMP-1 (Tissue Inhibitor of Metalloproteinase Type-1)	ng/mL	0.036	0.3 ± 0.12	0.3 ± 0.07	16.6 ± 8.33	***	18.4 ± 5.35	†††
Tissue Factor	ng/mL	0.10	1.84 ± 0.59	1.65 ± 0.25	2.38 ± 0.41		2.51 ± 0.14	††
TNF-alpha (Tumor Necrosis Factor-alpha)	ng/mL	0.027	0.02 ± 0	0.02 ± 0	0.17 ± 0.06	***	0.18 ± 0.02	†††
TPO (Thrombopoietin)	ng/mL	0.53	5.25 ± 1.55	4.69 ± 0.55	7.78 ± 1.22	*	8.68 ± 1.16	†††
VCAM-1 (Vascular Cell Adhesion Molecule-1)	ng/mL	0.19	11.6 ± 3.34	10.8 ± 1.79	48.4 ± 12	***	46 ± 9.4	†††
VEGF (Vascular Endothelial Cell Growth Factor)	pg/mL	7.6	1688 ± 392	1733 ± 403	2900 ± 734	**	2598 ± 207	†
vWF (von Willebrand Factor)	ng/mL	0.99	3.66 ± 1.07	3.63 ± 1.01	5.7 ± 0.91	*	5.88 ± 0.91	††

Tabular presentation of bead-array cytokine analysis in lung homogenates of animals given PBS or influenza virus intranasally on day 0, challenged with PBS or *B. parapertussis* on day 5, and sacrificed 1 day later. Data are presented as means ± SEMs, organized alphabetically by molecule name. n=4 per group. *, †, and ‡ denote a statistically significant difference at $p<0.05$ by 2-way ANOVA compared to PBS+PBS, PBS+*B. parapertussis*, and influenza virus+PBS-exposed mice, respectively. 2 icons denote $p<0.01$; 3 icons denote $p<0.001$.

Table 2: Flow cytometric analyses of lymphocyte subsets in the lungs

	PBS + PBS	PBS + *B. parapertussis*	Influenza virus + PBS	Influenza virus + *B. parapertussis*	
B cells	3.8 ± 0.2	2.7 ± 0.5	4.1 ± 0.6	3.9 ± 0.4	($x10^6$ cells/lung)
CD69+	7.7 ± 0.4	5.3 ± 1.2	8.2 ± 1.4	6.3 ± 0.6	($x10^4$)
NK cells	2.1 ± 0.6	2.3 ± 0.2	1.6 ± 0.2	1.9 ± 0.3	($x10^6$)
CD69+	5.2 ± 2.1	7.4 ± 0.3	2.5 ± 0.9	2.1 ± 1.3	($x10^4$) †
T cells	4.7 ± 0.6	4.0 ± 1.1	7.3 ± 3.9	12.9 ± 2.1	($x10^6$) †
CD4+	2.3 ± 0.2	1.7 ± 0.2	2.3 ± 0.9	3.5 ± 0.5	($x10^6$)
CD25+	1.9 ± 0.2	1.6 ± 0.3	2.0 ± 0.5	3.0 ± 0.3	($x10^5$)
CD69+	5.5 ± 0.8	4.6 ± 1.1	4.6 ± 2.0	10.0 ± 1.6	($x10^4$)
CD8+	1.9 ± 0.4	1.3 ± 0.6	4.4 ± 2.3	7.3 ± 1.4	($x10^6$) †††, ‡
CD25+	7.0 ± 3.8	5.3 ± 3.8	22.3 ± 10.4 *	36.3 ± 6.9	($x10^4$) †††, ‡‡
CD69+	5.5 ± 1.2	3.0 ± 1.3	10.0 ± 5.5	13.8 ± 2.2	($x10^4$) †
Tetramer+	0.0 ± 1.0	0.1 ± 2.3	6.8 ± 6.0 *	14.9 ± 3.6	($x10^5$) †††, ‡

Flow cytometric analyses of lymphocyte subsets in the lungs of mice given PBS or influenza virus on day 0, PBS or *B. parapertussis* on day 5, and then sacrificed 7 days later. Data are expressed as the means ± SEMs and were analysed by 2-way ANOVA. B-cells were defined by FSC/SSC/CD45R profile, natural killer (NK) cells FSC/SSC/Nk1.1, and T-cells by FSC/SSC/CD3. n=4 per group. *, †, and ‡ denote a statistically significant difference at $p<0.05$ compared to PBS+PBS, PBS+*B. parapertussis*, and influenza virus+PBS-exposed mice, respectively. 2 icons denote $p<0.01$; 3 icons denote $p<0.001$. Data are representative of two independent experiments.

Table 1: Biographical characteristics of human PBMC donors

Biographical characteristic	Smoking Status	
	Never-smokers	Smokers
Gender (m/f)	3/5	3/5
Age (years)	51.4 ± 3.2	57.88 ± 6.6
Pack-years (years)	N/A	25.6 ± 3.0

Biographical characteristics were acquired from subjects who volunteered to donate PBMCs for analysis of smoke's effects on human lymphocyte proliferative responses. Data were acquired from patient-reported medical histories. Ages and numbers of pack-years are presented as means ± SEMs. 1 pack year was defined as consumption of 1 self-defined pack of cigarettes per day for 1 year.

Chapter 6: References

1. Zavitz CC, Gaschler GJ, Robbins CS, Botelho FM, Cox PG, Stampfli MR. Impact of cigarette smoke on t and b cell responsiveness. *Cell Immunol* 2008;253:38-44.
2. Gaschler GJ, Bauer CM, Zavitz CC, Stampfli MR. Animal models of chronic obstructive pulmonary disease exacerbations. *Contrib Microbiol* 2007;14:126-141.
3. Lopez AD, Mathers CD, Ezzati M, Jamison DT, Murray CJL. Global burden of disease and risk factors. Measuring the global burden of disease and risk factors, 1990-2001. New York: Oxford University Press; 2006. p. 1-13.
4. WHO. The global burden of disease: 2004 update. Geneva, Switzerland: World Health Organization Press; 2008. p. 160.
5. Ezzati M, Lopez AD. Regional, disease specific patterns of smoking-attributable mortality in 2000. *Tob Control* 2004;13:388-395.
6. Peto R, Lopez A. Future worldwide health effects of current smoking patterns. In: Koop C, Pearson C, Schwartz M, editors. Critical issues in global health. San Francisco: Jossey-Bass; 2001. p. 472.
7. Ezzati M, Henley SJ, Lopez AD, Thun MJ. Role of smoking in global and regional cancer epidemiology: Current patterns and data needs. *Int J Cancer* 2005;116:963-971.
8. Eisner MD, Balmes J, Katz PP, Trupin L, Yelin EH, Blanc PD. Lifetime environmental tobacco smoke exposure and the risk of chronic obstructive pulmonary disease. *Environ Health* 2005;4:7.
9. The health consequences of smoking: A report of the surgeon general. Atlanta: U.S. Department of Health and Human Services, Centers for Disease Control and Prevention, National Center for Chronic Disease Prevention and Health Promotion, Office on Smoking and Health; 2004.
10. Murta-Nascimento C, Schmitz-Dräger B, Zeegers M, Steineck G, Kogevinas M, Real F, Malats N. Epidemiology of urinary bladder cancer: From tumor development to patient's death. *World Journal of Urology* 2007;25:285-295.
11. Tonetti MS. Cigarette smoking and periodontal diseases: Etiology and management of disease. *Ann Periodontol* 1998;3:88-101.
12. Birrenbach T, Bocker U. Inflammatory bowel disease and smoking: A review of epidemiology, pathophysiology, and therapeutic implications. *Inflamm Bowel Dis* 2004;10:848-859.
13. Costenbader KH, Feskanich D, Mandl LA, Karlson EW. Smoking intensity, duration, and cessation, and the risk of rheumatoid arthritis in women. *Am J Med* 2006;119:503 e501-509.
14. Jha P, Ranson MK, Nguyen SN, Yach D. Estimates of global and regional smoking prevalence in 1995, by age and sex. *Am J Public Health* 2002;92:1002-1006.
15. Levitzky MG. Pulmonary physiology. New York: McGraw-Hill; 2007.
16. Fokkens WJ, Scheeren RA. Upper airway defence mechanisms. *Paediatric Respiratory Reviews* 2000;1:336-341.
17. Sharry JM, Scanlan P, Marchesi J, Martin JG. Characterization of the bacterial community within the respiratory tract of healthy mice; a molecular approach. European Respiratory Society Annual Congress. Berlin, Germany; 2008. p. 293s.
18. Haytac MC, Oz IA. Atypical streptococcal infection of gingiva associated with chronic mouth breathing. *Quintessence Int* 2007;38:E577-582.

19. Pneumatikos IA, Dragoumanis CK, Bouros DE. Ventilator-associated pneumonia or endotracheal tube-associated pneumonia?: An approach to the pathogenesis and preventive strategies emphasizing the importance of endotracheal tube. *Anesthesiology* 2009;110:673-680 610.1097/ALN.1090b1013e31819868e31819860.
20. Sung JC, Pulliam BL, Edwards DA. Nanoparticles for drug delivery to the lungs. *Trends in Biotechnology* 2007;25:563-570.
21. Weibel ER. Morphological basis of alveolar-capillary gas exchange. *Physiol Rev* 1973;53:419-495.
22. Murphy KP, Travers P, Walport M, Janeway C. Janeway's immunobiology. New York: Garland Science; 2008.
23. Wright JR. Immunoregulatory functions of surfactant proteins. *Nat Rev Immunol* 2005;5:58-68.
24. Gardai SJ, Xiao Y-Q, Dickinson M, Nick JA, Voelker DR, Greene KE, Henson PM. By binding sirp[alpha] or calreticulin/cd91, lung collectins act as dual function surveillance molecules to suppress or enhance inflammation. *Cell* 2003;115:13-23.
25. Sato M, Sano H, Iwaki D, Kudo K, Konishi M, Takahashi H, Takahashi T, Imaizumi H, Asai Y, Kuroki Y. Direct binding of toll-like receptor 2 to zymosan, and zymosan-induced nf-kappa b activation and tnf-alpha secretion are down-regulated by lung collectin surfactant protein a. *J Immunol* 2003;171:417-425.
26. Guillot L, Balloy V, McCormack FX, Golenbock DT, Chignard M, Si-Tahar M. Cutting edge: The immunostimulatory activity of the lung surfactant protein-a involves toll-like receptor 4. *J Immunol* 2002;168:5989-5992.
27. Jack DL, Klein NJ, Turner MW. Mannose-binding lectin: Targeting the microbial world for complement attack and opsonophagocytosis. *Immunol Rev* 2001;180:86-99.
28. Conneely OM. Antiinflammatory activities of lactoferrin. *J Am Coll Nutr* 2001;20:389S-395.
29. Skerrett SJ. Lysozyme in pulmonary host defense: New tricks for an old dog. *Am J Respir Crit Care Med* 2004;169:435-436.
30. Landsman L, Jung S. Lung macrophages serve as obligatory intermediate between blood monocytes and alveolar macrophages. *J Immunol* 2007;179:3488-3494.
31. Murphy J, Summer R, Wilson AA, Kotton DN, Fine A. The prolonged life-span of alveolar macrophages. *Am J Respir Cell Mol Biol* 2008;38:380-385.
32. Takeuchi O, Akira S. Innate immunity to virus infection. *Immunol Rev* 2009;227:75-86.
33. Iwasaki A, Medzhitov R. Toll-like receptor control of the adaptive immune responses. *Nat Immunol* 2004;5:987.
34. Lee MS, Kim YJ. Signaling pathways downstream of pattern-recognition receptors and their cross talk. *Annu Rev Biochem* 2007;76:447-480.
35. Blander JM, Medzhitov R. Regulation of phagosome maturation by signals from toll-like receptors. *Science* 2004;304:1014-1018.
36. Le Goffic R, Pothlichet J, Vitour D, Fujita T, Meurs E, Chignard M, Si-Tahar M. Cutting edge: Influenza a virus activates tlr3-dependent inflammatory and rig-i-dependent antiviral responses in human lung epithelial cells. *J Immunol* 2007;178:3368-3372.
37. Herold S, Steinmueller M, von Wulffen W, Cakarova L, Pinto R, Pleschka S, Mack M, Kuziel WA, Corazza N, Brunner T, et al. Lung epithelial apoptosis in influenza virus pneumonia:

The role of macrophage-expressed tnf-related apoptosis-inducing ligand. *J Exp Med* 2008;205:3065-3077.
38. Ley K, Laudanna C, Cybulsky MI, Nourshargh S. Getting to the site of inflammation: The leukocyte adhesion cascade updated. *Nat Rev Immunol* 2007;7:678-689.
39. Choudhury S, Wilson MR, Goddard ME, O'Dea KP, Takata M. Mechanisms of early pulmonary neutrophil sequestration in ventilator-induced lung injury in mice. *Am J Physiol Lung Cell Mol Physiol* 2004;287:L902-910.
40. William MN. How human neutrophils kill and degrade microbes: An integrated view. *Immunological Reviews* 2007;219:88-102.
41. Medeiros AI, Serezani CH, Lee SP, Peters-Golden M. Efferocytosis impairs pulmonary macrophage and lung antibacterial function via pge2/ep2 signaling. *J Exp Med* 2009;206:61-68.
42. Rosenstiel P, Philipp EER, Schreiber S, Bosch TCG. Evolution and function of innate immune receptors -- insights from marine invertebrates. *Journal of Innate Immunity* 2009;1:291-300.
43. Pancer Z, Cooper MD. The evolution of adaptive immunity. *Annu Rev Immunol* 2006;24:497-518.
44. Kirby AC, Coles MC, Kaye PM. Alveolar macrophages transport pathogens to lung draining lymph nodes. *J Immunol* 2009;183:1983-1989.
45. Lyons CR, Ball EJ, Toews GB, Weissler JC, Stastny P, Lipscomb MF. Inability of human alveolar macrophages to stimulate resting t cells correlates with decreased antigen-specific t cell-macrophage binding. *J Immunol* 1986;137:1173-1180.
46. Toews GB, Vial WC, Dunn MM, Guzzetta P, Nunez G, Stastny P, Lipscomb MF. The accessory cell function of human alveolar macrophages in specific t cell proliferation. *J Immunol* 1984;132:181-186.
47. Lipscomb MF, Lyons CR, Nunez G, Ball EJ, Stastny P, Vial W, Lem V, Weissler J, Miller LM. Human alveolar macrophages: Hla-dr-positive macrophages that are poor stimulators of a primary mixed leukocyte reaction. *J Immunol* 1986;136:497-504.
48. Guth AM, Janssen WJ, Bosio CM, Crouch EC, Henson PM, Dow SW. Lung environment determines unique phenotype of alveolar macrophages. *Am J Physiol Lung Cell Mol Physiol* 2009;296:L936-946.
49. Chelen CJ, Fang Y, Freeman GJ, Secrist H, Marshall JD, Hwang PT, Frankel LR, DeKruyff RH, Umetsu DT. Human alveolar macrophages present antigen ineffectively due to defective expression of b7 costimulatory cell surface molecules. *J Clin Invest* 1995;95:1415-1421.
50. Lambrecht BN. Alveolar macrophage in the driver's seat. *Immunity* 2006;24:366-368.
51. Alvarez D, Vollmann EH, von Andrian UH. Mechanisms and consequences of dendritic cell migration. *Immunity* 2008;29:325-342.
52. Brunkow ME, Jeffery EW, Hjerrild KA, Paeper B, Clark LB, Yasayko SA, Wilkinson JE, Galas D, Ziegler SF, Ramsdell F. Disruption of a new forkhead/winged-helix protein, scurfin, results in the fatal lymphoproliferative disorder of the scurfy mouse. *Nat Genet* 2001;27:68-73.
53. Smith CM, Wilson NS, Waithman J, Villadangos JA, Carbone FR, Heath WR, Belz GT. Cognate cd4(+) t cell licensing of dendritic cells in cd8(+) t cell immunity. *Nat Immunol* 2004;5:1143-1148.
54. Stockinger B, Bourgeois C, Kassiotis G. Cd4+ memory t cells: Functional differentiation and homeostasis. *Immunol Rev* 2006;211:39-48.

55. Thepen T, Kraal G, Holt PG. The role of alveolar macrophages in regulation of lung inflammation. *Ann N Y Acad Sci* 1994;725:200-206.
56. Lipscomb MF, Pollard AM, Yates JL. A role for tgf-beta in the suppression by murine bronchoalveolar cells of lung dendritic cell initiated immune responses. *Reg Immunol* 1993;5:151-157.
57. Roth MD, Golub SH. Human pulmonary macrophages utilize prostaglandins and transforming growth factor beta 1 to suppress lymphocyte activation. *J Leukoc Biol* 1993;53:366-371.
58. Balbo P, Silvestri M, Rossi GA, Crimi E, Burastero SE. Differential role of cd80 and cd86 on alveolar macrophages in the presentation of allergen to t lymphocytes in asthma. *Clin Exp Allergy* 2001;31:625-636.
59. Snelgrove RJ, Goulding J, Didierlaurent AM, Lyonga D, Vekaria S, Edwards L, Gwyer E, Sedgwick JD, Barclay AN, Hussell T. A critical function for cd200 in lung immune homeostasis and the severity of influenza infection. *Nat Immunol* 2008;9:1074-1083.
60. van der Sluijs KF, van Elden LJ, Nijhuis M, Schuurman R, Pater JM, Florquin S, Goldman M, Jansen HM, Lutter R, van der Poll T. Il-10 is an important mediator of the enhanced susceptibility to pneumococcal pneumonia after influenza infection. *J Immunol* 2004;172:7603-7609.
61. Graham NM. The epidemiology of acute respiratory infections in children and adults: A global perspective. *Epidemiol Rev* 1990;12:149-178.
62. Mandell GL, Dolin R, Bennett JE. Principles and practice of infectious disease. New York: Elsevier/Churchill Livingstone; 2005.
63. Sikkel MB, Quint JK, Mallia P, Wedzicha JA, Johnston SL. Respiratory syncytial virus persistence in chronic obstructive pulmonary disease. *Pediatr Infect Dis J* 2008;27:S63-70.
64. Potter CW. Chronicle of influenza pandemics. In: Nicholson KG, Webster RG, Hay AJ, editors. Textbook of influenza. London: Blackwell Scientific Publications; 1998. p. 3-18.
65. Who | acute respiratory infections (update february 2009). 2009 February 11 2009 [cited 2009 February 23]. Available from: http://www.who.int/vaccine_research/diseases/ari/en/index.html.
66. Kieny MP, Girard MP. Human vaccine research and development: An overview. *Vaccine* 2005;23:5705-5707.
67. Girard MP, Cherian T, Pervikov Y, Kieny MP. A review of vaccine research and development: Human acute respiratory infections. *Vaccine* 2005;23:5708-5724.
68. Brammer TL, Murray EL, Fukuda K, Hall HE, Klimov A, Cox NJ. Surveillance for influenza--united states, 1997-98, 1998-99, and 1999-00 seasons. *MMWR Surveill Summ* 2002;51:1-10.
69. Simonsen L, Clarke MJ, Williamson GD, Stroup DF, Arden NH, Schonberger LB. The impact of influenza epidemics on mortality: Introducing a severity index. *Am J Public Health* 1997;87:1944-1950.
70. Olsen B, Munster VJ, Wallensten A, Waldenstrom J, Osterhaus AD, Fouchier RA. Global patterns of influenza a virus in wild birds. *Science* 2006;312:384-388.
71. Timothy K. W C, Leo L. M P. Biology of influenza a virus. *Annals of the New York Academy of Sciences* 2007;1102:1-25.
72. Wright PF, Neumann G, Kawaoka Y. Orthomyxoviruses. In: Knipe D, Howley P, editors. Fields virology, 5th ed. Phladelphia: Lippincott Williams & Wilkins; 2007. p. 1691-1740.

73. Normile D. Infectious diseases. Genetic analyses suggest bird flu virus is evolving. *Science* 2005;308:1234-1235.
74. Novel Swine-Origin Influenza AVIT. Emergence of a novel swine-origin influenza a (h1n1) virus in humans. *N Engl J Med* 2009:NEJMoa0903810.
75. Morens DM, Taubenberger JK, Fauci AS. Predominant role of bacterial pneumonia as a cause of death in pandemic influenza: Implications for pandemic influenza preparedness. *J Infect Dis* 2008;198:962-970.
76. McAuley JL, Hornung F, Boyd KL, Smith AM, McKeon R, Bennink J, Yewdell JW, McCullers JA. Expression of the 1918 influenza a virus pb1-f2 enhances the pathogenesis of viral and secondary bacterial pneumonia. *Cell Host Microbe* 2007;2:240-249.
77. McCullers JA. Insights into the interaction between influenza virus and pneumococcus. *Clin Microbiol Rev* 2006;19:571-582.
78. Spiller S, Elson G, Ferstl R, Dreher S, Mueller T, Freudenberg M, Daubeuf B, Wagner H, Kirschning CJ. Tlr4-induced ifn-{gamma} production increases tlr2 sensitivity and drives gram-negative sepsis in mice. *J Exp Med* 2008;205:1747-1754.
79. M. W. Pound DBM. Proposed mechanisms and preventative options of jarisch–herxheimer reactions. *Journal of Clinical Pharmacy & Therapeutics* 2005;30:291-295.
80. Annane D, Sebille V, Charpentier C, Bollaert PE, Francois B, Korach JM, Capellier G, Cohen Y, Azoulay E, Troche G, et al. Effect of treatment with low doses of hydrocortisone and fludrocortisone on mortality in patients with septic shock. *JAMA* 2002;288:862-871.
81. Root RK, Lodato RF, Patrick W, Cade JF, Fotheringham N, Milwee S, Vincent JL, Torres A, Rello J, Nelson S. Multicenter, double-blind, placebo-controlled study of the use of filgrastim in patients hospitalized with pneumonia and severe sepsis. *Crit Care Med* 2003;31:367-373.
82. Cole L, Bellomo R, Hart G, Journois D, Davenport P, Tipping P, Ronco C. A phase ii randomized, controlled trial of continuous hemofiltration in sepsis. *Crit Care Med* 2002;30:100-106.
83. Marshall JC. Such stuff as dreams are made on: Mediator-directed therapy in sepsis. *Nat Rev Drug Discov* 2003;2:391-405.
84. Muir R, Wilson GH. Influenza and its complications. *British Medical Journal* 1919;i:3-5.
85. Martin CM, Kunin CM, Gottlieb LS, Barnes MW, Liu C, Finland M. Asian influenza a in boston, 1957-1958. I. Observations in thirty-two influenza-associated fatal cases. *AMA Arch Intern Med* 1959;103:515-531.
86. Martin CM, Kunin CM, Gottlieb LS, Finland M. Asian influenza a in boston, 1957-1958. Ii. Severe staphylococcal pneumonia complicating influenza. *AMA Arch Intern Med* 1959;103:532-542.
87. Wolbach SB. Comments on the pathology and bacteriology of fatal influenza cases, as observed at camp devens. *Mass Bull J Hopkins Hosp* 1919;1:104-109.
88. Louria DB, Blumenfeld HL, Ellis JT, Kilbourne ED, Rogers DE. Studies on influenza in the pandemic of 1957-1958. Ii. Pulmonary complications of influenza. *J Clin Invest* 1959;38:213-265.
89. Avadhanula V, Rodriguez CA, Devincenzo JP, Wang Y, Webby RJ, Ulett GC, Adderson EE. Respiratory viruses augment the adhesion of bacterial pathogens to respiratory epithelium in a viral species- and cell type-dependent manner. *J Virol* 2006;80:1629-1636.
90. Hament JM, Aerts PC, Fleer A, van Dijk H, Harmsen T, Kimpen JL, Wolfs TF. Direct binding of respiratory syncytial virus to pneumococci: A phenomenon that enhances both pneumococcal

adherence to human epithelial cells and pneumococcal invasiveness in a murine model. *Pediatr Res* 2005;58:1198-1203.
91. Park K, Bakaletz LO, Coticchia JM, Lim DJ. Effect of influenza a virus on ciliary activity and dye transport function in the chinchilla eustachian tube. *Ann Otol Rhinol Laryngol* 1993;102:551-558.
92. Jakab GJ, Green GM. The effect of sendai virus infection on bactericidal and transport mechanisms of the murine lung. *J Clin Invest* 1972;51:1989-1998.
93. Navarini AA, Recher M, Lang KS, Georgiev P, Meury S, Bergthaler A, Flatz L, Bille J, Landmann R, Odermatt B, et al. Increased susceptibility to bacterial superinfection as a consequence of innate antiviral responses. *Proc Natl Acad Sci U S A* 2006;103:15535-15539.
94. Didierlaurent A, Goulding J, Patel S, Snelgrove R, Low L, Bebien M, Lawrence T, van Rijt LS, Lambrecht BN, Sirard JC, et al. Sustained desensitization to bacterial toll-like receptor ligands after resolution of respiratory influenza infection. *J Exp Med* 2008;205:323-329.
95. Jakab GJ, Green GM. Defect in intracellular killing of staphylococcus aureus within alveolar macrophages in sendai virus-infected murine lungs. *J Clin Invest* 1976;57:1533-1539.
96. Sun K, Metzger DW. Inhibition of pulmonary antibacterial defense by interferon-gamma during recovery from influenza infection. *Nat Med* 2008;14:558-564.
97. Kim KD, Zhao J, Auh S, Yang X, Du P, Tang H, Fu YX. Adaptive immune cells temper initial innate responses. *Nat Med* 2007;13:1248-1252.
98. Annual smoking-attributable mortality, years of potential life lost, and productivity losses--united states, 1997-2001. *MMWR Morb Mortal Wkly Rep* 2005;54:625-628.
99. Albano SA, Santana-Sahagun E, Weisman MH. Cigarette smoking and rheumatoid arthritis. *Semin Arthritis Rheum* 2001;31:146-159.
100. Marlow SP, Stoller JK. Smoking cessation. *Respir Care* 2003;48:1238-1254; discussion 1254-1236.
101. Mackay J, Amos A. Women and tobacco. *Respirology* 2003;8:123-130.
102. Fagerstrom K. The epidemiology of smoking: Health consequences and benefits of cessation. *Drugs* 2002;62 Suppl 2:1-9.
103. Sethi S, Murphy TF. Infection in the pathogenesis and course of chronic obstructive pulmonary disease. *N Engl J Med* 2008;359:2355-2365.
104. Smith CJ, Hansch C. The relative toxicity of compounds in mainstream cigarette smoke condensate. *Food Chem Toxicol* 2000;38:637-646.
105. Stampfli MR, Anderson GP. How cigarette smoke skews immune responses to promote infection, lung disease and cancer. *Nat Rev Immunol* 2009;9:377-384.
106. Heininger U, Cotter PA, Fescemyer HW, Martinez de Tejada G, Yuk MH, Miller JF, Harvill ET. Comparative phenotypic analysis of the *bordetella parapertussis* isolate chosen for genomic sequencing. *Infect Immun* 2002;70:3777-3784.
107. Harvill ET, Cotter PA, Miller JF. Pregenomic comparative analysis between bordetella bronchiseptica rb50 and bordetella pertussis tohama i in murine models of respiratory tract infection. *Infect Immun* 1999;67:6109-6118.
108. Heininger U, Stehr K, Schmitt-Grohe S, Lorenz C, Rost R, Christenson PD, Uberall M, Cherry JD. Clinical characteristics of illness caused by bordetella parapertussis compared with illness caused by bordetella pertussis. *Pediatr Infect Dis J* 1994;13:306-309.
109. Versteegh FG, Mooi-Kokenberg EA, Schellekens JF, Roord JJ. Bordetella pertussis and mixed infections. *Minerva Pediatr* 2006;58:131-137.

110. Bergey's manual of systematic bacteriology. New York: Springer; 2005.
111. Wood N, McIntyre P. Pertussis: Review of epidemiology, diagnosis, management and prevention. *Paediatric Respiratory Reviews* 2008;9:201-212.
112. Greenberg DP, von Konig CH, Heininger U. Health burden of pertussis in infants and children. *Pediatr Infect Dis J* 2005;24:S39-43.
113. Bonhoeffer J, Bar G, Riffelmann M, Soler M, Heininger U. The role of bordetella infections in patients with acute exacerbation of chronic bronchitis. *Infection* 2005;33:13-17.
114. Jackson LA, Cherry JD, Wang SP, Grayston JT. Frequency of serological evidence of bordetella infections and mixed infections with other respiratory pathogens in university students with cough illnesses. *Clin Infect Dis* 2000;31:3-6.
115. Widdicombe J, Kamath S. Acute cough in the elderly: Aetiology, diagnosis and therapy. *Drugs Aging* 2004;21:243-258.
116. Watanabe M, Nagai M. Whooping cough due to bordetella parapertussis: An unresolved problem. *Expert Rev Anti Infect Ther* 2004;2:447-454.
117. Liese JG, Renner C, Stojanov S, Belohradsky BH. Clinical and epidemiological picture of b pertussis and b parapertussis infections after introduction of acellular pertussis vaccines. *Arch Dis Child* 2003;88:684-687.
118. He Q, Viljanen MK, Arvilommi H, Aittanen B, Mertsola J. Whooping cough caused by bordetella pertussis and bordetella parapertussis in an immunized population. *JAMA* 1998;280:635-637.
119. Borska K, Simkovicova M. Studies on the circulation of bordetella pertussis and bordetella parapertussis in populations of children. *J Hyg Epidemiol Microbiol Immunol* 1972;16:159-172.
120. Keast D, Ayre DJ. Effects of chronic tobacco smoke exposure on immune responses in aged mice. *Arch Environ Health* 1981;36:201-207.
121. Baldwin CI, Todd A, Bourke S, Allen A, Calvert JE. Pigeon fanciers' lung: Effects of smoking on serum and salivary antibody responses to pigeon antigens. *Clin Exp Immunol* 1998;113:166-172.
122. Geng Y, Savage SM, Johnson LJ, Seagrave J, Sopori ML. Effects of nicotine on the immune response. I. Chronic exposure to nicotine impairs antigen receptor-mediated signal transduction in lymphocytes. *Toxicol Appl Pharmacol* 1995;135:268-278.
123. Kalra R, Singh SP, Savage SM, Finch GL, Sopori ML. Effects of cigarette smoke on immune response: Chronic exposure to cigarette smoke impairs antigen-mediated signaling in t cells and depletes ip3-sensitive ca(2+) stores. *J Pharmacol Exp Ther* 2000;293:166-171.
124. Skok M, Grailhe R, Changeux JP. Nicotinic receptors regulate b lymphocyte activation and immune response. *Eur J Pharmacol* 2005;517:246-251.
125. Loos BG, Roos MT, Schellekens PT, van der Velden U, Miedema F. Lymphocyte numbers and function in relation to periodontitis and smoking. *J Periodontol* 2004;75:557-564.
126. Parkhill J, Sebaihia M, Preston A, Murphy LD, Thomson N, Harris DE, Holden MT, Churcher CM, Bentley SD, Mungall KL, et al. Comparative analysis of the genome sequences of bordetella pertussis, bordetella parapertussis and bordetella bronchiseptica. *Nat Genet* 2003;35:32-40.
127. Wolfe DN, Kirimanjeswara GS, Harvill ET. Clearance of bordetella parapertussis from the lower respiratory tract requires humoral and cellular immunity. *Infect Immun* 2005;73:6508-6513.

128. Stainer DW, Scholte MJ. A simple chemically defined medium for the production of phase i bordetella pertussis. *J Gen Microbiol* 1970;63:211-220.
129. Brown EG, Bailly JE. Genetic analysis of mouse-adapted influenza a virus identifies roles for the na, pb1, and pb2 genes in virulence. *Virus Res* 1999;61:63-76.
130. Robbins CS, Bauer CMT, Vujicic N, Gaschler GJ, Lichty BD, Brown EG, Stampfli MR. Cigarette smoke impacts immune inflammatory responses to influenza in mice. *American Journal of Respiratory and Critical Care Medicine* 2006;174:1342-1351.
131. Drannik AG, Pouladi MA, Robbins CS, Goncharova SI, Kianpour S, Stampfli MR. Impact of cigarette smoke on clearance and inflammation after pseudomonas aeruginosa infection. *Am J Respir Crit Care Med* 2004;170:1164-1171.
132. Collins SE, Noyce RS, Mossman KL. Innate cellular response to virus particle entry requires irf3 but not virus replication. *J Virol* 2004;78:1706-1717.
133. Diaz-Granados N, Howe K, Lu J, McKay DM. Dextran sulfate sodium-induced colonic histopathology, but not altered epithelial ion transport, is reduced by inhibition of phosphodiesterase activity. *Am J Pathol* 2000;156:2169-2177.
134. Evanoff HL, Burdick MD, Moore SA, Kunkel SL, Strieter RM. A sensitive elisa for the detection of human monocyte chemoattractant protein-1 (mcp-1). *Immunol Invest* 1992;21:39-45.
135. Mehrad B, Strieter RM, Moore TA, Tsai WC, Lira SA, Standiford TJ. Cxc chemokine receptor-2 ligands are necessary components of neutrophil-mediated host defense in invasive pulmonary aspergillosis. *J Immunol* 1999;163:6086-6094.
136. Hebert CA, Chuntharapai A, Smith M, Colby T, Kim J, Horuk R. Partial functional mapping of the human interleukin-8 type a receptor. Identification of a major ligand binding domain. *J Biol Chem* 1993;268:18549-18553.
137. Simani A, Inoue S, Hogg J. Penetration of the respiratory epithelium of guinea pigs following exposure to cigarette smoke. *Lab Invest* 1974;31:75-81.
138. Hautamaki RD, Kobayashi DK, Senior RM, Shapiro SD. Requirement for macrophage elastase for cigarette smoke-induced emphysema in mice. *Science* 1997;277:2002-2004.
139. Didierlaurent A, Goulding J, Patel S, Snelgrove R, Low L, Bebien M, Lawrence T, van Rijt LS, Lambrecht BN, Sirard JC, et al. Sustained desensitization to bacterial toll-like receptor ligands after resolution of respiratory influenza infection. *J Exp Med* 2008.
140. Gaschler GJ, Zavitz CC, Bauer CM, Skrtic M, Lindahl M, Robbins CS, Chen B, Stampfli MR. Cigarette smoke exposure attenuates cytokine production by mouse alveolar macrophages. *Am J Respir Cell Mol Biol* 2008;38:218-226.
141. Lu LM, Zavitz CC, Chen B, Kianpour S, Wan Y, Stampfli MR. Cigarette smoke impairs nk cell-dependent tumor immune surveillance. *J Immunol* 2007;178:936-943.
142. Robbins CS, Bauer CM, Vujicic N, Gaschler GJ, Lichty BD, Brown EG, Stampfli MR. Cigarette smoke impacts immune inflammatory responses to influenza in mice. *Am J Respir Crit Care Med* 2006;174:1342-1351.
143. Robbins CS, Dawe DE, Goncharova SI, Pouladi MA, Drannik AG, Swirski FK, Cox G, Stampfli MR. Cigarette smoke decreases pulmonary dendritic cells and impacts antiviral immune responsiveness. *Am J Respir Cell Mol Biol* 2004;30:202-211.
144. Robbins CS, Pouladi MA, Fattouh R, Dawe DE, Vujicic N, Richards CD, Jordana M, Inman MD, Stampfli MR. Mainstream cigarette smoke exposure attenuates airway immune

inflammatory responses to surrogate and common environmental allergens in mice, despite evidence of increased systemic sensitization. *J Immunol* 2005;175:2834-2842.
145. Binnie V, McHugh S, Macpherson L, Borland B, Moir K, Malik K. The validation of self-reported smoking status by analysing cotinine levels in stimulated and unstimulated saliva, serum and urine. *Oral Dis* 2004;10:287-293.
146. de Weerd S, Thomas CM, Kuster JE, Cikot RJ, Steegers EA. Variation of serum and urine cotinine in passive and active smokers and applicability in preconceptional smoking cessation counseling. *Environ Res* 2002;90:119-124.
147. Siu EC, Tyndale RF. Characterization and comparison of nicotine and cotinine metabolism in vitro and in vivo in dba/2 and c57bl/6 mice. *Mol Pharmacol* 2007;71:826-834.
148. Savage SM, Donaldson LA, Cherian S, Chilukuri R, White VA, Sopori ML. Effects of cigarette smoke on the immune response. Ii. Chronic exposure to cigarette smoke inhibits surface immunoglobulin-mediated responses in b cells. *Toxicol Appl Pharmacol* 1991;111:523-529.
149. O'Leary JG, Goodarzi M, Drayton DL, von Andrian UH. T cell- and b cell-independent adaptive immunity mediated by natural killer cells. *Nat Immunol* 2006;7:507-516.
150. Sethi S, Evans N, Grant BJB, Murphy TF. New strains of bacteria and exacerbations of chronic obstructive pulmonary disease. *N Engl J Med* 2002;347:465-471.
151. Ashkar AA, Mossman KL, Coombes BK, Gyles CL, Mackenzie R. Fimh adhesin of type 1 fimbriae is a potent inducer of innate antimicrobial responses which requires tlr4 and type 1 interferon signalling. *PLoS Pathog* 2008;4:e1000233.
152. Sajic D, Ashkar AA, Patrick AJ, McCluskie MJ, Davis HL, Levine KL, Holl R, Rosenthal KL. Parameters of cpg oligodeoxynucleotide-induced protection against intravaginal hsv-2 challenge. *J Med Virol* 2003;71:561-568.
153. Pyles RB, Higgins D, Chalk C, Zalar A, Eiden J, Brown C, Van Nest G, Stanberry LR. Use of immunostimulatory sequence-containing oligonucleotides as topical therapy for genital herpes simplex virus type 2 infection. *J Virol* 2002;76:11387-11396.
154. Ashkar AliÂ A, Yao XD, Gill N, Sajic D, Patrick AmyÂ J, Rosenthal KennethÂ L. Tollâ€ like receptor (tlr)â€"3, but not tlr4, agonist protects against genital herpes infection in the absence of inflammation seen with cpg DNA. *The Journal of Infectious Diseases* 2004;190:1841-1849.
155. Tsai WC, Strieter RM, Mehrad B, Newstead MW, Zeng X, Standiford TJ. Cxc chemokine receptor cxcr2 is essential for protective innate host response in murine pseudomonas aeruginosa pneumonia. *Infect Immun* 2000;68:4289-4296.
156. Belperio JA, Keane MP, Burdick MD, Londhe V, Xue YY, Li K, Phillips RJ, Strieter RM. Critical role for cxcr2 and cxcr2 ligands during the pathogenesis of ventilator-induced lung injury. *J Clin Invest* 2002;110:1703-1716.
157. Erickson SE, Martin GS, Davis JL, Matthay MA, Eisner MD. Recent trends in acute lung injury mortality: 1996-2005. *Crit Care Med* 2009;37:1574-1579.
158. Phua J, Badia JR, Adhikari NK, Friedrich JO, Fowler RA, Singh JM, Scales DC, Stather DR, Li A, Jones A, et al. Has mortality from acute respiratory distress syndrome decreased over time?: A systematic review. *Am J Respir Crit Care Med* 2009;179:220-227.
159. Villard J, Dayer-Pastore F, Hamacher J, Aubert JD, Schlegel-Haueter S, Nicod LP. Gro alpha and interleukin-8 in pneumocystis carinii or bacterial pneumonia and adult respiratory distress syndrome. *Am J Respir Crit Care Med* 1995;152:1549-1554.

160. McNamee LA, Harmsen AG. Both influenza-induced neutrophil dysfunction and neutrophil-independent mechanisms contribute to increased susceptibility to a secondary streptococcus pneumoniae infection. *Infect Immun* 2006;74:6707-6721.
161. Wissinger E, Goulding J, Hussell T. Immune homeostasis in the respiratory tract and its impact on heterologous infection. *Semin Immunol* 2009;21:147-155.
162. Shahangian A. Type i ifns mediate development of postinfluenza bacterial pneumonia in mice. *The Journal of Clinical Investigation* 2009;0:0-0.
163. Yu X, Tsibane T, McGraw PA, House FS, Keefer CJ, Hicar MD, Tumpey TM, Pappas C, Perrone LA, Martinez O, et al. Neutralizing antibodies derived from the b cells of 1918 influenza pandemic survivors. *Nature* 2008;455:532.
164. Seki M, Kosai K, Yanagihara K, Higashiyama Y, Kurihara S, Izumikawa K, Miyazaki Y, Hirakata Y, Tashiro T, Kohno S. Disease severity in patients with simultaneous influenza and bacterial pneumonia. *Intern Med* 2007;46:953-958.
165. Al-Delaimy WK, Pierce JP, Messer K, White MM, Trinidad DR, Gilpin EA. The california tobacco control program's effect on adult smokers: (2) daily cigarette consumption levels. *Tob Control* 2007;16:91-95.
166. Franco F, Riese J, Tomassetti S, Shapiro S. Effect of cigarette smoking on antigen presentation by lung dendritic cells to cd4+ cells in thoracic lymph nodes American Thoracic Society International Conference. San Diego, California, USA; 2006.
167. Gaschler GJ, Skrtic M, Zavitz CC, Lindahl M, Onnervik PO, Murphy TF, Sethi S, Stampfli MR. Bacteria challenge in smoke-exposed mice exacerbates inflammation and skews the inflammatory profile. *Am J Respir Crit Care Med* 2009;179:666-675.
168. Marshall MD, Kales SN, Christiani DC, Goldman RH. Are reference intervals for carboxyhemoglobin appropriate? A survey of boston area laboratories. *Clin Chem* 1995;41:1434-1438.
169. Andersen P, Pedersen OF, Bach B, Bonde GJ. Serum antibodies and immunoglobulins in smokers and nonsmokers. *Clin Exp Immunol* 1982;47:467-473.
170. Sopori M. Effects of cigarette smoke on the immune system. *Nat Rev Immunol* 2002;2:372-377.
171. Berghall H, Siren J, Sarkar D, Julkunen I, Fisher PB, Vainionpaa R, Matikainen S. The interferon-inducible rna helicase, mda-5, is involved in measles virus-induced expression of antiviral cytokines. *Microbes Infect* 2006;8:2138-2144.
172. Tissari J, Siren J, Meri S, Julkunen I, Matikainen S. Ifn-alpha enhances tlr3-mediated antiviral cytokine expression in human endothelial and epithelial cells by up-regulating tlr3 expression. *J Immunol* 2005;174:4289-4294.
173. Dauphinee SM, Karsan A. Lipopolysaccharide signaling in endothelial cells. *Lab Invest* 2006;86:9-22.
174. Andonegui G, Zhou H, Bullard D, Kelly MM, Mullaly SC, McDonald B, Long EM, Robbins SM, Kubes P. Mice that exclusively express tlr4 on endothelial cells can efficiently clear a lethal systemic gram-negative bacterial infection. *J Clin Invest* 2009;119:1921-1930.
175. An H, Hou J, Zhou J, Zhao W, Xu H, Zheng Y, Yu Y, Liu S, Cao X. Phosphatase shp-1 promotes tlr- and rig-i-activated production of type i interferon by inhibiting the kinase irak1. *Nat Immunol* 2008;9:542-550.
176. O'Neill LA. 'fine tuning' tlr signaling. *Nat Immunol* 2008;9:459-461.

177. Christophi GP, Hudson CA, Gruber R, Christophi CP, Massa PT. Promoter-specific induction of the phosphatase shp-1 by viral infection and cytokines in cns glia. *J Neurochem* 2008.
178. Sriskandan S, Altmann DM. The immunology of sepsis. *The Journal of Pathology* 2008;214:211-223.